APPENDIX A

Bernalillo Bridge Reach
Hwy 550 Bridge (old Hwy 44) to Corrales Flood Channel
Hydraulic Modeling Analysis
1962-2001

Middle Rio Grande, New Mexico
June 2003

Report prepared by:
Claudia Leon
Mike Sixta
Jason Albert
Pierre Y. Julien

CSU – Engineering Research Center
Department of Civil Engineering
Fort Collins, Colorado

BERNALILLO BRIDGE REACH

HIGHWAY 44 BRIDGE TO CORRALES FLOOD CHANNEL OUTFALL

HYDRAULIC MODELING ANALYSIS

1962-2001

MIDDLE RIO GRANDE, NEW MEXICO

JUNE 2003

PREPARED FOR:

US BUREAU OF RECLAMATION

ALBUQUERQUE, NEW MEXICO

PREPARED BY:

MIKE SIXTA

JASON ALBERT

DR. CLAUDIA LEÓN

DR. PIERRE Y. JULIEN

COLORADO STATE UNIVERSITY

ENGINEERING RESEARCH CENTER

DEPARTMENT OF CIVIL ENGINEERING

FORT COLLINS, COLORADO 80523

ABSTRACT

The Bernalillo Bridge reach spans 5.10 miles downstream from Highway 44 at Bernalillo to cross-section CO-33. This reach is included in the habitat designation for two federally-listed endangered species, the Rio Grande silvery minnow and the southwestern willow flycatcher. Restoration efforts for these species require the understanding of historic, current and potential future geomorphic characteristics of the channel. Analysis of water and suspended sediment data at the USGS gaging stations, aerial photos, cross-section surveys and bed material size, reveal the temporal and spatial changes in the processes acting on the channel.

Geomorphic analyses indicate that the general trends of the Bernalillo Bridge reach include a decrease in width, width-depth ratio, wetted perimeter, and velocity and an increase in cross sectional area and depth during the 1962 to 2001 time period. Water surface and friction slopes did not change during this time period. The channel planform has remained straight with a sinuosity close to 1.10. The channel width has decreased since 1918 and the rate of change in channel width decreased with time from 1918 to 1992.

The entire reach aggraded between 1962 and 1972, with sand deposits of d_{50} = 0.20 mm. Subsequently, the bed degraded between 1972 and 2001. This degradation resulted in a coarsening of the bed material from sand to sand-gravel sized material of about d_{10} = 0.36 mm and d_{50} = 2.4 mm. From 1992 to 2001, subreaches 1 and 2 coarsened, while subreach 3 exhibited an opposite trend, whereby becoming finer. This resulted in a non-homogeneous reach. This is indicative of a depletion of sand within the reach.

The sand-load (0.0625 mm < d_s < 2 mm) at a discharge of 5,000 cfs is 21,672 tons/day at the Albuquerque gage. The corresponding bed-material load (0.36 mm < d_s < 2 mm) is about 10,836 tons/day. The calculated sediment transport capacity using 6 different methods and the hydraulic geometry data of 1992 is on average 7,139 tons/day and no method exceeds 15,000 tons/day. This transport capacity is fairly comparable to the incoming bed-material load (0.36 mm <d_s < 2 mm). The method of Yang (d_{50} and size fraction) seems appropriate for the bed-material load calculations in 1992. According to the hydraulic geometry characteristics in 1992 and the above equations, the channel slope in 1992 is able to transport the incoming bed-material load of about 10,836 tons/day.

The calculated sediment transport capacities using 5 different methods and the hydraulic

geometry characteristics in 2001 are on average 401 tons/day and 997 tons/day for subreaches 1 and 2, respectively. These results are much lower than the bed-material load (10,836 tons/day) at the Albuquerque gage. The low transport capacities of these two subreaches are likely due to the significant coarsening of the bed from 1992 to 2001. The sediment transport capacity for the sand fractions (0.0625 mm to 2 mm) was calculated using 6 different equations and the 2001 channel geometry data for subreach 3. The averaged transport capacity of subreach 3 is 3,693 tons/day, which is less than 50 % of the bed-material load at the Albuquerque gage and is about half of the capacity of that subreach in 1992. This reduction of capacity is likely due to the decrease in velocity and water surface slope from 1992 to 2001.

TABLE OF CONTENTS

Abstract ..... **ii**
Table of Contents ..... **iv**
List of Figures ..... **vii**
List of Tables ..... **x**
1 Introduction **1**
2 Site Description and Background **4**
2.1 Subreach Definition 6
2.2 Available Data 11
2.3 Channel Forming Discharge 14
3 Geomorphic Characterization **17**
3.1 Methods 17
Channel Classification 17
Sinuosity 22
Valley Slope 22
Longitudinal Profile 23
Thalweg Elevation 23
Mean Bed Elevation 23
Friction and Water Surface Slopes 23
Channel Geometry 24
Overbank Flow/Channel Capacity 25
Sediment 25
Bed Material 25
3.2 Results 26
Channel Classification 26
Historic and Current Channel Pattern Description 26
Sinuosity 32
Longitudinal Profile 32
Thalweg Elevation 32
Mean Bed Elevation 33
Friction Slope 35

Water Surface Slope 35
Channel Geometry 39
Width 40
Overbank Flow/Channel Capacity 41
Sediment 41
Bed Material 41
4 Suspended Sediment and Water History 45
4.1 Methods 45
4.2 Results 45
Single Mass Curves 45
Discharge Mass Curves 45
Suspended Sediment Mass Curve 46
Double Mass Curve 48
5 Equilibrium State Predictors 50
5.1 Methods 50
Sediment Transport Analysis 50
Hydraulic Geometry 52
Equilibrium Channel Width Analyses 58
5.2 Results 60
Sediment Transport Analysis 60
Hydraulic Geometry 64
Equilibrium Channel Width Analyses 67
6 Discussion 72
6.1 Historic Trend analysis and Current Conditions 72
Entire Bernalillo Bridge Reach 72
Subreach Trends 74
6.2 Schumm's (1969) River Metamorphosis Model 76
6.3 Potential Future Equilibrium Conditions 79
Sediment Transport Analysis 79
Equilibrium Channel Width Analysis 80
Hydraulic Geometry 81
7 Summary 82

8 References 85

Appendix A A-1

Appendix B B-1

Appendix C C-1

Appendix D D-1

Appendix E E-1

Appendix F F-1

Appendix G G-1

LIST OF FIGURES

Figure 1-1 Bernalillo Bridge reach location map 3
Figure 2-1 1995 Rio Grande spring runoff hydrograph 5
Figure 2-2 Annual suspended sediment yield in the Rio Grande in tons/year at Otowi Gage (upstream of Cochiti Dam), Cochiti Gage (just downstream of Cochiti dam) and Albuquerque Gage (downstream of Cochiti Gage) from 1974 to 2000. Cochiti gage record ends in 1988. 6
Figure 2-3 Bernalillo Bridge reach subreach definitions 7
Figure 2-4 Aerial photo of subreach 1. Date of photography: Winter 2000 8
Figure 2-5 Aerial photo of subreach 2. Date of photography: Winter 2000 9
Figure 2-6 Aerial photo of subreach 3. Date of photography: Winter 2000 10
Figure 2-7 2001 River planform of the Bernalillo Bridge Reach indicating locations of CO-lines and subreaches 13
Figure 2-8 Maximum mean daily annual discharge in cfs on the Rio Grande at San Felipe (1927-2001) 15
Figure 2-9 Maximum mean daily annual discharge histograms on the Rio Grande at San Felipe (1927 – 2001) 15
Figure 3-1 Channel pattern, width/depth ratio and potential specific stream power relative to reference values, as defined by Eqs. 1 and 2 (after van den Berg 1995)..... 20
Figure 3-2 Channel patterns of sand streams (after Chang 1979) 22
Figure 3-3 Non-vegetated active channel of the Bernalillo Bridge reach. 1918 planform from topographic survey. 1935, 1962,1992 and 2001 planform from aerial photos..... 27
Figure 3-4 Time series of sinuosity of the Bernalillo Bridge Reach as measured from the digitized aerial photos by dividing the thalweg length by the valley length 32
Figure 3-5 Change in thalweg elevation with time at the CO-lines 33
Figure 3-6 Change in mean bed elevation with time at CO-lines 34
Figure 3-7 Time series of reach-averaged mean bed elevation, computed from the 1962, 1972 and 1992 agg/deg surveys and 2001 CO-line surveys..... 35
Figure 3-8 Mean Bed Elevation Profile of entire Bernalillo Bridge Reach for 1962,1972, 1992 and 2001. Distance downstream is measured from agg/deg 298. 36

Figure 3-9 Mean bed elevation profiles of the subreaches from the agg/deg surveys of 1962,1972 and 1992. Thalweg elevation profile from CO-line surveys of 2001. (a) Subreach 1, (b) Subreach 2, (c) Subreach 3. 37
Figure 3-10 Time series of friction slope of the subreaches and the entire reach from HEC-RAS modeling results 38
Figure 3-11 Time series of water surface slope (ft/ft) of the subreaches and the entire reach from HEC-RAS modeling results 38
Figure 3-12 Reach-averaged main channel geometry from HEC-RAS results for Q = 5,000 cfs. (a) Mean Velocity, (b) Cross-section Area, (c) Average Depth, (d) Width-depth ratio, (e) Wetted Perimeter 39
Figure 3-13 Reach averaged active channel width from digitized aerial photos 40
Figure 3-14 Reach averaged main channel width from HEC-RAS at Q =5,000 cfs 40
Figure 3-15 Comparison of 1992 and 2001 bed material gradation curves for subreach 1 42
Figure 3-16 Comparison of 1992 and 2001 bed material gradation curves for subreach 2 43
Figure 3-17 Comparison of 1992 and 2001 bed material gradation curves for subreach 3 43
Figure 3-18 2001 Bed-material samples used in the sediment transport and equilibrium analyses 44
Figure 4-1 Discharge mass curve at Bernalillo and Albuquerque gages (1942-2000) 46
Figure 4-2 Suspended sediment mass curve at Bernalillo and Albuquerque gages (1956-1999) 47
Figure 4-3 Cumulative discharge vs. cumulative suspended sediment load at Rio Grande at Bernalillo and Rio Grande at Albuquerque (1956 - 1999) 48
Figure 5-1 Variation of wetted perimeter P with discharge Q and type of channel (after Simons and Albertson 1963) 54
Figure 5-2 Variation of average width W with wetted perimeter P (after Simons and Albertson 1963) 55
Figure 5-3 Albuquerque gage sand-load rating curve for the Spring and Summer seasons from 1978 to 1999 61
Figure 5-4 – Downstream hydraulic geometry equation results – Predicted equilibrium width in feet vs. measured reach-averaged non-vegetated active channel width in feet 66
Figure 5-5 Empirical width-discharge relationships for the Bernalillo Bridge reach and subreaches 67

Figure 5-6 Relative decrease in channel width in (a) Subreach 1, (b) Subreach 2, (c) Subreach 3 and (d) Bernalillo Bridge Reach..... 68
Figure 5-7 Linear regression results of subreach and entire reach data – observed width change (ft/year) with observed channel width (feet). (a) Subreach 1, (b) Subreach 2, (c) Subreach 3, (d) Entire Reach..... 69
Figure 5-8 Application of exponential model of width change using methods 1 and 2 to estimate k_1 and W_e values. (a) Subreach 1, (b) Subreach 2, (c) Subreach 3 and (d) Entire Reach . 70

LIST OF TABLES

Table 2-1 Bernalillo Bridge reach subreach definition 7
Table 2-2 Periods of record for discharge and continuous suspended sediment data collected by the USGS 11
Table 2-3 Periods of record for bed material particle size distribution data collected by the USGS 11
Table 2-4 Surveyed dates for bed material particle size distribution data at CO-lines and BI-lines collected by the US Bureau of Reclamation 12
Table 2-5 Surveyed dates for BB and CR Lines collected by the US Bureau of Reclamation 14
Table 2-6 Surveyed dates for the Cochiti range lines collected by the US Bureau of Reclamation 14
Table 3-1 Source of bed material data used for the bed sediment subreach characterization and in the 2001 sediment transport and equilibrium analyses 25
Table 3-2 Input Parameters for Channel Classification Methods 28
Table 3-3 Channel Pattern Classification for 1962 and 1972 30
Table 3-4 Channel Pattern Classification for 1992 and 2001 31
Table 3-5 Reach averaged change in mean bed elevation in feet from agg/deg surveys. 34
Table 3-6 Range of median grain sizes in Subreaches 1, 2 and 3 for 1962, 1972, 1992 and 2001 41
Table 3-7 Median grain size statistics from the bed material samples at Bernalillo gage, CO-lines and BI-lines. 42
Table 4-1 Summary of the discharge mass curve slope breaks at Bernalillo and Albuquerque gages (1942-2000) 46
Table 4-2 Summary of the suspended sediment discharge mass curve slope breaks at Bernalillo and Albuquerque gages (1956-1999) 47
Table 4-3 Summary of suspended sediment concentrations at Bernalillo and Albuquerque gages (1956-1999) 49
Table 5-1 Percents of total load that behave as washload and bed material load at flows close to 5,000 cfs 50
Table 5-2 Appropriateness of bedload and bed-material load transport equations (Stevens et al. 1989). 52

Table 5-3 Hydraulic input data at all subreaches for sediment transport capacity computations from 1992 and 2001 HEC-RAS runs at 5,000 cfs. 52
Table 5-4 Input data for the empirical width-discharge relationship 57
Table 5-5 Input data for the hydraulic geometry calculations 58
Table 5-6 Hyperbolic regression input data 59
Table 5-7 Bed-material transport capacity for the 1992 channel geometry data for subreaches 1 and 2 61
Table 5-8 Bed-material and bedload transport capacity for the 2001 channel geometry data for subreaches 1 and 2 62
Table 5-9 Bed material transport capacity for the 1992 and 2001 channel geometry data for subreach 3 63
Table 5-10 Predicted Equilibrium Widths in ft from downstream hydraulic geometry equations for Q = 5,000 cfs 65
Table 5-11 Change in width with time hyperbolic equations and regression coefficients 68
Table 5-12 Empirical estimation of k_1 and W_e from linear regressions of width vs. width change data (Method 1) 69
Table 5-13 Exponential model results using methods 1 and 2 71
Table 5-14 Exponential equations of change in width with time using methods 1 and 2 71
Table 6-1 Summary of channel changes between 1962 and 2001 based on reach-averaged main channel parameters from HEC-RAS modeling runs at Q = 5,000 cfs. 74
Table 6-2 Summary of channel changes during 1962-1972 and 1972-1992 periods based on reach-averaged main channel parameters from HEC-RAS modeling run at Q = 5,000 cfs. 75
Table 6-3 Summary of Schumm's (1969) channel metamorphosis model. 77
Table 6-4 Summary of channel changes during 1962-1972, 1972-1992, and 1992-2001 periods. 78
Table 6-5 1991-1992 rate of decrease in channel width according to the hyperbolic model and 2001 predicted and measured widths 80
Table 6-6 1985-1992 rate of decrease in channel width according to the exponential model and 2001 predicted and measured widths 81

1 INTRODUCTION

The hydrologic and sediment regime of the Middle Rio Grande, New Mexico has been altered in the last century through construction of several dams and channelization. The quantity and quality of habitat for native species, such as the silvery minnow (*Hybognathus amarus*), the southwestern willow flycatcher (*Empidonax traillii extimus*) and the southwestern cottonwood-willow riparian habitat, has been significantly reduced.

The Rio Grande silvery minnow occurs only in less than 10% of its original range (Bestgen 1996) and reaches its most upstream distribution in the Cochiti Reach (Platania 1999). Remaining populations of this species continue to decline primarily due to the lack of warm, slow-moving, silt-sand substrate pools, dewatering of the river and abundance of non-native and exotic fish species (Platania 1991, Bestgen et. al 1991, Burton 1997, Robinson 1995, Arritt 1996). The silvery minnow became a federally listed endangered species in July 1999, after the US Fish and Wildlife Service (USFWS) designated the Middle Rio Grande, New Mexico from just downstream of Cochiti Dam to the railroad bridge at San Marcial as critical habitat for this species.

In addition, deterioration of riparian bosque habitat has occurred (Taylor et. al 2001). The USFWS listed the southwestern willow flycatcher (*Empidonax traillii extimus*) as an endangered species in February 27, 1995. This species is a small, grayish-green migratory songbird found primarily in riparian habitats characterized by dense growths of willows, arrowweed and other species that provide foraging and nesting habitat (USFWS 2000). The loss of southwestern cottonwood-willow riparian habitat has been the main reason for the decline of the population of the southwestern willow flycatcher (USFWS 2000).

The Bernalillo Bridge reach (Figure 1-1) in the Middle Rio Grande is included in both critical habitat designations. This reach begins at the Highway 44 Bridge in Bernalillo and ends 5.10 miles downstream from the bridge at cross section CO-33. Bernalillo Bridge reach is the next downstream reach from the Santa Ana Restoration Project.

The objective of this work is to analyze historical data and estimate potential conditions of the river channel. Prediction of future equilibrium conditions of the Bernalillo Bridge reach will facilitate the identification of sites that are more conducive to restoration efforts.

In order to achieve this objective, the following analyses were performed:

- Identification of spatial and temporal trends in channel geometry through the analysis of cross-section survey data.
- Planform classification through analysis of aerial photos and channel geometry data.
- Analysis of temporal trends in water and sediment discharge and sediment concentration using USGS gaging station data.
- Evaluation of the equilibrium state of the river through the application of hydraulic geometry methods, empirical width-time relationships and sediment transport analysis.

This work consists of eight sections. The introduction is included in section 1. Description and background of the study site is in section 2. Geomorphic characterization of the reach, including planform classification, sinuosity computations, longitudinal profiles, channel geometry and bed material sediment characterizations are presented in section 3. Section 4 presents the sediment continuity analysis of the reach, including single and double discharge and suspended sediment mass curves. Section 5 contains the predicted equilibrium states of the channel based on sediment transport analyses, hydraulic geometry equations and minimum stream power methods. Section 6 presents the discussion of the results. Summary of the results is included in section 7 and finally the list of cited references is presented in section 8.

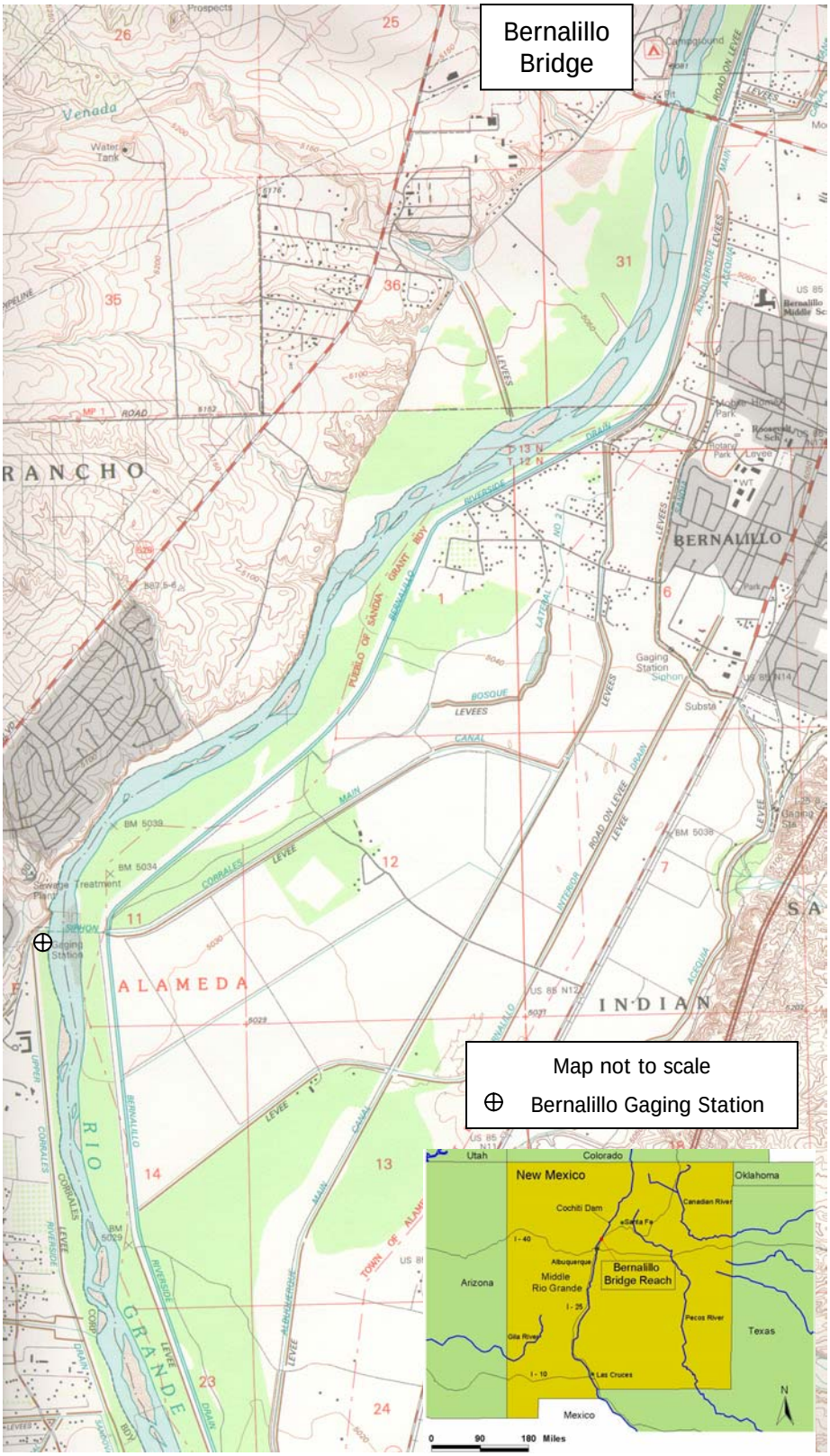

Figure 1-1 Bernalillo Bridge reach location map

2 SITE DESCRIPTION AND BACKGROUND

The Bernalillo Bridge reach of the Middle Rio Grande spans 5.10 miles from New Mexico Highway 44 (agg/deg 298) to cross section CO-33 (agg/deg line 351) (Figure 1-1). The reach is generally straight with a sinuosity close to one and an average valley slope of 0.0010. This reach is characterized by a bimodal sediment size distribution, from medium sand to coarse gravel.

Historically, the middle Rio Grande was a relatively straight, braided channel (Baird 1996). In addition, the river bed was characterized by an aggradational trend, which might have started about 11,000 to 22,000 years ago (Sanchez et al. 1997). Increasing sedimentation of the river bed began after 1850 due to water shortage and increasing sediment input from tributaries and arroyos (Scurlock 1998). The aggradation of the river bed induced severe flooding, waterlogged lands and failing irrigation facilities (Scurlock 1998).

The Middle Rio Grande Conservancy District was organized in 1925 for the main purpose of improving drainage, irrigation and flood control in the middle valley (Woodson and Martin 1962). A floodway was constructed in the early 1930's to provide flood protection to the adjacent irrigated and urban areas (Woodson 1961). In addition, the Conservancy District built El Vado Dam on the Rio Chama in 1935, four diversion dams along the main stem, two canal headings and many miles of drainage and irrigation canals (Lagasse 1980).

Further aggradation and seepage induced deterioration of the floodway and suggested the need for regulation of flood flows, sediment retention and channel stabilization (Woodson and Martin 1962). The Corps of Engineers and the United States Bureau of Reclamation (USBR) together with other Federal, State and local agencies recommended a comprehensive plan of improvement for the Rio Grande in New Mexico in 1948 (Pemberton 1964). The plan consisted of constructing a system of reservoirs on the Rio Grande (Cochiti) and its tributaries (Abiquiu, Jemez, Galisteo) as well as the rehabilitation of the floodway constructed by the Rio Grande Conservancy District in 1935 (Woodson and Martin 1962).

Cochiti Dam, built in the Rio Grande, began impounding water and sediment in November 1973 (Lagasse 1980). Cochiti Dam was intended for flood and sediment control, preventing aggradation and inducing degradation of the main stem (Lagasse 1980). Additionally, other dams on the main tributaries (Jemez, Galisteo) and agricultural diversions (Angostura) in the main stem decrease the flow between Cochiti Dam and the Bernalillo Bridge reach.

Figure 2-1 shows a typical spring runoff hydrograph in the Middle Rio Grande. The Otowi stream gage station is located upstream of Cochiti Dam. Attenuation of the spring runoff peak between Otowi and the gages located downstream of the dam is evident in the hydrographs (Figure 2-1). Peak outflows from Cochiti can historically occur as much as 62 days after, or as much as 225 days prior to the peak inflows to the reservoir (Bullard and Lane 1993).

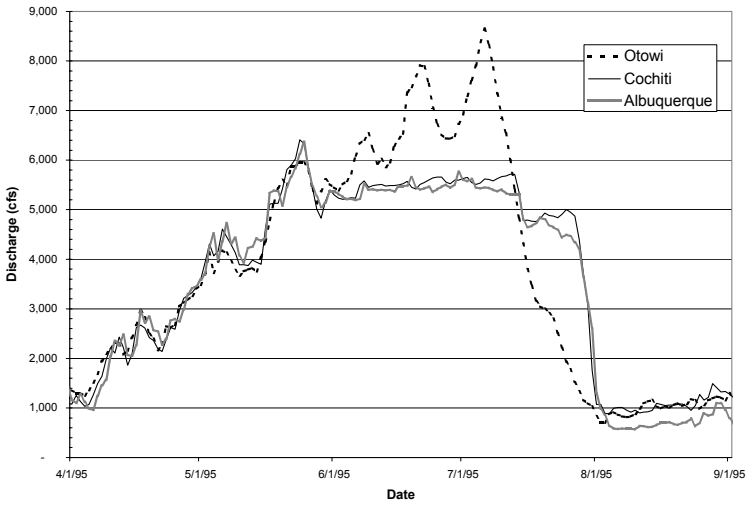

Figure 2-1 1995 Rio Grande spring runoff hydrograph

Cochiti dam also traps most of the sediment entering the reservoir from upstream. Figure 2-2 shows the change in annual suspended sediment yield from upstream of Cochiti dam to downstream. Tributary input and erosion of the channel bed and banks are the major sources of sediment to the middle Rio Grande downstream from Cochiti Dam. Increase of sediment yield between Cochiti Dam and Albuquerque gaging station is evident in Figure 2-2.

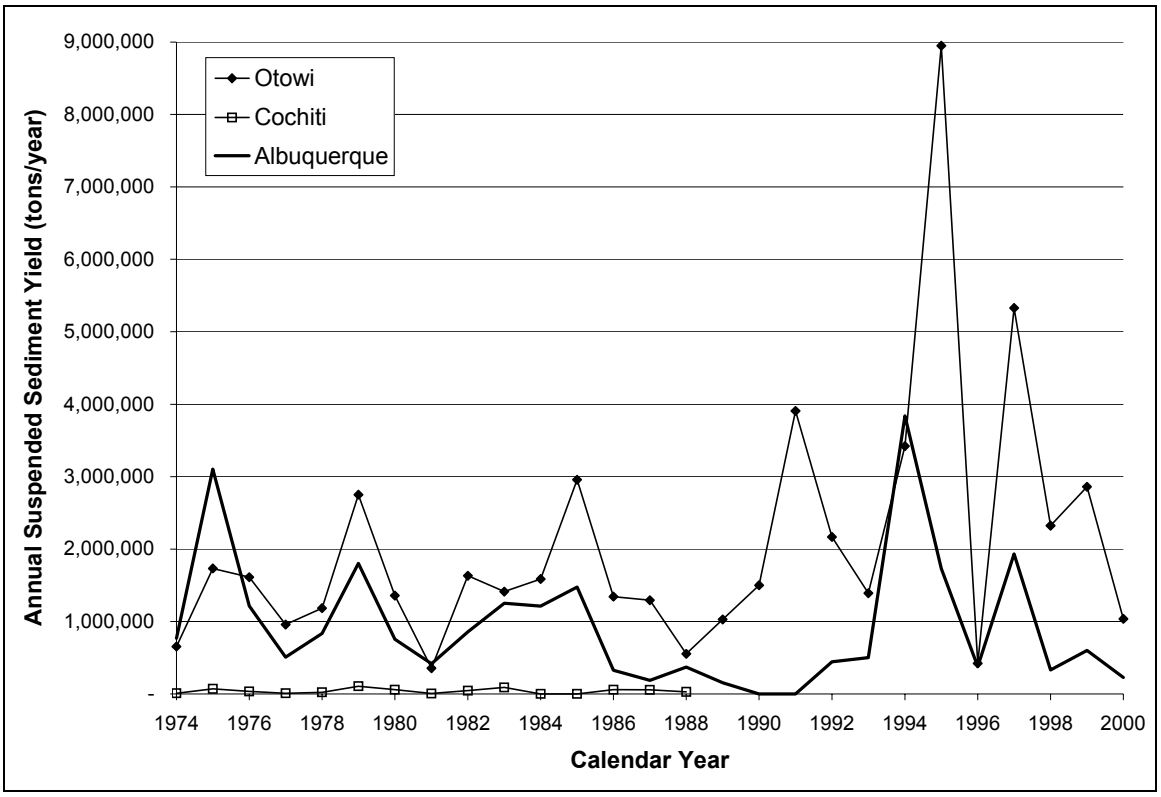

Figure 2-2 Annual suspended sediment yield in the Rio Grande in tons/year at Otowi Gage (upstream of Cochiti Dam), Cochiti Gage (just downstream of Cochiti dam) and Albuquerque Gage (downstream of Cochiti Gage) from 1974 to 2000. Cochiti gage record ends in 1988.

Two ephemeral tributaries, Arroyo Venada and Arroyo de la Barranca, join the study reach from the west. A third tributary, Arroyo de las Lomitas Negras, enters the river from the west just downstream of the study reach. Arroyo de la Barranca has a noticeable delta at the confluence with the main channel. The locations of these arroyos are indicated in the aerial photo in Figures 2-4 and 2-6.

2.1 SUBREACH DEFINITION

The Bernalillo Bridge reach was subdivided into three subreaches that exhibit similar channel characteristics, such as width, planform and slope to facilitate the geomorphic characterization. Subreach 1 is 1.79 miles long and spans from Highway NM-44 (Agg/Deg 298) to cross section Agg/Deg 316. Subreach 2 is 1.93 miles long and spans from cross section Agg/Deg 316 to cross section Agg/Deg 337. Subreach 3 is 1.38 miles long and spans from Agg/Deg 337 to Agg/Deg 351 (CO-33). The three subreaches are fairly straight, yielding an

average sinuosity of 1.10. Subreach 1 has vegetated bars lateral to the low flow channel. Subreach 2 has some vegetated bars within the low flow channel and subreach 3 does not exhibit vegetated islands. Subreach 1 exhibits a low flow single thread channel. Subreaches 2 and 3 show some short reaches with multiple channel patterns. Besides planform differences, the 1992 longitudinal profile reveals two slope breaks at cross sections Agg/deg 316 and Agg/deg 337. Only few cross sections were surveyed in the year 2001. Therefore, the same breaks in slopes are not noticeable in the 2001 longitudinal profile. The subreach definition is outlined in Table 2-1 and in Figures 2-3, 2-4, 2-5 and 2-6.

Table 2-1 Bernalillo Bridge reach subreach definition

	Agg/Deg Line		
	From	To	Length (miles)
Subreach 1	298	316	1.79
Subreach 2	316	337	1.93
Subreach 3	337	351	1.38

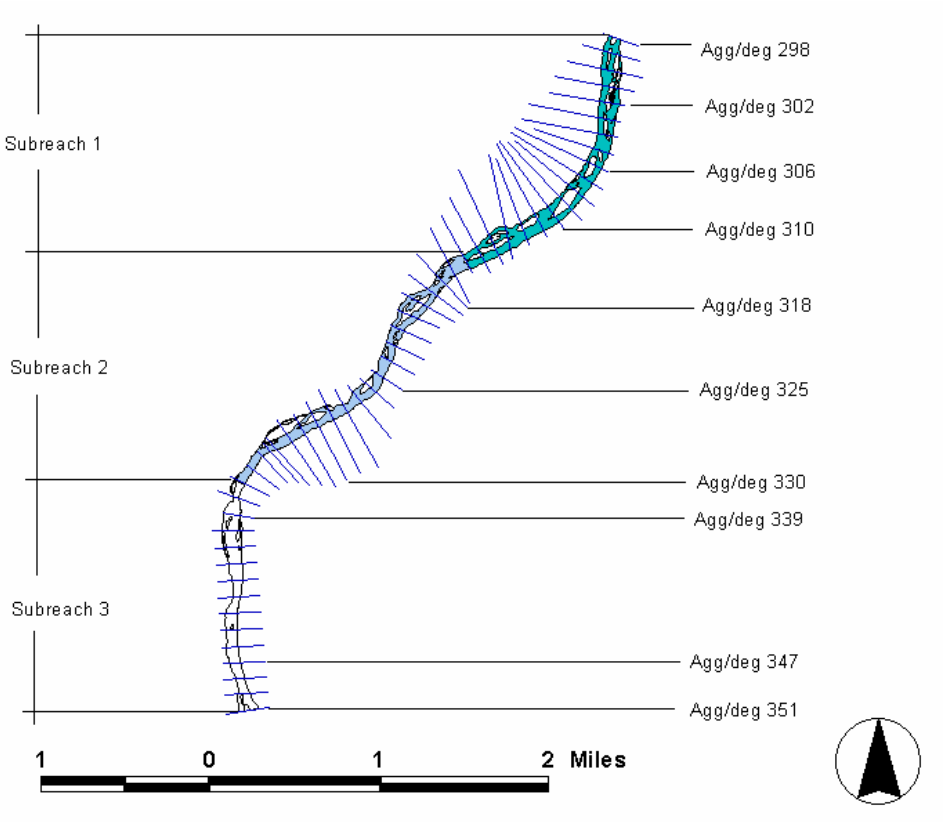

Figure 2-3 Bernalillo Bridge reach subreach definitions

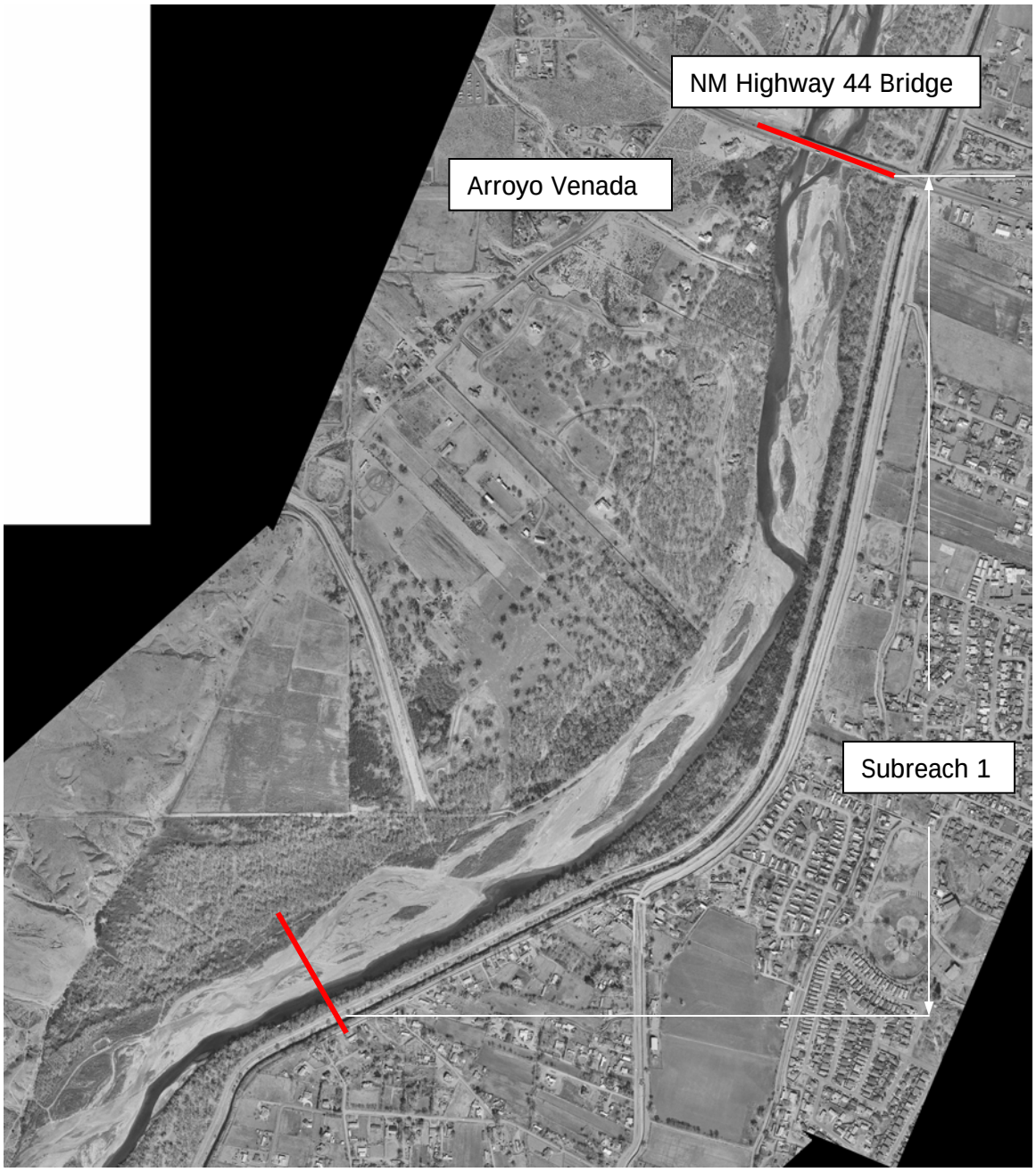

Figure 2-4 Aerial photo of subreach 1. Date of photography: Winter 2000

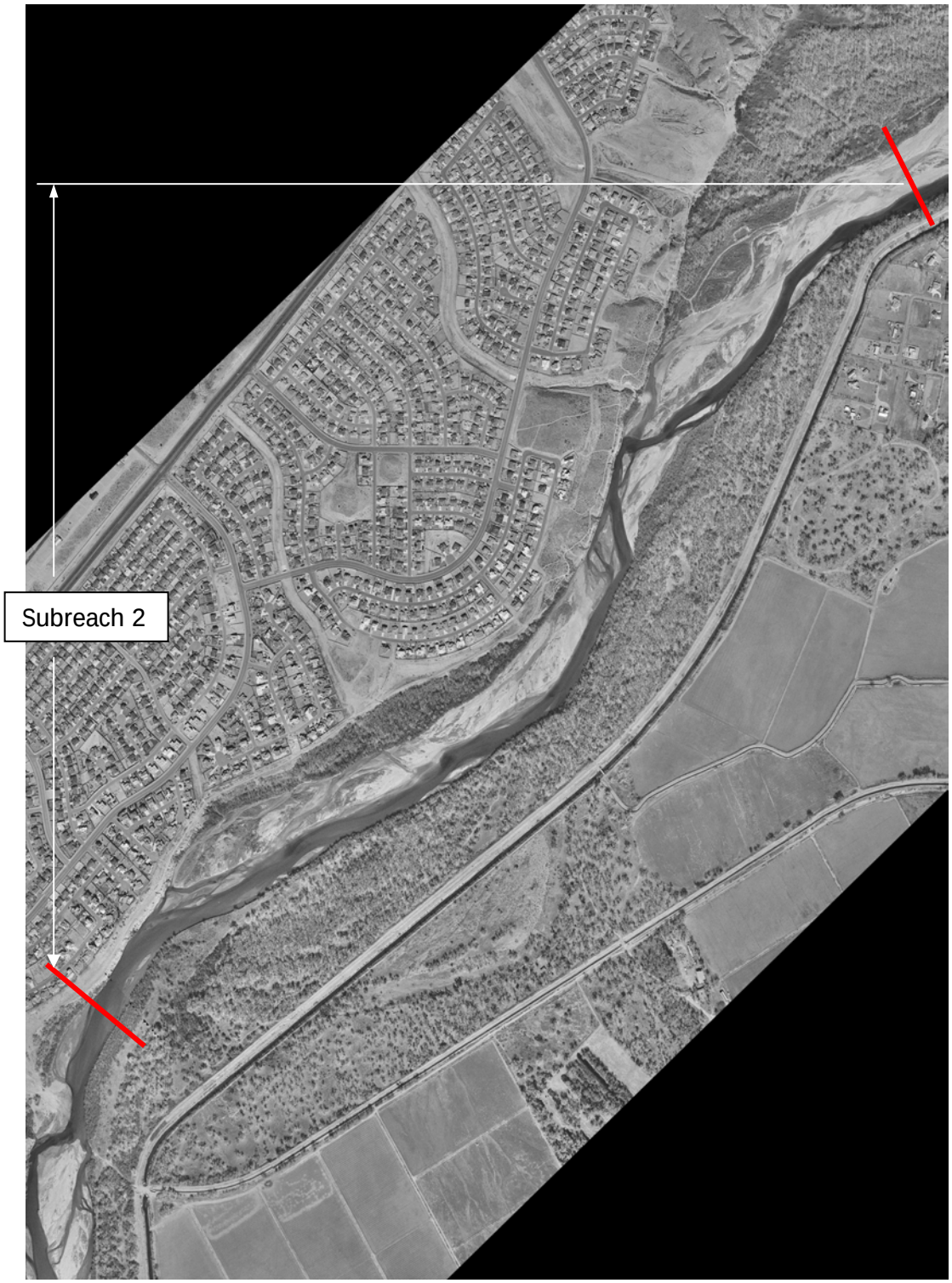

Figure 2-5 Aerial photo of subreach 2. Date of photography: Winter 2000

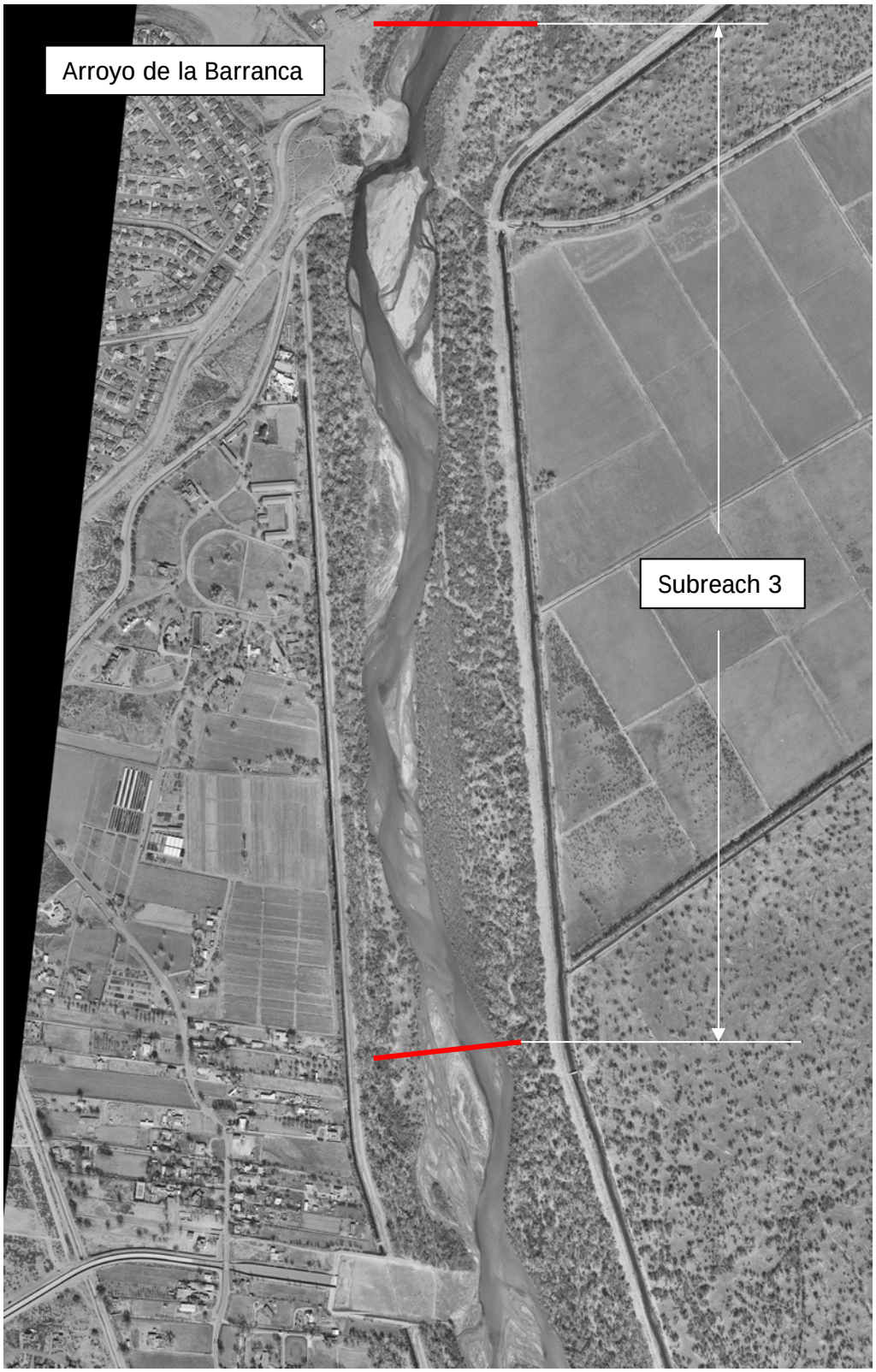

Figure 2-6 Aerial photo of subreach 3. Date of photography: Winter 2000

2.2 AVAILABLE DATA

There is one U.S. Geological Survey (USGS) gaging station (Rio Grande at Bernalillo) located in the Bernalillo reach, upstream of subreach 3 (Figure 1-1). In addition, there are two gaging stations upstream and downstream of the study reach. Rio Grande at San Felipe gaging station is located about 13 miles upstream from New Mexico Highway 44 and Rio Grande at Albuquerque gaging station is about 16.5 miles downstream from cross section CO-33. Table 2-2 summarizes the available water discharge and suspended sediment data from the USGS gages.

Table 2-2 Periods of record for discharge and continuous suspended sediment data collected by the USGS

Stations	***Mean Daily Discharge***	***Continuous Suspended Sediment Discharge***
	Period of Record	Period of Record
Rio Grande at San Felipe	1927-2001	----
Rio Grande near Bernalillo	1942-1968	1956-1969
Rio Grande at Albuquerque	1942-2001	1969-1989 1992-1999

Bed material particle size distribution data were collected at the USGS gaging stations at San Felipe, Bernalillo and Albuquerque. Table 2-3 summarizes the periods of record for the bed material data from the above-mentioned USGS gages. Additionally, bed material samples were collected at the CO-lines, BI-lines and BB-lines. BI-296 is about 0.16 miles upstream of the study reach. Table 2-4 lists the bed material surveyed dates at the CO-lines, BI-lines and BB-lines.

Table 2-3 Periods of record for bed material particle size distribution data collected by the USGS

Stations	***Bed Material Particle Size Distributions***
	Period of Record
Rio Grande at San Felipe	1970 - 1974
Rio Grande near Bernalillo	1961, 1966 - 1969
Rio Grande at Albuquerque	1969 - 2001

Table 2-4 Surveyed dates for bed material particle size distribution data at CO-lines and BI-lines collected by the US Bureau of Reclamation

Stations	***Bed Material Particle Size Distributions***
	Surveyed Date
CO-30	1971 - 1982, 1997
CO-31	1971 - 1982, 1992, 1995, 1997
CO-32	1971 1982, 1997
CO-33	1970 - 1982, 1992, 1995
BI-296	1990 - 1997
BB-301	2001
BB-307	2001
BB-318	2001
BB-327	2001
BB-340	2001
BB-345	2001

Reclamation's GIS and Remote Sensing group in Denver, CO digitized the aerial photos and topographic surveys of the study reach which are available for 1918, 1935, 1949, 1962, 1972, 1992 and 2001. Dates and scales of the aerial photos as well as the estimated mean daily discharges in the channel on the dates of the photos, according to USGS gaging stations, are summarized in Appendix A.

Aggradation/Degradation (agg/deg) line surveys, collected by the USBR, are available for 1962, 1972 and 1992. These cross section lines are photogrammetrically surveyed. The mean bed elevations were estimated by the USBR based on the water surface elevation, slope, channel roughness and discharge at the time of the survey. Agg/deg lines are approximately spaced every 500 feet apart.

There are three different sets of cross sections that have been field surveyed in this reach. The Cochiti (CO) range lines were field surveyed for the US Bureau of Reclamation. There are four lines located in this study reach (Figure 2-7). CO-30 is located 1.55 miles downstream from New Mexico Highway 44 (agg/deg 298) in subreach 1. CO-31 is located in subreach 2 and coincides with agg/deg 324. CO-32 is also located in subreach 2 and coincides with agg/deg 335. CO-33 is the last cross section in subreach 3 and corresponds to the agg/deg line 351. In addition to these four lines, there is one CO-line (CO-29) just upstream from the study reach. Table 2-5 summarizes the survey dates for the CO-Lines within the reach. CO-line plots and their corresponded agg/deg lines are included in Appendix B. There are a total of seven

Bernalillo Bridge (BB) lines along the study reach. There are two in subreach 1, three in subreach 2 and two in subreach 3. The CR-lines are downstream from the study reach. Table 2-5 lists the surveyed dates for these cross sections.

Reclamation's GIS and Remote Sensing group in Denver, CO digitized the aerial photos and topographic surveys of the study reach available for 1918, 1935, 1949, 1962, 1972, 1992 and 2001. Dates and scales of the photos as well as the estimated flow discharges in the channel during the date of the photos are summarized in Appendix A.

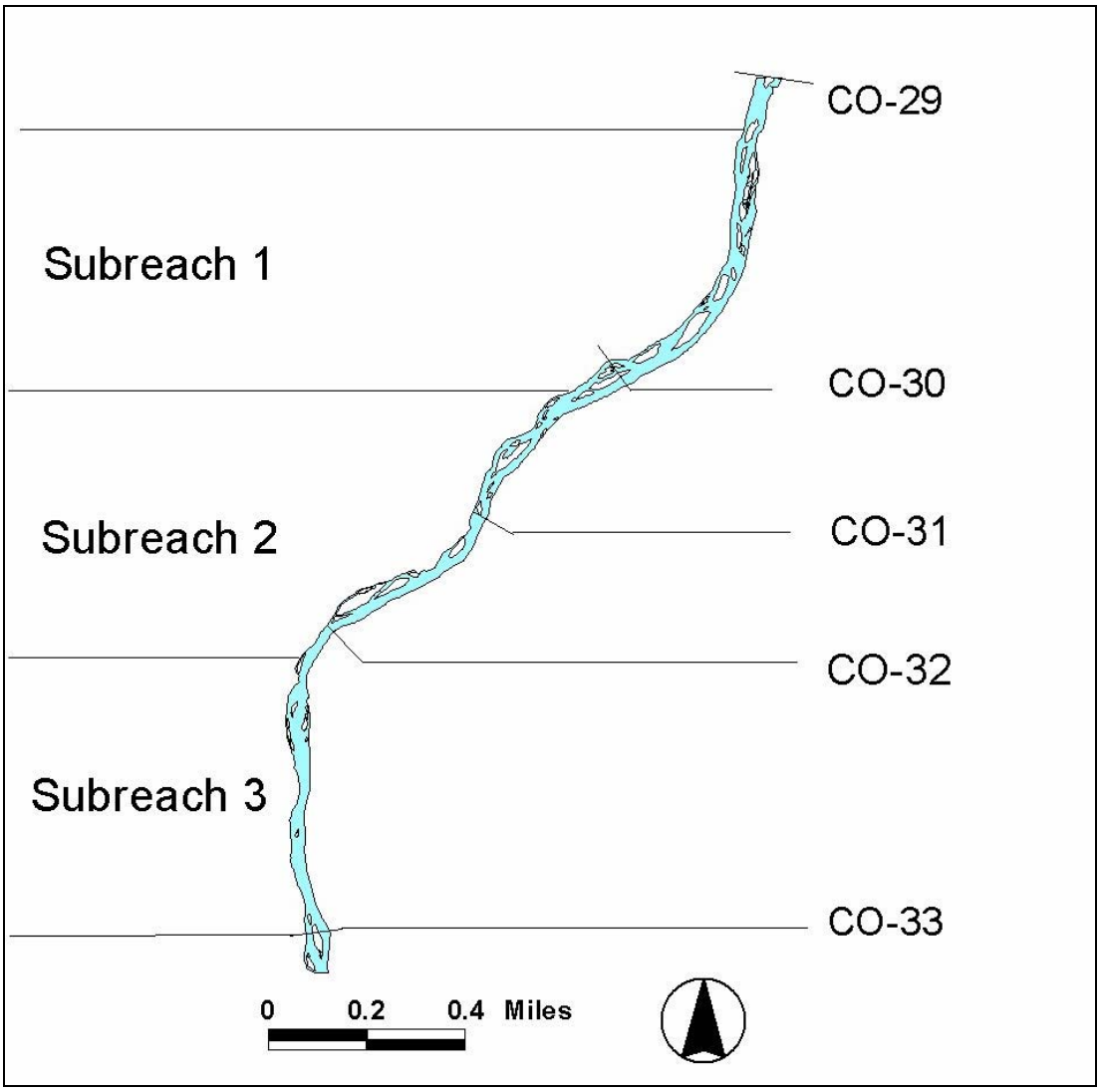

Figure 2-7 2001 River planform of the Bernalillo Bridge Reach indicating locations of CO-lines and subreaches

Table 2-5 Surveyed dates for BB and CR Lines collected by the US Bureau of Reclamation

Cross section	Dates
BB-301	13/04/01
BB-307	13/04/01
BB-318	13/04/01
BB-323	13/04/01
BB-327	13/04/01
BB-340	15/05/01
BB-345	15/05/01
CR-355	May-01
CR-361	May-01
CR-367	May-01

Table 2-6 Surveyed dates for the Cochiti range lines collected by the US Bureau of Reclamation

	Cross Section Number			
Date	CO-30	CO-31	CO-32	CO-33
May-71	x	x	x	x
Sep-71	x	x	x	x
Mar-72	x	x	x	x
Nov-72	x	x	x	x
May-73	x			
Jun-73		x	x	x
May-74	x	x	x	x
Sep-74	x		x	x
Nov-74	x	x	x	x
May-75	x	x	x	x
Jul-75	x	x	x	x
Nov-75	x	x	x	x
Apr-79	x	x	x	x
May-79			x	x
Jul-79		x	x	x
Jan-80	x	x	x	x
Oct-82	x	x	x	x
Nov-83	x	x	x	x
Nov-86	x	x	x	
Jul-92	x	x	x	x
Aug-95	x	x	x	x
Sep-98	x	x	x	x

2.3 CHANNEL FORMING DISCHARGE

Reclamation's Albuquerque office determined the channel forming discharge from discharge/frequency analysis in the Santa Ana Reach. The Bernalillo Bridge reach is the next downstream reach from the Santa Ana Restoration Project. The two year instantaneous peak discharge (Q_{2y}= 5,000 cfs) used as the channel forming discharge in the Santa Ana Geomorphic Analysis (Mosley and Boelman 1998) is also used in this work.

Figure 2-8 shows the annual maximum daily mean discharges recorded by the USGS at the San Felipe gaging station. Since 1958, there have been no flows recorded at San Felipe exceeding 10,000 cfs. Since flow regulation began at Abiquiu Dam on the Rio Chama in 1963

and on Cochiti Dam on the Rio Grande in 1973, the regulated two-year flow has decreased to 5,650 cfs (Bullard and Lane, 1993). Figure 2-9 shows annual peak flow histograms before and after 1963. Most of the flows are between 3,000 cfs and 7,000 cfs after 1963. Annual peak daily-mean discharge plots at Bernalillo and Albuquerque gages are included in Appendix C.

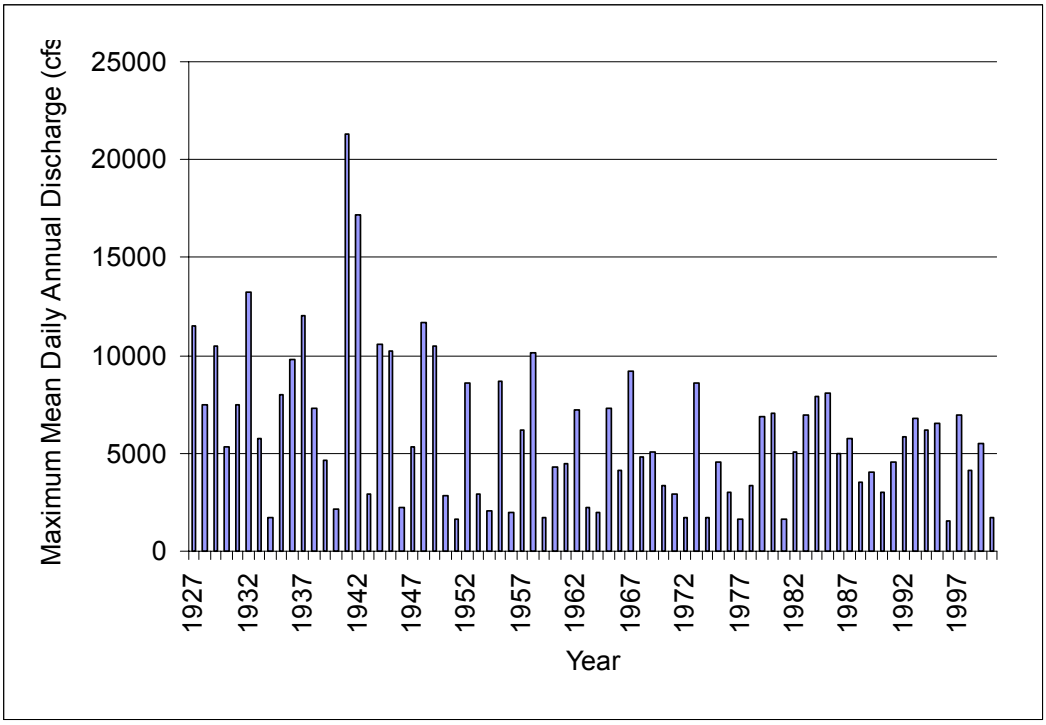

Figure 2-8 Maximum mean daily annual discharge in cfs on the Rio Grande at San Felipe (1927-2001)

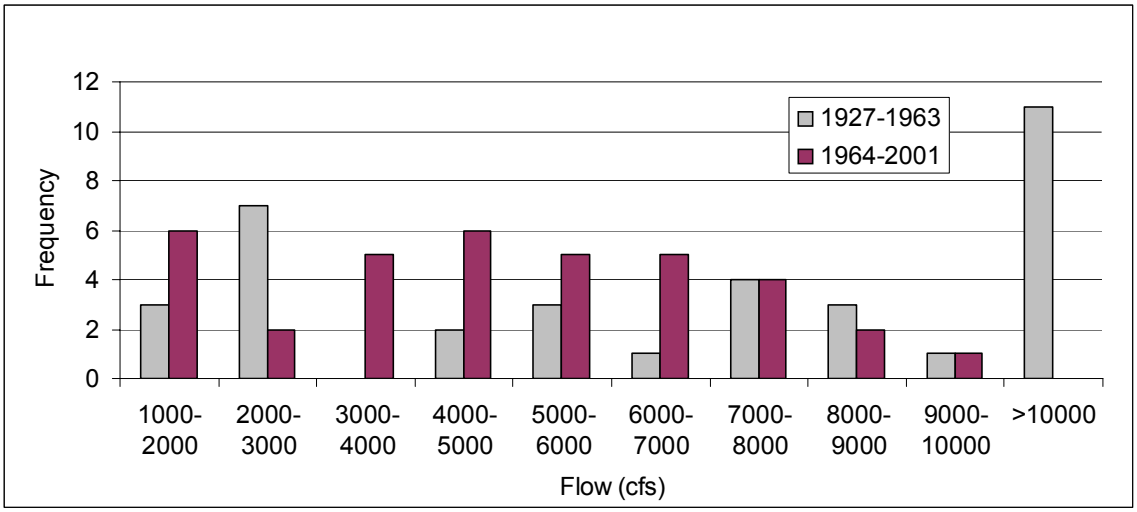

Figure 2-9 Maximum mean daily annual discharge histograms on the Rio Grande at San Felipe (1927 – 2001)

Besides flood regulation, climate changes seem to have a strong influence in the flow regime of the Rio Grande. Richard (2001) observed that the magnitude of the annual peak flows at Otowi and Cochiti gage declined with time since 1895, prior to the construction of main dams in the Rio Grande system. Cochiti gage data show a dry period from about 1942 to about 1978 (Richard 2001). Richard (2001) also determined that peak flows between 1943 and 1973 (pre-Cochiti dam) are not statistically different from those between 1974 and 1996 (post-Cochiti dam).

Molnár (2001) analyzed trends in precipitation and streamflow in the Rio Puerco, one of the largest tributary arroyos of the Rio Grande downstream from the Bernalillo Bridge reach. He concluded that statistically significant increasing trend in precipitation in the basin at the annual timescale occurred between 1948 and 1997. This increase is due to increases in non-summer precipitation, in particular in the frequency and intensity of moderate rainfall events (Molnár 2001). Molnár also concluded that there is a strong relationship between the long-term precipitation trends in the Rio Puerco Basin and the sea surface temperature anomalies in the Northern Pacific (Molnár 2001).

Also, annual maximum precipitation events seem to produce lower annual maximum runoff events in the last 50 years, most likely due to vegetation cover and hydraulic characteristics of the basin (Molnár 2001). Even though this type of analysis has not been performed in other sub-basins of the Rio Grande other than the Rio Puerco Basin, it is likely that the same trends occur in nearby areas along the Rio Grande.

3 GEOMORPHIC CHARACTERIZATION

3.1 METHODS

Channel Classification

Current channel pattern was qualitatively described from the 2001 set of aerial photos. In addition, qualitative descriptions of the non-vegetated channel planform were performed from the GIS coverages from 1918 to 2001.

Several channel classification methods were applied to the study reach to characterize the spatial and temporal trend of the channel planform. These methods are based on different concepts, such as slope-discharge relationships, channel morphology and unit stream power. The following methods were computed for the study reach: Leopold and Wolman (1957), Lane (1957, from Richardson et al. 1990), Henderson (1963, from Henderson 1966), Ackers and Charlton (1970, from Ackers 1982), Schumm and Khan (1972), Rosgen (1996), Parker (1976), Van den Berg (1995), Knighton and Nanson (1993) and Chang (1979).

The methods that incorporate slope-discharge relationships are as follows:

Leopold and Wolman (1957) classify channel planform as meandering, braided and straight based on a slope-discharge relationship. The criterion $S_o = 0.06\ Q^{-0.44}$ distinguishes between braided and meandering rivers. Q is the bankfull discharge in cfs and S_o is the channel slope in ft/ft. Straight channels (sinuosity (thalweg length to valley length) < 1.5) have slopes above and below the discriminator. In other words, straight channels occur throughout the range of slopes. They define meandering as channels with sinuosity > 1.5. Braiding refers to channels with relatively stable alluvial islands.

Lane (1957, from Richardson et al. 1990) also proposed a slope-discharge relationship to discriminate meandering from braided channel patterns. The relationship between mean discharge in cfs and slope in ft/ft in sand bed rivers is $SQ^{0.25} = K$. When $SQ^{0.25} \leq 0.0017$ the sand bed channel is considered to be meandering and when $SQ^{0.25} \geq 0.010$ the sand bed channel is considered braided. Between these two values the channel is classified as intermediate sand bed stream.

Henderson (1963, from Henderson 1966) incorporated bed material into Leopold and Wolman's slope-discharge relationship to describe channel pattern. Plotting the ratio of $S/0.06Q^{-0.44}$

against median bed size d (in feet), the following discriminator was proposed:

$$S = 0.64d^{1.14}Q^{0.44}$$

Two-thirds of the data points representing straight or meandering channels fell close to the line of distinction. All braided channels had S values that were substantially greater than indicated by the equation.

Ackers and Charlton (1979, Ackers 1982) proposed slope-discharge relationships to distinguish straight channels from straight channels with alternating bars and meandering channels. These relationships are as follows:

- Straight channels:

  $S < 0.001Q^{-0.12}$

- Straight channels with alternating bars:

  $0.001Q^{-0.12} < S < 0.0014Q^{-0.12}$

- Meanders develop if:

  $S_v > 0.0014Q^{-0.12}$

In these relationships S is the water surface slope (m/m) along a straight axial line for straight channels and channels with prominent shoals, S_v is the straight line slope (m/m) for meandered channels and Q is the water discharge (m^3/s).

It was later discovered by Ackers (1982) that a straight line of the form $S_v = 0.0008\ Q^{-0.21}$ separates the straight and meandered data of sand-bed rivers and canals.

Schumm and Khan (1972) proposed the following valley slope thresholds to define channel pattern:

- Straight $S < 0.0026$
- Meandering thalweg $0.0026 < S < 0.016$
- Braided $S > 0.016$

In these distinctions S is the valley slope (ft/ft).

The methods that are based on channel morphology are as follows:

Rosgen (1996) classified rivers based on channel morphology and sediment characteristics. Classification is determined from slope, entrenchment, sinuosity, width-depth ratio and bed material.

Parker (1976) indicates that rivers with sediment transport and depth to width ratio (d_o/B) << 1 at formative discharge have a tendency toward meandering or braiding. His classification is based on the relative magnitude of the depth-width ratio to the channel slope-Froude number ratio (S/F). Meandering occurs when S/F << d_o/B, braiding occurs for S/F >> d_o/B and transition between the two occurs when S/F ~ d_o/B.

The methods based on the concept of stream power are as follows:

Van den Berg (1995) proposed a discriminator between braided and single-thread channels with sinuosity larger than 1.3 that is based on potential specific stream power and bed material size. The discriminator is defined as:

$$\omega_{v,t} = 900 \cdot D_{50}^{0.42} \qquad \text{Eq. 1}$$

$\omega_{v,bf}$ = potential specific stream power, for sand-bed:

$$\omega_{v,bf} = 2.1 \cdot S_v \sqrt{Q_{bf}} \ \ (kW/m^2)$$

$\omega_{v,bf}$ = potential specific stream power, for gravel-bed:

$$\omega_{v,bf} = 3.3 \cdot S_v \sqrt{Q_{bf}} \ \ (kW/m^2)$$

In these relationships Q_{bf} is the bankfull discharge (m^3/s), D_{50} is the median grain size (mm) and S_v is the Valley slope (m/m).

Straight, single-thread rivers with sinuosity < 1.3 plot on both sides of the discriminator. Low stream power straight channels generally have a much smaller width-depth ratio than high stream power channels. Plotting the ratio of measured to reference bankfull channel width ($w=aQ_{bf}^b$ (Eq. 2)) against the ratio of potential specific stream power to the value of the discriminating function straight single thread channels can be classified as high or low energy channels. From the developed relationships Van den Berg established the following criteria:

- If $\frac{\omega_{v,bf}}{\omega_{v,t}} > 1$ the channel pattern corresponds to low sinuosity single-thread and multi-thread channel.
- If $\frac{\omega_{v,bf}}{\omega_{v,t}} < 1$ the river is a single-thread channel (see Figure 3-1).

- If measure to reference width ratio > 1 the river is a high energy wide channel (see Figure 3-1).
- If measure to reference width ratio < 1 the river is a low energy narrow channel (see Figure 3-1).

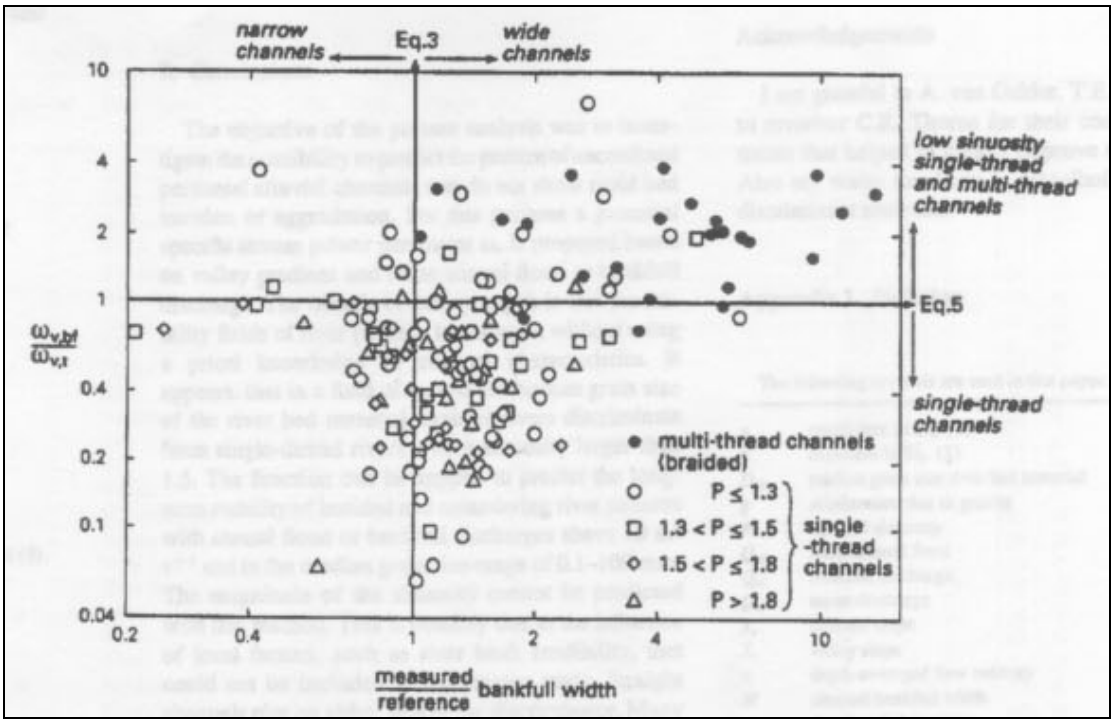

Figure 3-1 Channel pattern, width/depth ratio and potential specific stream power relative to reference values, as defined by Eqs. 1 and 2 (after van den Berg 1995)

Knighton and Nanson (1993) defined channel pattern in terms of the following three variables:

- Flow strength
- Bank erodibility
- Relative sediment supply: rate at which material is supplied either from bank erosion or from upstream relative to the rate it is transported downstream.

This classification is based on the continuum from straight to meandering to braided corresponding to increases in the three variables listed above. Flow strength can be defined through specific stream power, total power, or shear stress. Bank erodibility could be estimated by the silt-clay content of the bank material.

Knighton and Nanson (1993) do not quantify thresholds for these variables, but rather expressed the continuum concept on the following ordinal scale:

LOW (L)	**FLOW STRENGTH**	**HIGH (H)**
	----------→	
Straight	*Meandering*	*Braided*
LOW (L)	BANK ERODIBILITY	**HIGH (H)**
	----------→	
Straight	*Meandering*	*Braided*
LOW (L)	**RELATIVE SEDIMENT SUPPLY RATE**	**HIGH (H)**
	----------→	
Straight	*Meandering*	*Braided*

In order to apply this method to the Bernallilio Bredge Reach, changes in flow strength were evaluated as changes in water discharge (Chapter 4). Changes in bank erodibility were considered as changes in channel width (Chapter 3) and changes in sediment supply rate as the changes in suspended sediment with time (Chapter 4).

Chang (1979) classifies channel patterns based on stream power and slope-discharge relationships. For a given water and sediment discharge, a stable channel geometry and slope correspond to a minimum stream power per unit channel length. For small values of water and sediment discharge a unique minimum exists and therefore a unique stable channel configuration and slope (Chang 1979). When this unique stable channel slope equals the valley slope, the channel pattern is straight (Chang 1979). Above a certain threshold valley slope the stream power has two minimums, indicating two possible stable channel configurations and slopes (Chang 1979). Highly sinuous rivers, with small width-depth ratios occur on flatter valley slopes and they become braided and less sinuous as the valley slope increases (Chang 1979). Figure 3-2 shows Chang's (1979) channel pattern diagram.

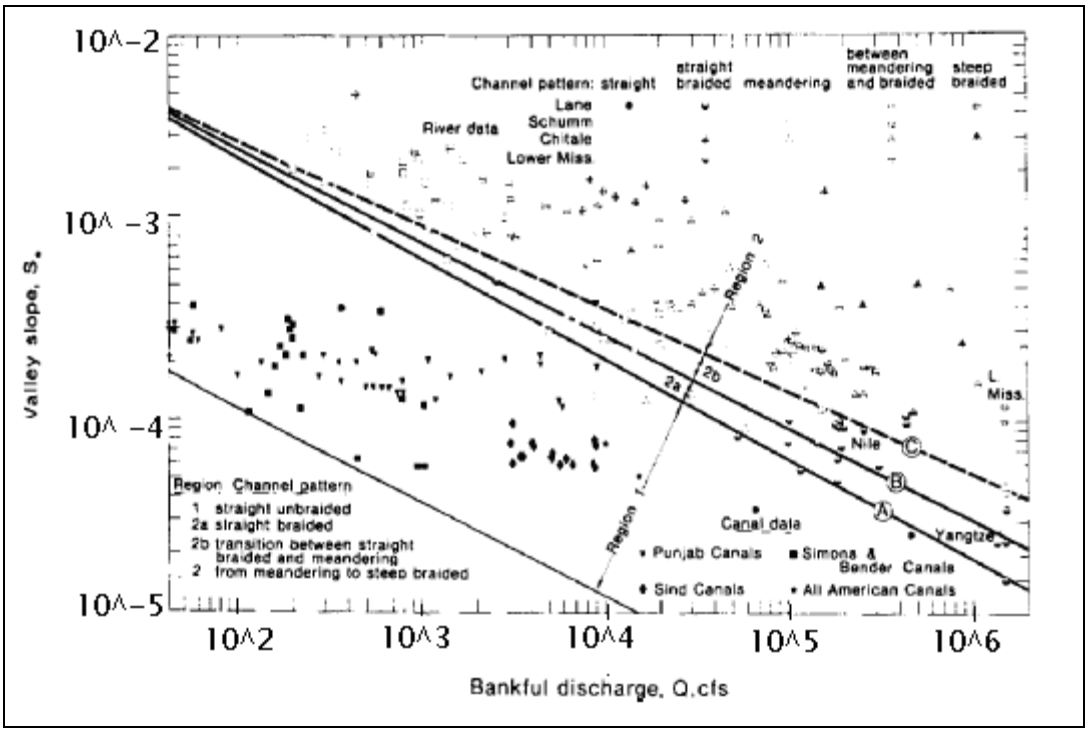

Figure 3-2 Channel patterns of sand streams (after Chang 1979)

Sinuosity

The sinuosity of the study reach and subreaches were estimated as the ratio of the channel thalweg length to the valley length. Reclamation's GIS and Remote Sensing Group in Denver, CO digitized the channel thalweg and measured valley lengths from aerial photos and topographic maps. The thalweg length was used as the active channel length in the sinuosity computations. Identification of the channel length is subject to the quality of the photos and surveys.

Valley Slope

Valley slopes were estimated as the ratio of the difference of valley elevations between the upper and lower end of the reach to the valley length. Valley elevations were estimated from the agg/deg data. Agg/deg data contains elevation data outside of the main channel. Averaged elevations of those areas were computed and considered as valley elevations. There are not agg/deg data available for 1998 or 2001. Therefore, the valley slope could not be estimated for these years. The valley slope for 2001 was determined through using the CO-line cross sectional data from 1998. Reclamation's GIS and Remote Sensing Group, Denver, CO measured valley lengths from aerial photos and topographic maps. Valley slope values were

used as input to some of the channel classification methods as described in the Channel Classification section.

Longitudinal Profile

Thalweg Elevation

The thalweg elevation is the lowest elevation in a channel cross section. The photogrammetrically surveyed agg/deg lines are available for 1962, 1972 and 1992, but are not available for 2001. Consequently, the only available thalweg elevation data for the Bernalillo Bridge Reach in 2001 are the BB-lines and CR-lines for the survey dates listed in Table 2-5 and the CO-lines for the survey dates listed in Table 2-6. Changes in the thalweg elevation with time for each CO cross section were plotted to identify temporal trends in the thalweg elevation at these four locations.

Mean Bed Elevation

Longitudinal profiles were plotted for the study reach for the years of 1962, 1972, 1992 and 1998. The profiles for the first three sets of years were generated from the agg/deg data. The longitudinal profile for 2001 was generated from the CO, BI, and CR data and plotted together with the agg/deg line longitudinal profiles. All profiles were generated using the same methodology. Parameters calculated from the U.S. Army Corps of Engineers' Hydrologic Engineering Center-River Analysis System (HEC-RAS) version 3.1 program (USACE 1998) were utilized in this methodology. The HEC-RAS runs that were executed using the channel forming discharge (5,000 cfs). To calculate the mean bed elevation (MBE), the following equation was used:

$$MBE = WSE - \frac{A}{Tw} = WSE - h$$

In this equation, WSE represents the water surface elevation (ft), A represents the channel area (ft^2), Tw represents the channel top width (ft) and h represents the hydraulic depth (ft) which is seen to be equivalent to the area-to-top width ratio.

Friction and Water Surface Slopes

The friction and water surface slopes were estimated at each cross section at a channel-forming discharge of 5,000 cfs using HEC-RAS. The slopes were then averaged over the reach

using a weighting factor equal to the sum of one half of the distances to each of the adjacent upstream and downstream cross-sections.

Channel Geometry

Two methods were used to describe the channel geometry characteristics of the study reach: 1) HEC-RAS model and 2) digitized aerial photo interpretation. HEC-RAS was used to model the channel geometry of the study reach with the available agg/deg line data for 1962, 1972 and 1992 and BB-line, CO-line and CR-line data for 2001. A total of 53 agg/deg cross sections spaced approximately 500 feet apart, were modeled. The model for 2001 was performed with seven BB-lines together with five CO-lines and three CR-lines, spaced about 500 feet to 3,500 feet apart. Channel-forming discharge of 5,000 cfs was routing through the reach. HEC-RAS was not calibrated. A Manning's n value of 0.02 was used for the channel and 0.1 for the floodplain for the simulations of the years 1962, 1972 and 1992. Manning's n of 0.032 was used for the channel bed for the simulation of the year 2001. The channel bed material is coarser in 2001 than before 1992. Therefore, the roughness coefficient was considered higher for the 2001 simulations. Main channel delineation was performed with the assistance of the aerial photos and cross-section surveys. Digitized aerial photos were used to measure the non-vegetated channel width at each agg/deg line.

The resulting channel geometry parameters at each cross section were then averaged over each subreach and the entire reach by using a weighting factor equal to the sum of one half of the distances to each of the adjacent upstream and downstream cross sections.

The following channel geometry parameters were computed:

Wetted Perimeter = P

Wetted Cross Section Area = A

Mean Flow Velocity = V = Q/A

where, Q = Flow discharge

Top Width = W

Mean Depth = h = A/W

Width-Depth ratio = W/h

Froude Number Fr = $V/\sqrt{gD}$, where D = A/W

Overbank Flow/Channel Capacity

The HEC-RAS results are divided into main channel flow and overbank flow. The main channel results were used for the analyses of this work, because this is where the majority of the sediment transport occurs.

Sediment

Bed Material

Characterization of the spatial and temporal variability of median bed material size (d_{50}) was performed for each subreach. Median grain sizes were computed for 1962, 1972, 1992 and 2001 from USGS gaging station, CO-line and BB-line data. Apparent temporal and spatial trends were noted. Table 3-1 lists the source of the bed material data used for the bed material subreach characterization, the 2001 sediment transport and equilibrium analysis, and hydraulic geometry computations.

Table 3-1 Source of bed material data used for the bed sediment subreach characterization and in the 2001 sediment transport and equilibrium analyses

	Subreach 1	Subreach 2	Subreach 3
1962	Bernalillo gage	Bernalillo gage	Bernalillo gage
1972	CO-30	CO-31 and 32	CO-33
1992	BI-296	CO-31	CO-33
2001	BB-301, BB-307	BB-318, BB-323, BB-327	BB-340, BB-345

Several samples were collected across each cross section. Average of the median bed material sizes (d_{50}) of all the samples collected in the bed of the channel at each station were performed to characterize the bed material of the subreaches. These averages were input into the channel classification methods (see Table 3-2). In addition, different statistics such as minimum, maximum and standard deviation of the median bed material sizes were computed at each station.

For the 2001 sediment transport and equilibrium analyses, bed material samples collected at BB-lines were used to determine the grain size distributions for each subreach (Table 3-1). The arithmetic averages of the values of percentages finer than a given size were computed to generate the average curves (Nordin et. al 1961).

3.2 Results

Channel Classification

Historic and Current Channel Pattern Description

Historically, the Middle Rio Grande was a relatively straight, braided and aggrading channel (Baird 1996). As a result of the aggradation trend, the Middle Rio Grande Conservancy District constructed a floodway along the river during the 1930 to 1936 period (Woodson and Martin 1962) to contain the river in its channel and prevent avulsions from forming in the adjacent areas (Sanchez et. al 1997). The levee system, constructed as a part of the floodway, was laid out to contain the pattern of the river prevailing at that time and no significant attempts were performed to straighten and shorten the channel (Woodson and Martin 1962). By the 1950's, the Rio Grande occupied a wide shallow channel between the levees of the floodway (Woodson and Martin 1962). The channel had no banks and the average level of the bed was above the elevation of the land outside the levees (Woodson and Martin 1962). After the major flood year of 1941, the levees were breached at 25 places and extensive flood damage was experienced (Woodson and Martin 1962). In 1948 the Corps of Engineers and the Bureau of Reclamation recommended the comprehensive plan of improvement for the Rio Grande in New Mexico (Woodson and Martin 1962). As a part of this plan rehabilitation of the floodway was performed and several jetty fields were placed along the floodway.

Figure 3-3 was produced from Reclamation's GIS coverages of the Bernalillo Bridge reach and represents the changes in river planform that occurred in the non-vegetated active channel in 1918, 1935, 1962, 1992 and 2001. It is evident that the study reach planform has not experienced significant changes since 1935, except for subreach 1, which was confined to a single channel after removing the large vegetated island shown in the 1935 planform. The Bernalillo Bridge channel has been confined since the 1930's, after the Middle Rio Grande Conservancy District constructed the floodway along the river. Narrowing of the channel is evident in subreaches 1 and 2. Subreach 3 depicts almost no change since 1918. The greatest decrease in width for the entire reach occurs from 1918 to 1935.

The current channel pattern description is based on observation of the 2000 set of aerial photos, which were taken during the winter season (Figures 2-4, 2-5 and 2-6). At flows below bankfull (<5,000 cfs), the Bernalillo Bridge reach exhibits a multi channel pattern in some short reaches of subreaches 2. Vegetated bars lateral to the low flow channels are present in

subreach 1. Some vegetated bars within the channel are present in subreach 2. Channel width is almost constant along the entire reach. According to the results from HEC-RAS, using the 2001 cross section data, most of the middle channel bars in subreaches 1 and 2 are not under water at discharge equal to 5,000 cfs.

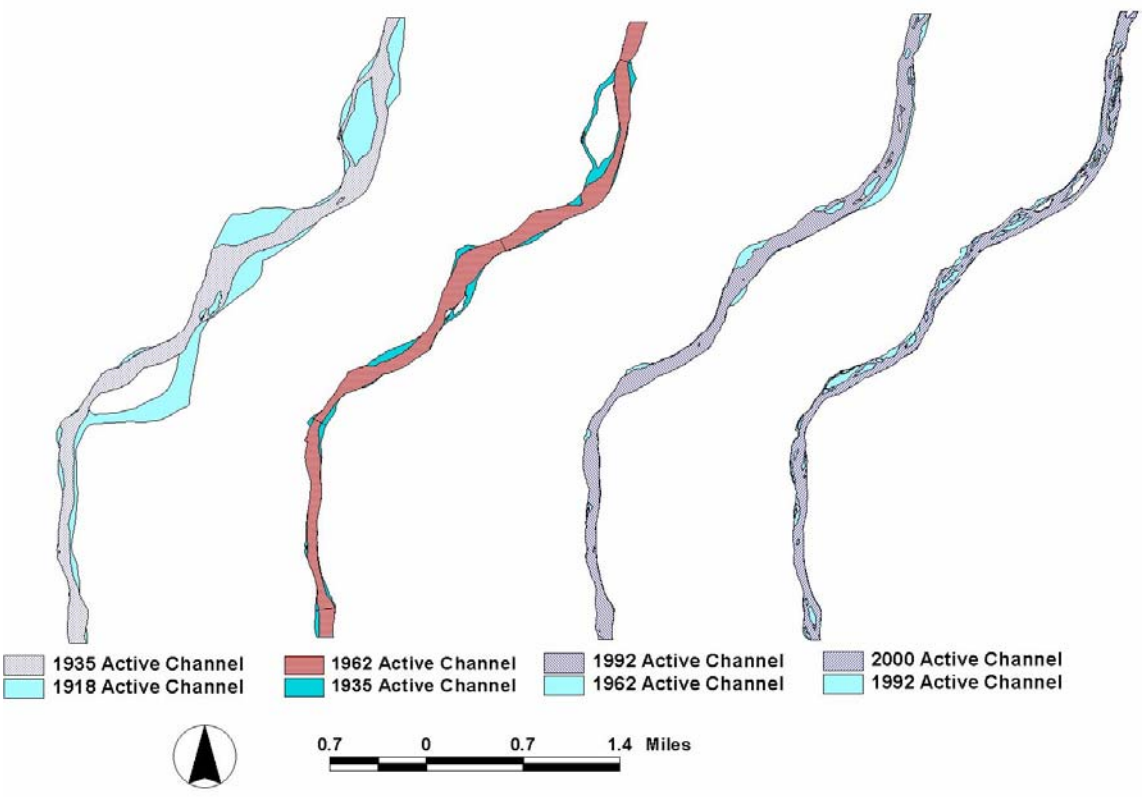

Figure 3-3 Non-vegetated active channel of the Bernalillo Bridge reach. 1918 planform from topographic survey. 1935, 1962,1992 and 2001 planform from aerial photos

The values of the input parameters for the different channel classification methods applied to the 1962, 1972, 1992 and 2001 surveys of the Bernalillo Bridge reach are in Table 3-2. These methods produce descriptions of the channel that range from straight to meandering and braided (Table 3-3 and Table 3-4).

Table 3-2 Input Parameters for Channel Classification Methods

1962	Q (cfs)	Channel Slope (ft/ft)	Valley Slope (ft/ft)	d50 (mm)	d50 (ft)	Width (ft) from Hec-Ras	Depth (ft)	Velocity (ft/s)	Fr	EG Slope (ft/ft)
1	5,000	0.0007	0.0009	0.21	0.000689	595	2.36	3.89	0.44	0.0009
2	5,000	0.0008	0.0011	0.21	0.000689	586	2.38	3.99	0.46	0.0010
3	5,000	0.0010	0.0007	0.21	0.000689	432	2.74	4.35	0.47	0.0010
Total	5,000	0.0008	0.0009	0.21	0.000689	546	2.48	4.05	0.46	0.0009
1972										
1	5,000	0.0009	0.0011	0.21	0.000689	641	3.38	2.60	0.30	0.0006
2	5,000	0.0009	0.0010	0.21	0.000689	595	2.29	3.80	0.45	0.0010
3	5,000	0.0010	0.0007	0.24	0.000787	446	2.50	4.43	0.50	0.0012
Total	5,000	0.0009	0.0010	0.22	0.000722	574	2.74	3.50	0.40	0.0008
1992										
1	5,000	0.0008	0.0009	1.38	0.004528	565	2.34	3.86	0.45	0.0009
2	5,000	0.0011	0.0011	1.09	0.003576	501	2.56	4.17	0.46	0.0010
3	5,000	0.0007	0.0005	5.73	0.018799	418	2.75	4.58	0.50	0.0012
Total	5,000	0.0009	0.0009	2.73	0.008968	501	2.52	4.20	0.47	0.0010
2001										
1	5,000	0.0011	0.0009	15.43	0.050607	560	3.12	2.95	0.29	0.0009
2	5,000	0.0008	0.0011	11.29	0.037041	421	3.79	3.37	0.31	0.0009
3	5,000	0.0008	0.0005	1.24	0.004060	546	3.17	3.01	0.30	0.0009
Total	5,000	0.0008	0.0009	9.32	0.030569	504	3.38	3.12	0.27	0.0009

The methods based on slope-discharge relationships (Leopold and Wolman 1957, Lane 1957 - from Richarson et al. 1990, Henderson 1963 - from Henderson 1966, Ackers and Charlton 1970 - from Ackers 1982, Schumm and Khan 1972) produced varying results. Leopold and Wolman (1957), Lane (from Richardson et. al 1990), Henderson (from Henderson 1966) and Schumm and Khan (1972) methods do not show any spatial and temporal planform trend, since they predict the same pattern for the entire reach for all years. Leopold and Wolman's (1957) and Schumm and Khan's (1972) methods yield a straight channel planform. Henderson's (1963) method predicts a braided planform and Lane's (1957) method predicts an intermediate channel. Ackers and Charlton's (1970) classification system (when comparing with valley slope) produces a meandering pattern for subreaches 1 and 2 for all the years, a straight channel with alternating bars configuration for subreach 3 for 1962 and 1972 and a straight channel for 1992 and 2001.

Rosgen's (1996) and Parker's (1976) classification systems are based on channel morphology variables. According to Rosgen's method, the Bernalillo Bridge Reach best fits as a D5c for 1962 and 1972 and D4c for 1992 and 2001. The D5c is a multiple-channel with very high width-depth ratio (> 40), low sinuosity (<1.2), slope < 0.001 and sand bed. The D4c has the same configuration as the D5c except for the gravel bed material. Typically D5c streams are characterized by a braided pattern, a channel slope that approximates the valley slope and high bank erosion rates. Using Parker's (1976) method, the entire reach is classified as

meandering for all years. Prior to 1992, subreach 1 classifies as meandering with three to ten braids.

Van den Berg's (1995) method, which is based on stream power, classifies the Bernalillo Bridge Reach as high energy single thread wide channel in 1962 and 1972, and as a low stream power single thread narrow channel in 1992 and 2001. Chang's (1979) method, which is also based on stream power as well, yields a meandering to steep braided channel planform for the entire reach for all the years. All the subreaches plot above the line C in Chang's diagram (see Chang's diagram in Section 3.1), which corresponds to region 2. According to Chang (1979), region 2 predicts that highly sinuous rivers with low width-depth ratios occur on flat valley slopes and as the valley slope increases, more braided and less sinuous channel patterns are predicted.

Knighton and Nanson (1993) do not quantify thresholds values for flow strength, bank erodibility and sediment supply. However, it is possible to interpret the change in these variables in the Bernalillo Bridge reach as follows: flow strength (peak water discharge) started to decrease before regulation of flows began in the middle Rio Grande basin, probably due to climatic changes and intensification of agricultural activities in the upper Rio Grande basin. According to Richard (2001) the magnitude of peak flows at Otowi and Cochiti gaging stations declined with time since 1895. Sediment supply rates (suspended sediment concentration at Albuquerque gage) have decreased since the closure of Cochiti Dam in 1973 (Richard 2001). Bank erodibility has decreased due to the construction of the floodway and other river works that control the lateral movement of the channel (Figure 3-3). A combination of these factors would indicate a likely shift from a braiding to meandering planform.

Table 3-3 Channel Pattern Classification for 1962 and 1972

Reach #	Slope-discharge						Channel Morphology		Stream Power	
	Leopold and Wolman	Lane	Henderson	Ackers & Charlton		Schumm & Khan	Rosgen	Parker	van den Berg	Chang
				Comparing with channel slope	Comparing with valley slope					
1962										
1	Straight	Intermediate	Braided	Straight w/alternating bars	Meandering	Straight	D5c	Meandering	High energy single thread wide channel	from meandering to steep braided
2	Straight	Intermediate	Braided	Meandering	Meandering	Straight	D5c	Meandering	High energy single thread wide channel	from meandering to steep braided
3	Straight	Intermediate	Braided	Meandering	Straight w/alternating bars	Straight	D5c	Meandering/3-10 Braids	High energy single thread wide channel	from meandering to steep braided
Total	Straight	Intermediate	Braided	Meandering	Meandering	Straight	D5c	Meandering	High energy single thread wide channel	from meandering to steep braided
1972										
1	Straight	Intermediate	Braided	Meandering	Meandering	Straight	D5c	Meandering	High energy single thread wide channel	from meandering to steep braided
2	Straight	Intermediate	Braided	Meandering	Meandering	Straight	D5c	Meandering	High energy single thread wide channel	from meandering to steep braided
3	Straight	Intermediate	Braided	Meandering	Straight w/alternating bars	Straight	D5	Meandering/3-10 Braids	High energy single thread wide channel	from meandering to steep braided
Total	Straight	Intermediate	Braided	Meandering	Meandering	Straight	D5c	Meandering	High energy single thread wide channel	from meandering to steep braided

Table 3-4 Channel Pattern Classification for 1992 and 2001

Reach #	Slope-discharge						Channel Morphology		Stream Power	
	Leopold and Wolman	Lane	Henderson	Ackers & Charlton		Schumm & Khan	Rosgen	Parker	van den Berg	Chang
				Comparing with channel slope	Comparing with valley slope					
1992										
1	Straight	Intermediate	Braided	Meandering	Meandering	Straight	D5c	Meandering	High energy single thread wide channel	from meandering to steep braided
2	Straight	Intermediate	Braided	Meandering	Meandering	Straight	D5	Meandering	Low stream power single thread narrow channel	from meandering to steep braided
3	Straight	Intermediate	Braided	Straight w/alternating bars	Straight	Straight	D4c	Meandering	Low stream power single thread narrow channel	from meandering to steep braided
Total	Straight	Intermediate	Braided	Meandering	Meandering	Straight	D4c	Meandering	Low stream power single thread narrow channel	from meandering to steep braided
2001										
1	Straight	Intermediate	Braided	Meandering	Meandering	Straight	D4	Meandering	Low stream power single thread narrow channel	from meandering to steep braided
2	Straight	Intermediate	Braided	Meandering	Meandering	Straight	D4c	Meandering	Low stream power single thread narrow channel	from meandering to steep braided
3	Straight	Intermediate	Braided	Meandering	Straight	Straight	D5c	Meandering	High energy single thread wide channel	from meandering to steep braided
Total	Straight	Intermediate	Braided	Meandering	Meandering	Straight	D4c	Meandering	Low stream power single thread narrow channel	from meandering to steep braided

Sinuosity

The sinuosity of the entire Bernalillo Bridge reach has remained close to 1.10 since 1918 (Figure 3-4). From 1918 to 1992, subreach 1 has decreased in sinuosity while subreaches 2 and 3 have increased in sinuosity. After 1962, the sinuosities of all three subreaches are similar and tend to a value close to 1.10. These results indicate that the channel is straight.

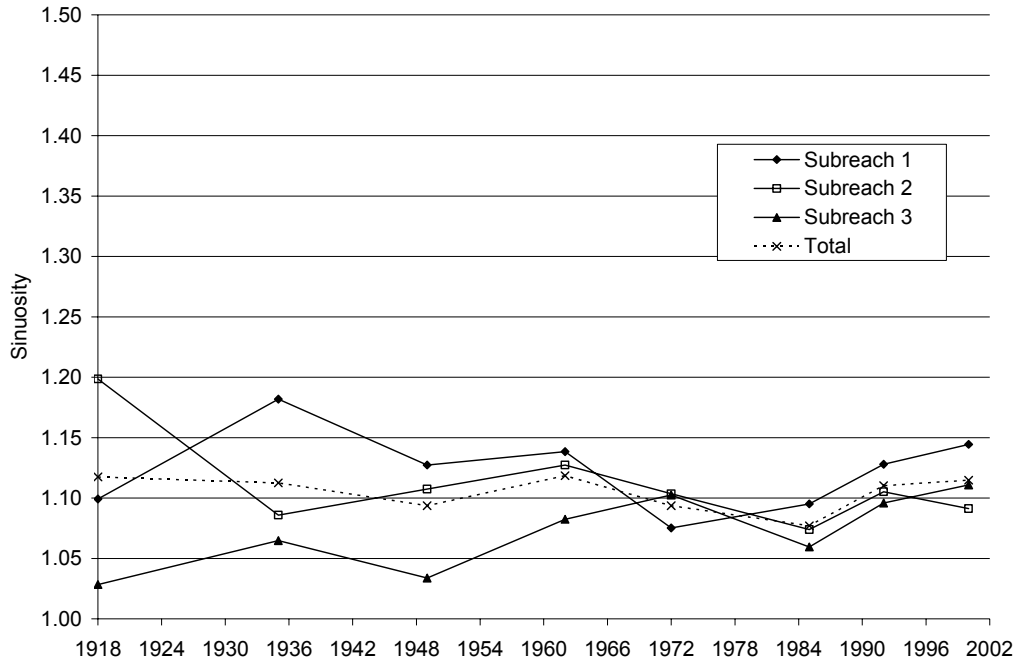

Figure 3-4 Time series of sinuosity of the Bernalillo Bridge Reach as measured from the digitized aerial photos by dividing the thalweg length by the valley length

Longitudinal Profile

Thalweg Elevation

Changes in thalweg elevation with time at each of the four CO-lines are presented in Figure 3-5. These surveys were collected at different times of the year and therefore at different points in the annual flow regime (Table 2-6). Most of the surveys from 1971 to 1986 were taken during winter and summer runoffs. Recent surveys were performed during early summer. It is expected to observe more degradation in the channel during the spring flows. The general trend is degradation at cross sections CO-30 and CO-31 since 1971. Cross sections CO-32 and CO-33 seems to have maintained almost the same thalweg elevation throughout the entire period analyzed.

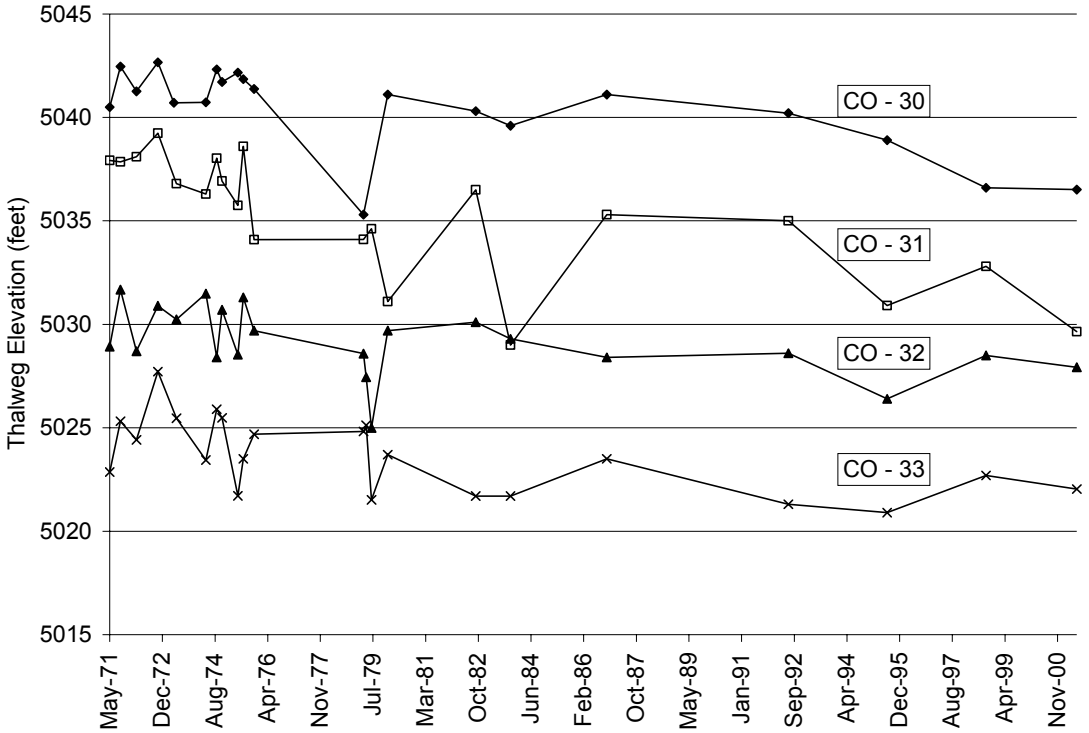

Figure 3-5 Change in thalweg elevation with time at the CO-lines

Mean Bed Elevation

Changes in mean bed elevation with time at the CO-lines are illustrated in Figure 3-6. The general trend is degradation of the bed since 1971. Mean bed elevations at cross sections CO-32 and CO-33 have not changed dramatically between 1986 and 1998.

Mean bed elevations from the agg/deg surveys show trends of aggradation between 1962 and 1972 and degradation between 1972 and 1992 (Figure 3-7). The degradation trend continues from 1992 to 2001 for subreach 1 while subreaches 2 and 3 aggraded (Figure 3-7). Table 3-5 summarizes the reach averaged bed elevations from the agg/deg surveys in the 1962-1972, 1972-1992 and 1962-1992 periods. Minimum amounts of aggradation and degradation occurred at the lower end of subreach 3.

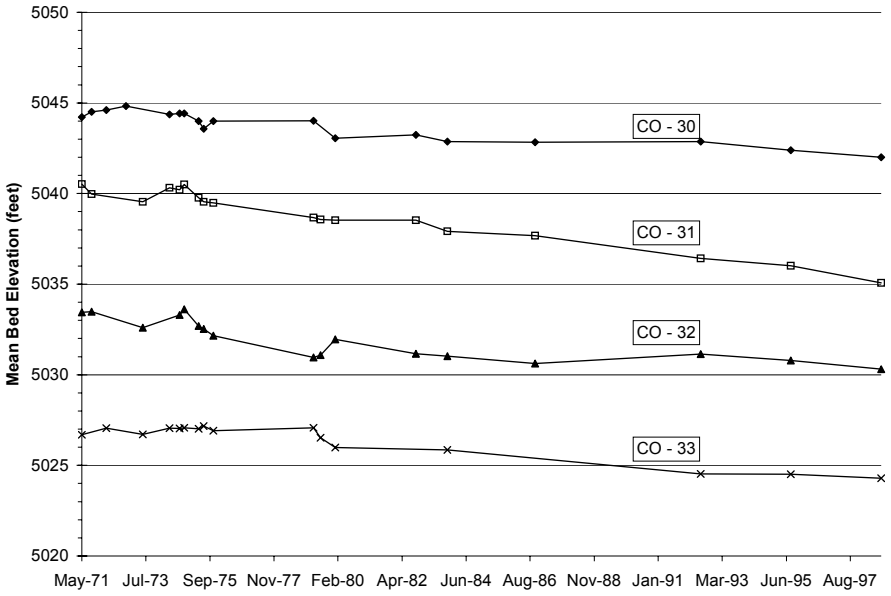

Figure 3-6 Change in mean bed elevation with time at CO-lines

Table 3-5 Reach averaged change in mean bed elevation in feet from agg/deg surveys.

Reach #	1962-72 Agg/Deg	1972-92 Agg/Deg	1962-92 Agg/Deg
1	1.52	-2.72	-1.20
2	1.24	-2.38	-1.14
3	1.33	-2.25	-0.92
Total	1.29	-2.55	-1.26

Longitudinal profiles of the mean bed elevations for 1962, 1972, 1992 and 2001 are presented in Figures 3-8 and 3-9. The entire reach portrayed a general aggradational trend upwards of 3 feet between 1962 and 1972 and a general degradational trend upwards of 5 feet from 1972 to 2001. The 1992 channel elevations are slightly lower than the 1962 elevations. A general trend of degradation of up to 2 feet occurred between 1992 and 2001 with subreach 3 displaying an opposite aggradational trend of approximately 1 foot during this time period (Figure 3-9).

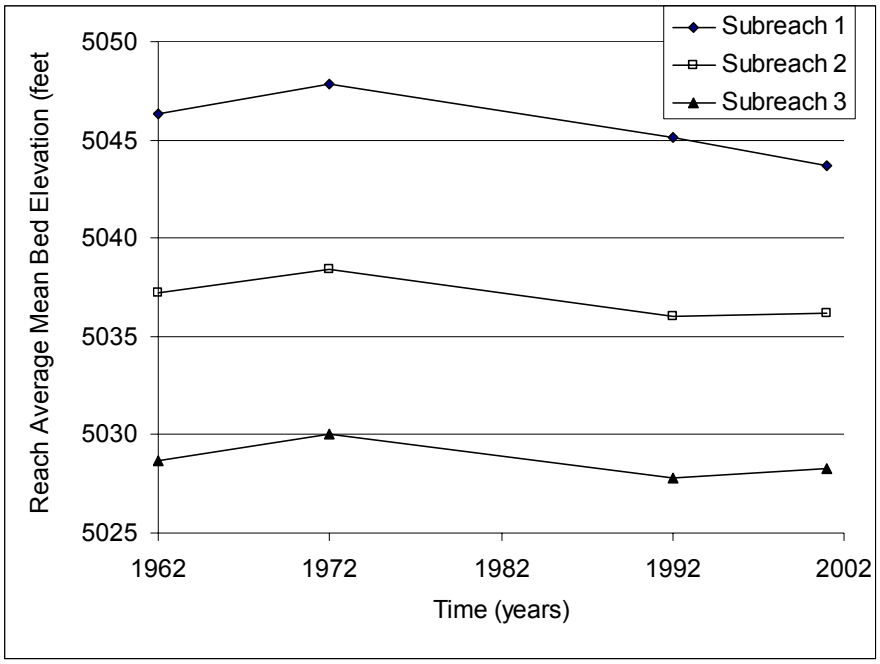

Figure 3-7 Time series of reach-averaged mean bed elevation, computed from the 1962, 1972 and 1992 agg/deg surveys and 2001 CO-line surveys.

Friction Slope

A time series of the friction slope is shown in Figure 3-10. The friction slopes in the entire reach and subreach 1 decreased from 1962 to 1972 and increased from 1972 to 1992. Subreach 2 maintained an almost constant slope from 1962 to 1992. The slope of subreach 3 increased from 1962 to 1992. The friction slope decreased in all the subreaches from 1992 to 2001. The slopes are the same in all the subreaches and are similar to the slopes in 1962.

Water Surface Slope

Figure 3-11 shows a time series of the water surface slope. From 1962 to 1972, the water surface slope increased in subreaches 1, 3 and in the entire reach, but decreased in subreach 2. From 1972 to 1992, the slope increased in subreaches 2, 3 and in the entire reach. Water surface slope in subreach 1 decreased and reached a value close to the 1962 slope. The slope decreased at all reaches from 1992 to 2001.

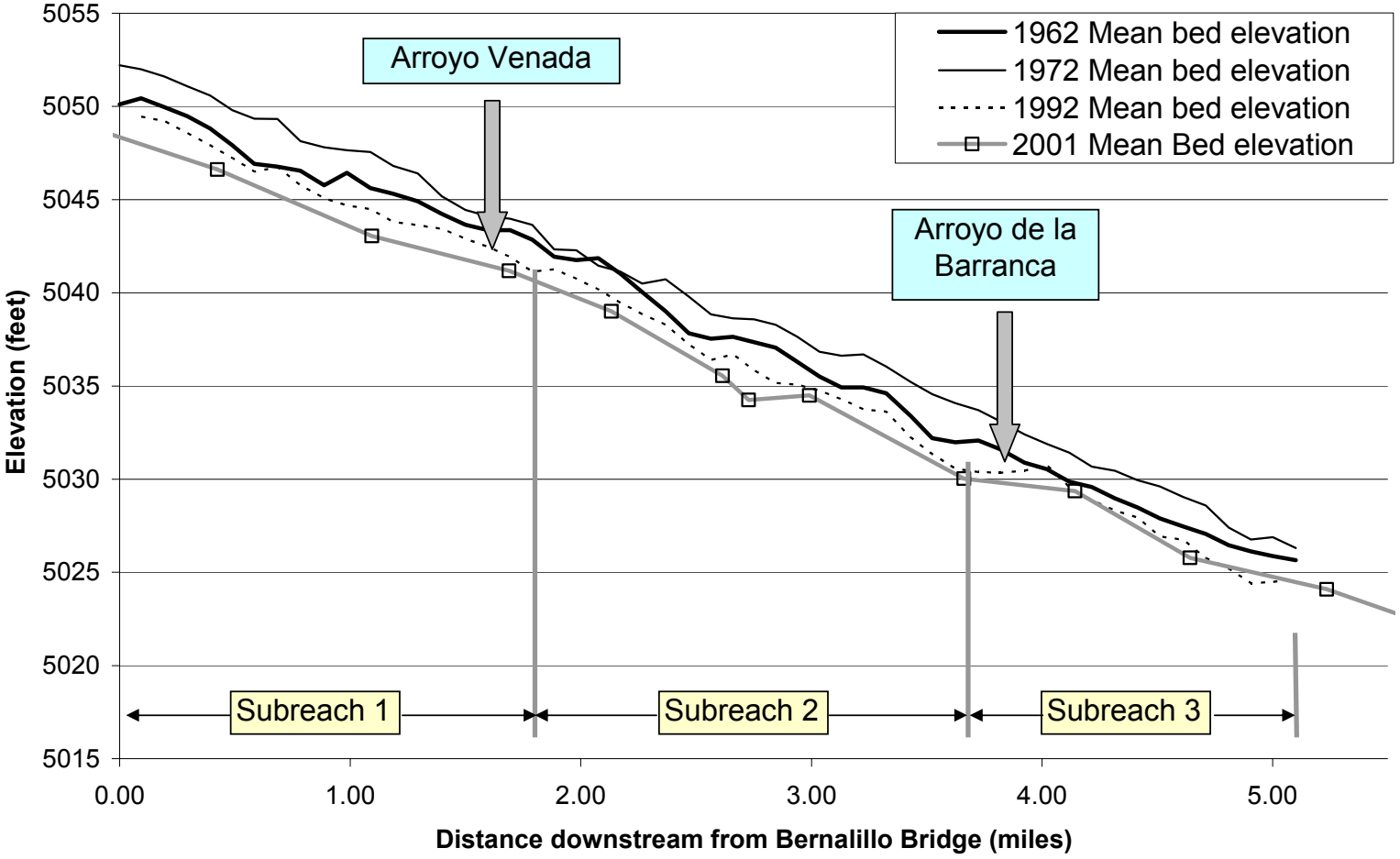

Figure 3-8 Mean Bed Elevation Profile of entire Bernalillo Bridge Reach for 1962,1972, 1992 and 2001. Distance downstream is measured from agg/deg 298.

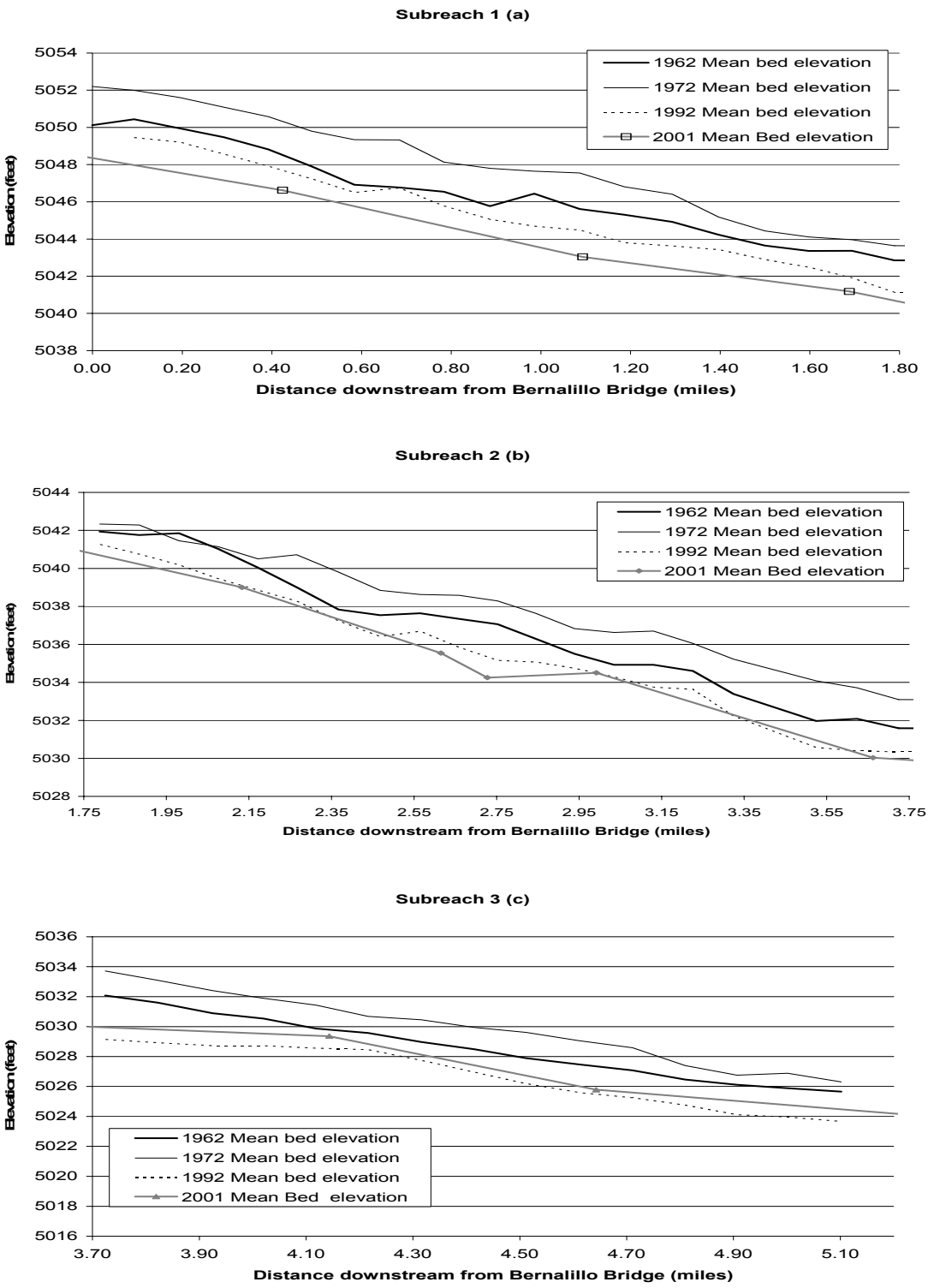

Figure 3-9 Mean bed elevation profiles of the subreaches from the agg/deg surveys of 1962,1972 and 1992. Thalweg elevation profile from CO-line surveys of 2001. (a) Subreach 1, (b) Subreach 2, (c) Subreach 3.

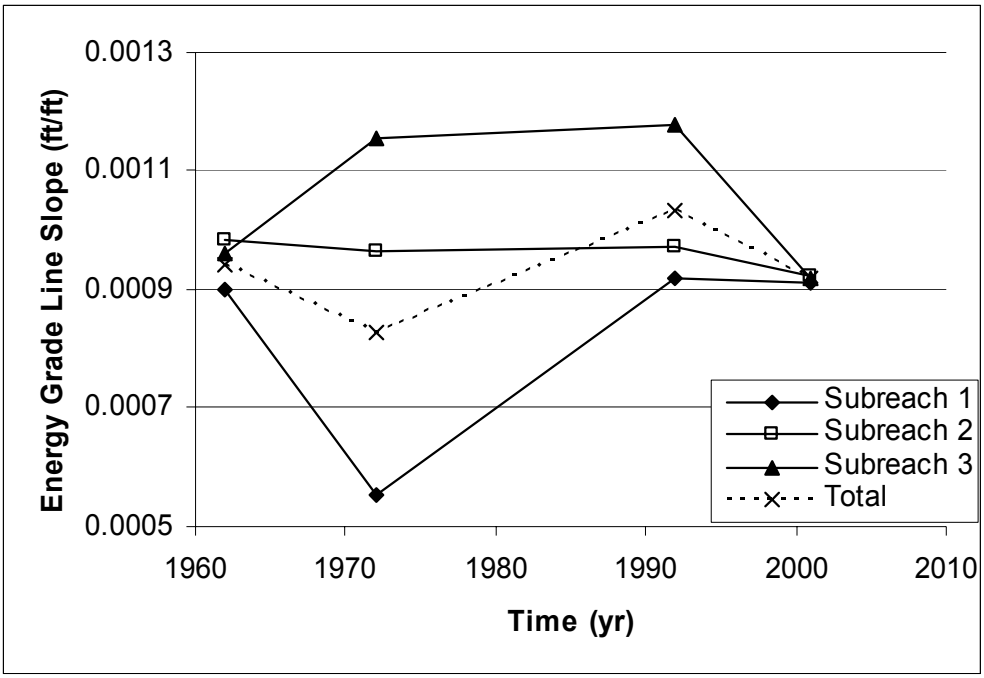

Figure 3-10 Time series of friction slope of the subreaches and the entire reach from HEC-RAS modeling results

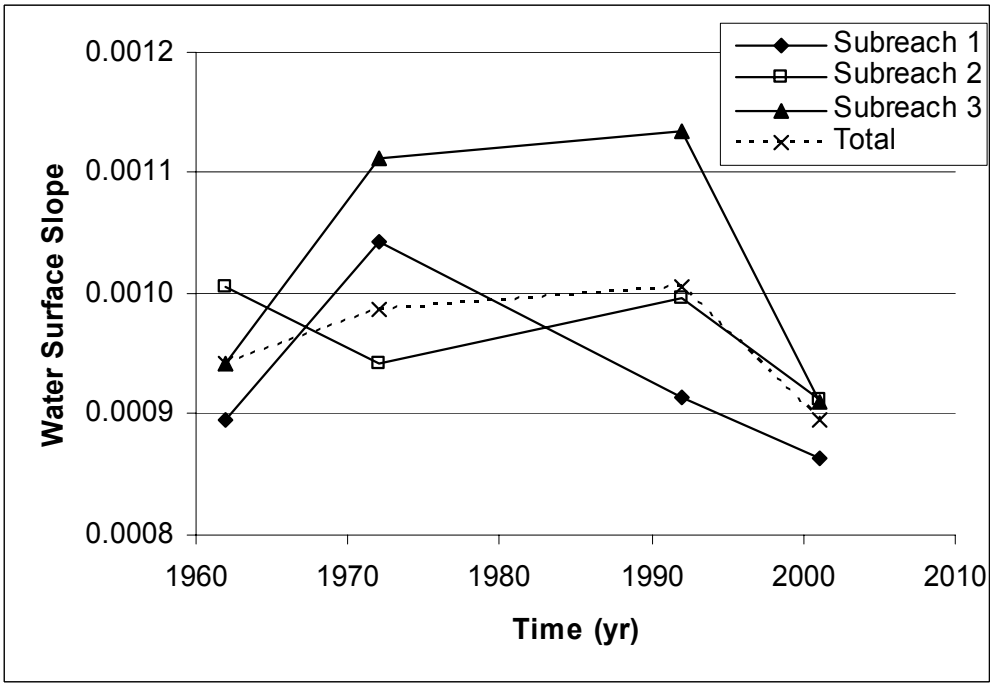

Figure 3-11 Time series of water surface slope (ft/ft) of the subreaches and the entire reach from HEC-RAS modeling results

Channel Geometry

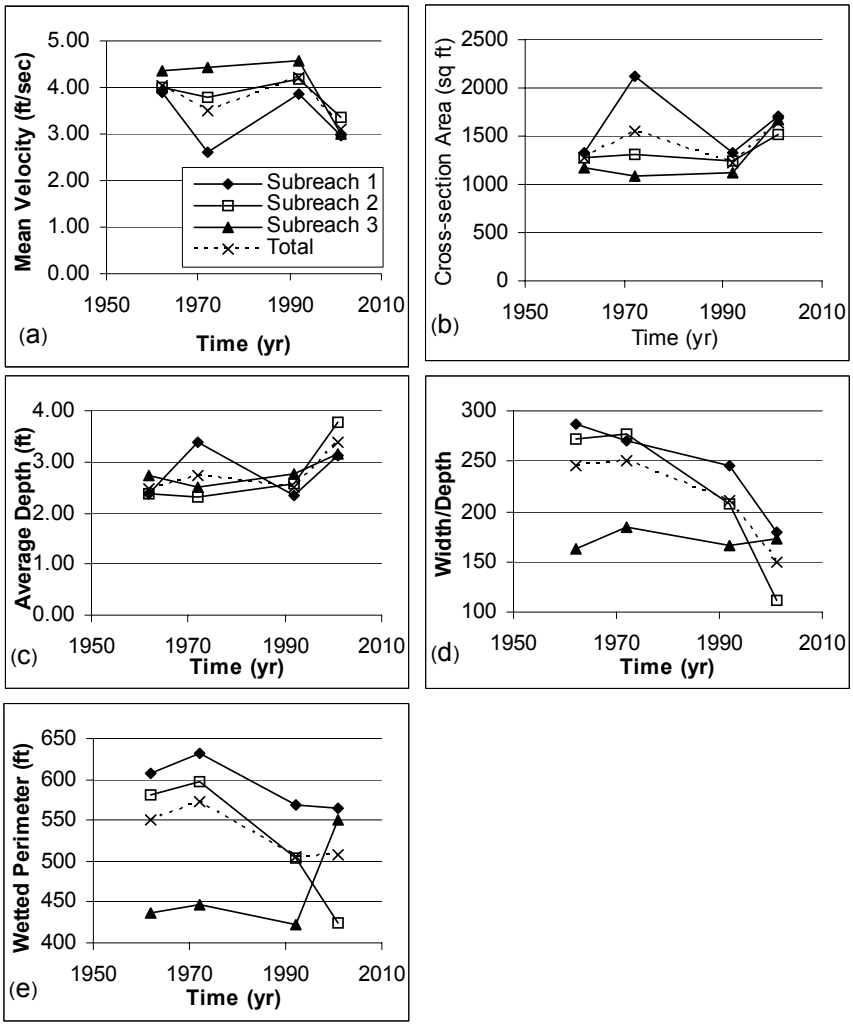

Figure 3-12 Reach-averaged main channel geometry from HEC-RAS results for Q = 5,000 cfs. (a) Mean Velocity, (b) Cross-section Area, (c) Average Depth, (d) Width-depth ratio, (e) Wetted Perimeter

The temporal changes in reach-averaged channel geometry are summarized in Figure 3-12. The changes in mean velocity, average depth, width-depth ratio and wetted perimeter generally are similar in subreaches 2 and 3 from 1962 to 1972 and from 1972 to 1992. Changes in mean velocity, width-depth ratio and wetted perimeter are similar in subreaches 1,2 and 3 from 1972 to 1992. The channel incised from 1992 to 2001, as evidenced by the increase in flow depth and decrease in width-depth ratio. Cross sectional area increased at all reaches during this period. Mean velocity decreased at all reaches as well, probably due to the increase in roughness.

Width

Active channel width time series from the digitized vegetation boundaries are presented in Figure 3-13. All of the reaches exhibit declining width with time. The width of subreach 1 slightly increases in 1972 and 1985. Subreach 3 appears to have leveled off from 1949 to 1992 while subreach 2 has consistently decreased since 1918. In general, the largest change in channel width occurred between 1918 and 1935. All reaches narrowed after 1992. The main-channel widths at 5,000 cfs obtained from HEC-RAS modeling exhibit almost no change between 1962 and 1992 and a slightly increase in 1972 for all reaches (Figure 3-14). The width of subreaches 1 and 2 decreased and the width of subreach 3 increased from 1992 to 2001.

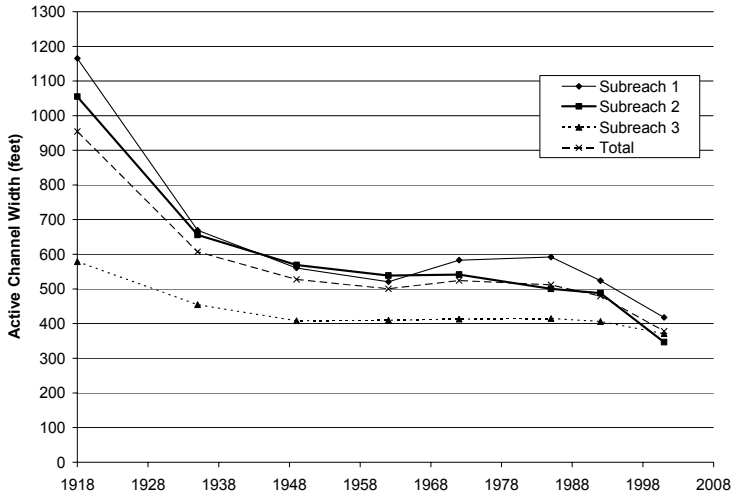

Figure 3-13 Reach averaged active channel width from digitized aerial photos

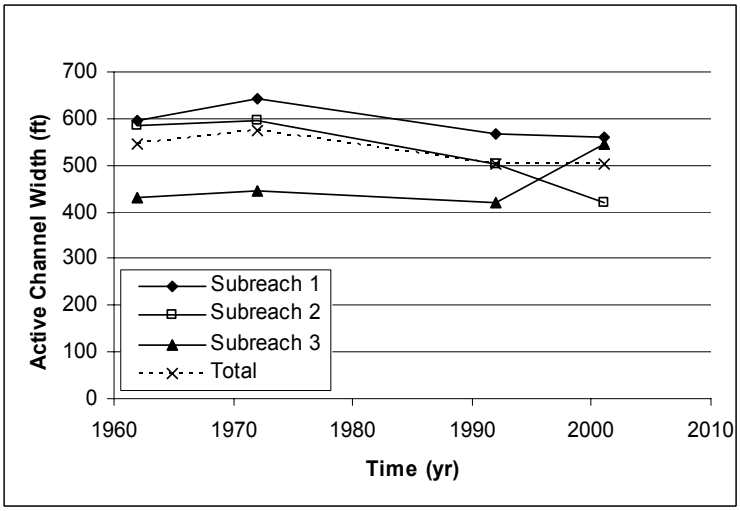

Figure 3-14 Reach averaged main channel width from HEC-RAS at Q =5,000 cfs

Overbank Flow/Channel Capacity

Most of the flow occurs in the main channel and not in the overbank region in 1962, 1992, and 2001 according to the HEC-RAS results at 5,000 cfs. This demonstrates the aggradational trend evident in the 1972 mean bed elevation profiles (Figures 3-8 and 3-9).

Sediment

Bed Material

The median grain sizes from the bed material samples at the Bernalillo gage are comprised of fine sand for all the subreaches for 1962. In 1972, CO-line samples report median sizes of fine sand for subreaches 1 and 2 and fine to medium sand for subreach 3. In 1992, the median size material is medium to very fine gravel for subreaches 1 and 2 and medium sand to coarse gravel in subreach 3. The median size material coarsens from 1992 to 2001. Table 3-6 summarizes these results.

Table 3-6 Range of median grain sizes in Subreaches 1, 2 and 3 for 1962, 1972, 1992 and 2001

	Median Bed Material Size		
	Subreach 1	**Subreach 2**	**Subreach 3**
1962	fine sand	fine sand	fine sand
1972	fine sand	fine sand	fine to medium sand
1992	medium to very fine gravel	medium to very fine gravel	medium sand to coarse gravel
2001	medium to coarse gravel	very coarse sand to coarse gravel	medium sand to very coarse sand

In general, it appears that the grain size coarsens with distance and time downstream from Bernalillo Bridge, probably due to sediment input from the Arroyo de la Barranca, between cross sections CO-32 and CO-33 from 1962 to 2001. The 2001 bed material is coarser than the 1992 bed material at reaches 1 and 2, and is finer at subreach 3. The average, maximum, minimum and standard deviation of the median bed material sizes at each station were computed for all the years. Table 3-7 summarizes these results.

Table 3-7 Median grain size statistics from the bed material samples at Bernalillo gage, CO-lines and BI-lines.

					d50					
Reach	Year	Station	Number of Observations	Range of flow discharges (cfs)	Minimum value (mm)	Maximum value (mm)	Mean value (mm)	Standard deviation (mm)	# of d50 in the sand range	# of d50 in the gravel range
Entire reach	1961	Bernalillo Gage	3	2140-3850	0.20	0.22	0.21	0.01	3	
Subreach 1	1972	CO-30	2	549-1070 (*)	0.18	0.21	0.20	0.02	2	
Subreach 2	1972	CO-31	2	549-1070 (*)	0.18	0.22	0.20	0.03	2	
Subreach 2	1972	CO-32	2	549-1070 (*)	0.20	0.20	0.20	0.00	2	
Average Subreach 2	1972	CO31, CO-32	4	549-1070 (*)	0.18	0.22	0.20	0.00	4	
Subreach 3	1972	CO-33	2	549-1070 (*)	0.19	0.27	0.23	0.060	2	
Subreach 1	1992	BI-296	5	3690 (*)	0.48	2.9	1.38	0.92	4	1
Subreach 2	1992	CO-31	5	517 (*)	0.46	2.20	1.09	0.76	4	1
Subreach 3	1992	CO-33	5	517 (*)	0.70	16.05	5.73	6.29	2	3
Subreach 1	2001	BI- 301, BI-307	2	No data	12.72	18.13	15.43	3.83	0	2
Subreach 2	2001	BI-318, BI-323, BI-327	3	No data	1.10	16.77	11.29	8.83	1	2
Subreach 3	2001	BI-340, BI-345	4	No data	0.46	1.85	1.24	0.58	4	0

(*) Rio Grande at Albuquerque gaging station

All of the median grain sizes (d_{50}) are in the sand range for 1961 and 1972. Some of the samples contain median grain sizes in the gravel range in 1992. Gravel sediment particles were surveyed at both high (3,690 cfs) and low (517 cfs) flows. Bed material sediment coarsened from 1992 to 2001 in subreaches 1 and 2 (Figures 3-15 and 3-16). Subreach 3 is the coarser reach in 1992. However, subreach 3 contains the finest sediment in 2001 (Figure 3-17).

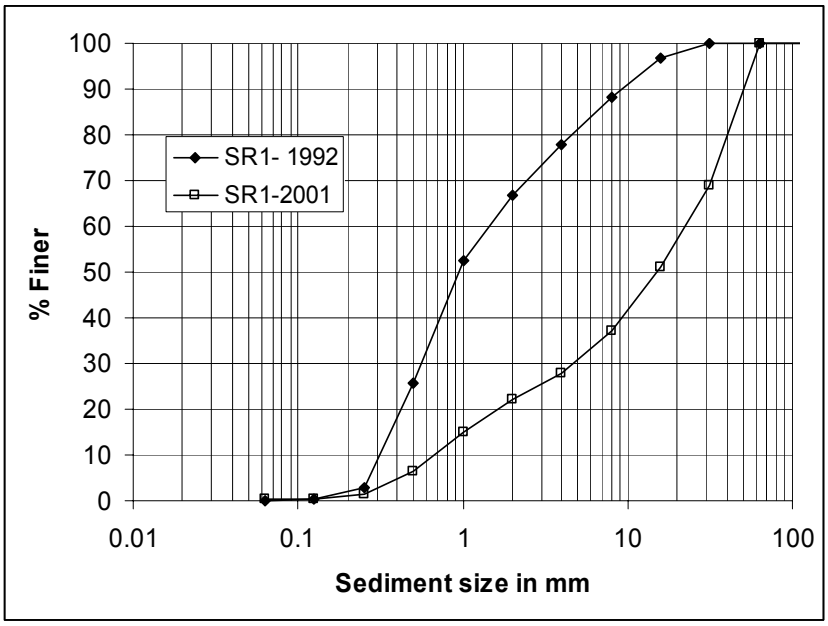

Figure 3-15 Comparison of 1992 and 2001 bed material gradation curves for subreach 1

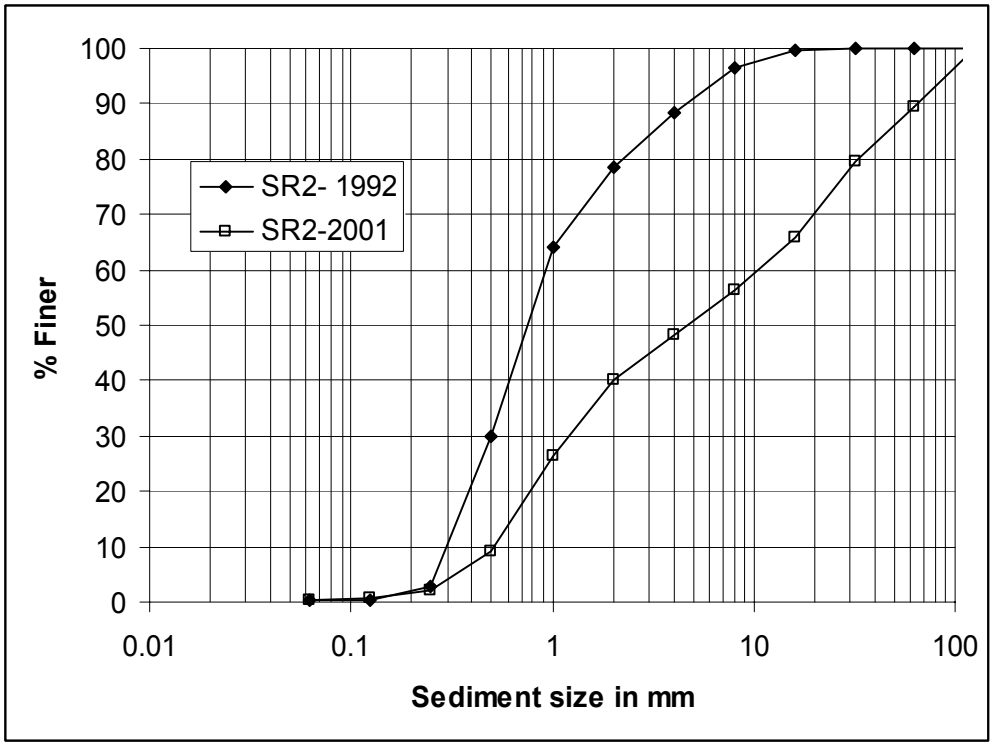

Figure 3-16 Comparison of 1992 and 2001 bed material gradation curves for subreach 2

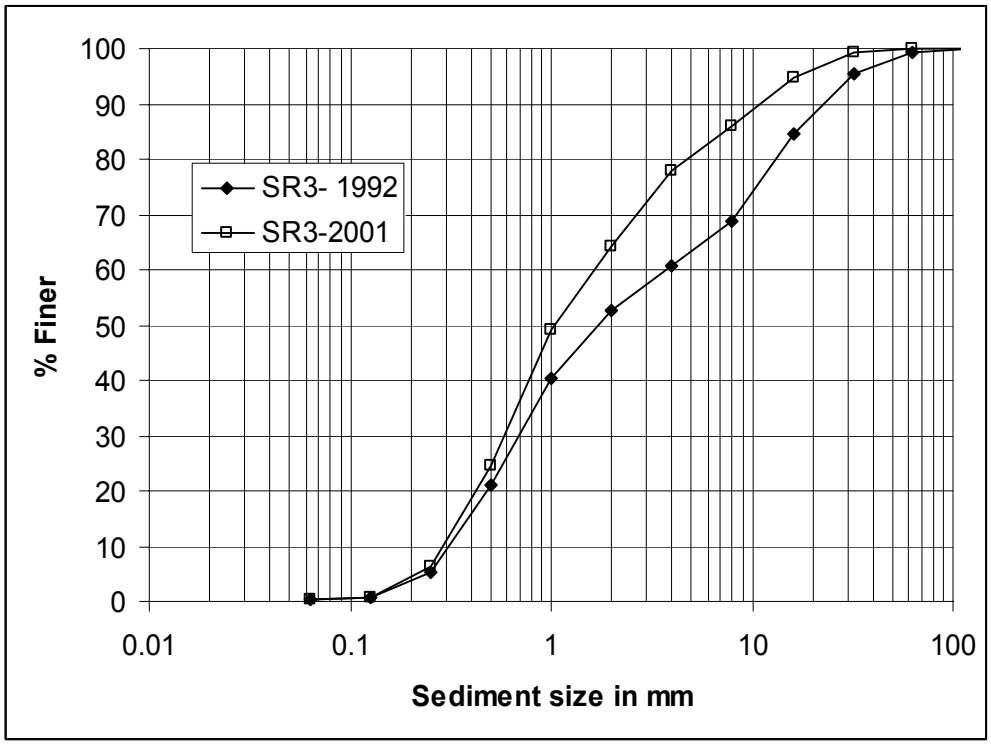

Figure 3-17 Comparison of 1992 and 2001 bed material gradation curves for subreach 3

Figure 3-18 shows the averaged bed material size distribution curves for each subreach and the entire reach for 2001. These curves are the input bed material data for the 2001 sediment transport and equilibrium analyses. The 1992 gradation curves in Figures 3-15 to 3-17 are also used in the sediment transport analysis for that year.

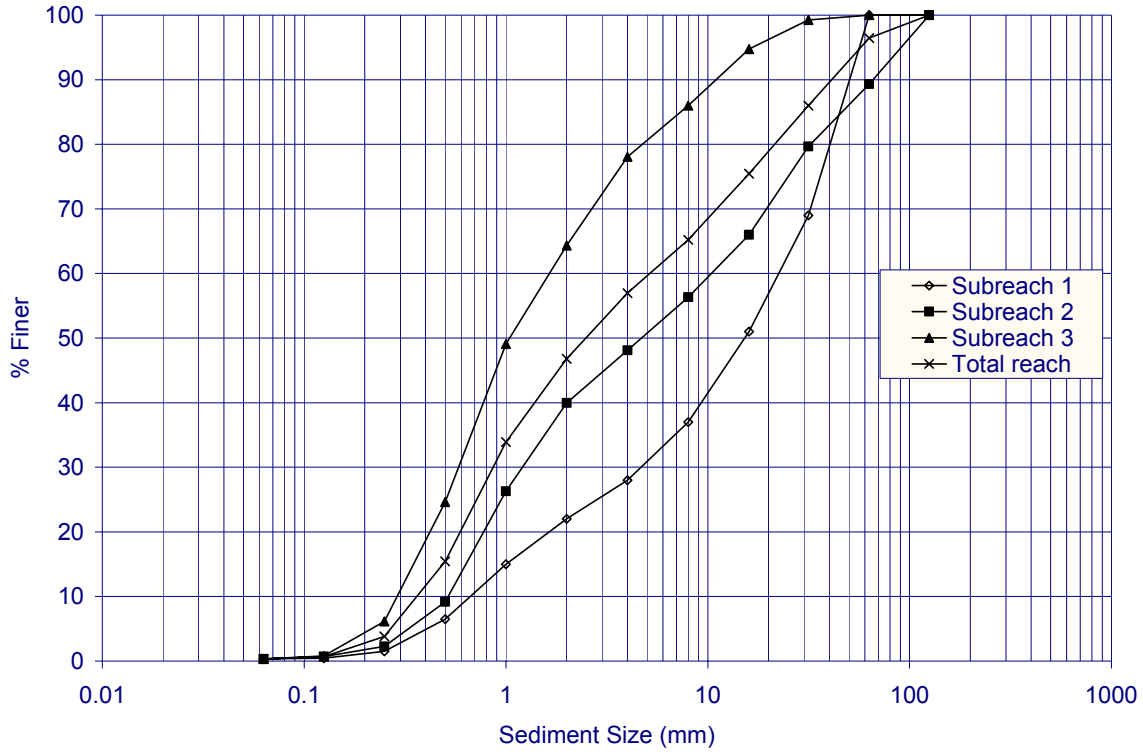

Figure 3-18 2001 Bed-material samples used in the sediment transport and equilibrium analyses

4 SUSPENDED SEDIMENT AND WATER HISTORY

4.1 METHODS

Water and sediment flow trends in the Bernalillo Bridge reach were analyzed through the development of single-mass curves and double-mass curves. Not enough suspended sediment data were available to generate difference-mass curves and perform a sediment continuity analysis of the reach.

The following curves were developed for the Bernalillo and Albuquerque gages, for the entire period of record:

- Mass curve of water discharge (acre-feet/year) from 1942 to 2000
- Mass curve of sediment discharge (tons/year) from 1956 to 1999
- Double mass curve with water and sediment discharge for trends in sediment concentration (mg/l) from 1956 to 1999

The slopes of each curve and the time periods of breaks in the curves were also estimated.

4.2 RESULTS

Single Mass Curves

Discharge Mass Curves

The discharge mass curves for Bernalillo and Albuquerque gages (Figure 4-1) have similar trends, indicating that there is not significant water input from the ephemeral tributaries between the two gages. There are three breaks in slope in the discharge mass curve (1942-1978, 1978 - 1987 and 1987 – 2000 periods), with an increase in annual discharge rate from 1978 to 1987 and a slight decrease from 1987 to 2000 (Figure 4-1 and Table 4-1). The drier water discharge period (1942-1978) at Bernalillo and Albuquerque gages coincides with the drier water period at Cochiti gage, as identified by Richard (2001). These slope breaks in the mass curve represent changes in water regime in the river. These changes may be due to changes in climate and/or flood management or regulation in the Rio Grande basin.

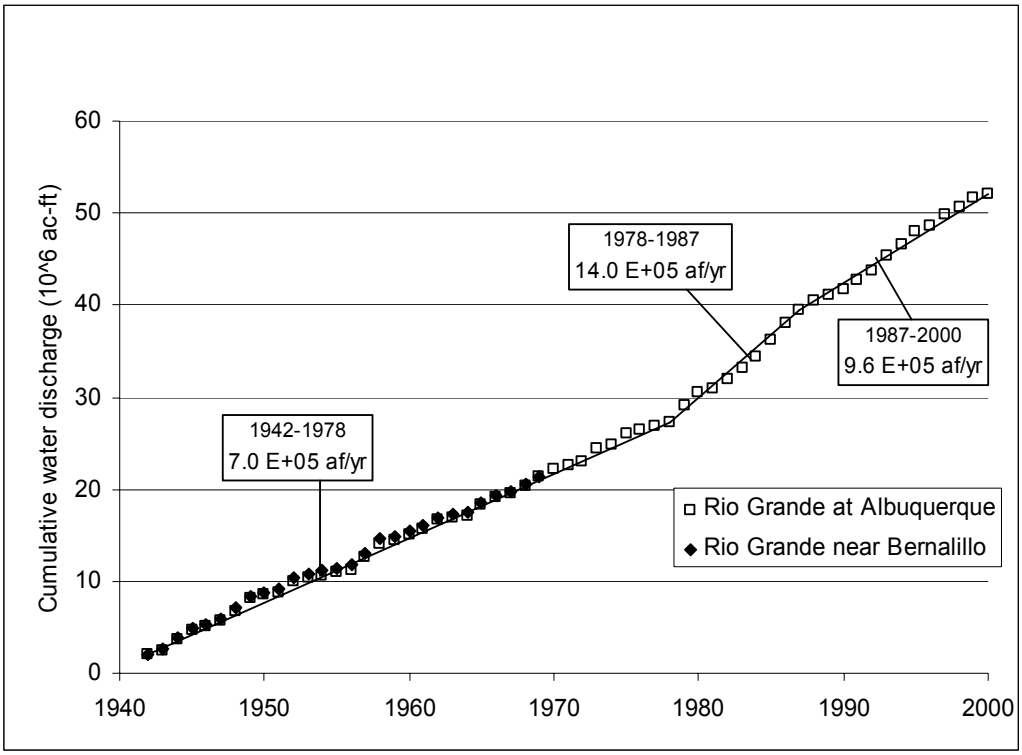

Figure 4-1 Discharge mass curve at Bernalillo and Albuquerque gages (1942-2000)

Table 4-1 Summary of the discharge mass curve slope breaks at Bernalillo and Albuquerque gages (1942-2000)

Time Period	Slopes of the water discharge mass curve (10^6 ac-ft/yr)
1942-1978	7.0 E+05
1978-1987	14.0 E+05
1987-2000	9.6 E+05

Suspended Sediment Mass Curve

The suspended sediment mass curve for Bernalillo and Albuquerque shows nine slope breaks (Figure 4-2). In general, the slopes are steeper from 1956 to 1973 than after 1973. The slope values range from 2.3 to 10.8 tons per year between 1956 and 1973. After 1973, the slope values are between 0.25 to 2.79 tons per year. This change in sediment rate in 1973 coincides with the closure of Cochiti Dam. There was an increase of suspended sediment discharge from 1993 to 1995 (2.79 E+06 tons/yr) with respect to the 1978-1993 discharges

(1.11 E+06 tons/yr and 0.25 E+06 tons/yr). However, the 1995-1999 suspended sediment discharge has decreased to 0.8 E+06 tons/yr and is comparable to the 1978-1985 sediment discharge (1.11 E+06 tons/yr). Table 4-2 summarizes the slope values of the suspended sediment discharge mass curve.

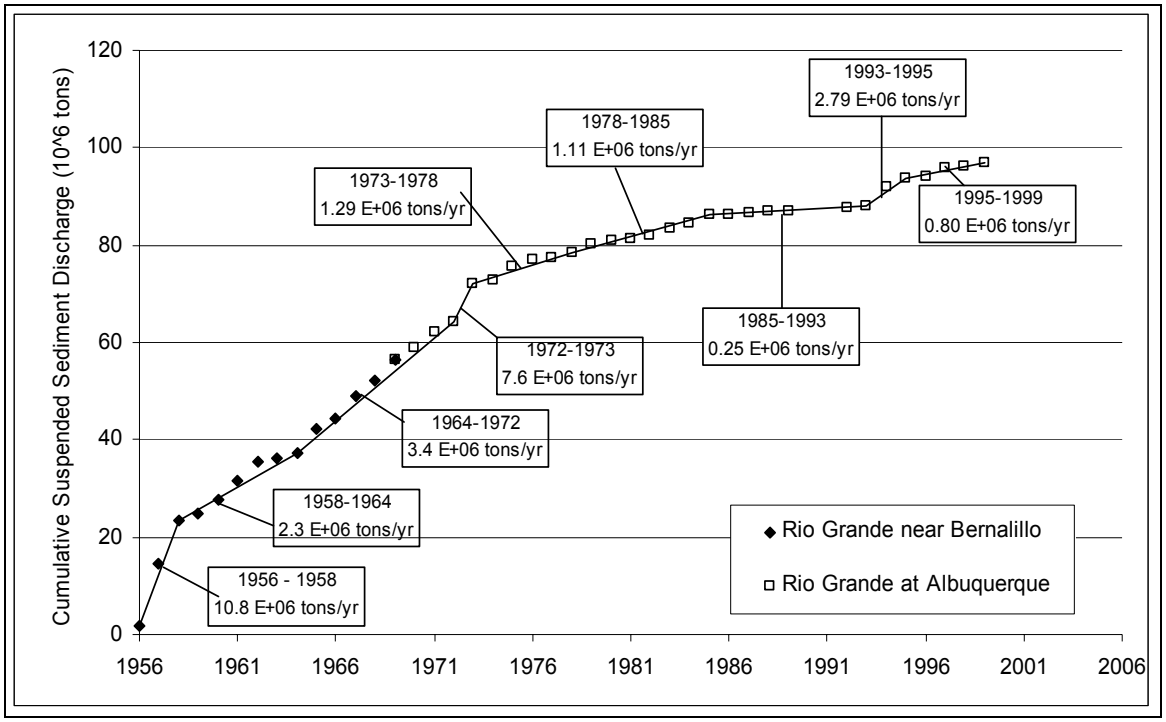

Figure 4-2 Suspended sediment mass curve at Bernalillo and Albuquerque gages (1956-1999)

Table 4-2 Summary of the suspended sediment discharge mass curve slope breaks at Bernalillo and Albuquerque gages (1956-1999)

Time Period	Slopes of the suspended sediment discharge mass
1956-1958	10.8E+0.6
1958-1964	2.30E+06
1964-1972	3.40E+06
1972-1973	7.55E+06
1973-1976	1.29E+06
1976-1985	1.11E+06
1985-1993	0.25E+06
1993-1995	2.79E+06
1995-1999	0.80E+06

Double Mass Curve

The double mass curve of cumulative water discharge versus cumulative sediment discharge shows the changes of suspended sediment concentration with time. Figure 4-3 shows higher concentrations of suspended sediment from 1956 to 1973 with average concentration varying from 3,741 mg/l to 6,670 mg/l. After 1973, the concentration does not exceed 1,602 mg/l. In general, the double mass curve shows a similar trend as the suspended sediment single mass curve. An average concentration of 664 mg/l has persisted from 1995 to 1999 and is comparable to the 1978-1984 average concentration (650 mg/l). Table 4-3 summarizes the suspended sediment concentrations at Bernalillo and Albuquerque gages between 1956 and 1999.

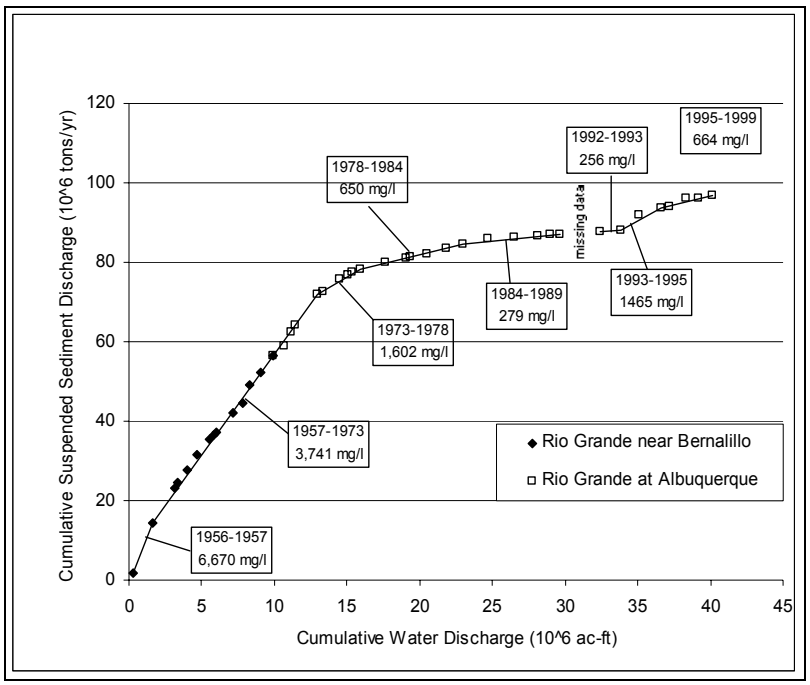

Figure 4-3 Cumulative discharge vs. cumulative suspended sediment load at Rio Grande at Bernalillo and Rio Grande at Albuquerque (1956 - 1999)

Table 4-3 Summary of suspended sediment concentrations at Bernalillo and Albuquerque gages (1956-1999)

Time Period	Concentration (mg/l)
1956-1957	6670
1957-1973	3741
1973-1978	1602
1978-1984	650
1984-1989	279
1992-1993	256
1993-1995	1465
1995-1999	664

5 EQUILIBRIUM STATE PREDICTORS

5.1 METHODS

Sediment Transport Analysis

The purpose of this section is to compare the subreach transport capacity with: 1) the incoming sand load (0.0625 mm < d_s < 2 mm); and 2) the incoming bed material load (0.30 mm < d_s < 2 mm).

Field observations performed by the USBR indicate that sand size particles are mobile at all flows greater than 300 cfs as bedload material and become suspended at flows greater than 3,000 cfs (Massong pers. communication 2001). According to these field observations, it is believed that the bed material load is comparable to the sand load (0.0625 mm and 2 mm) (Massong pers. communication 2001).

However, very fine and fine sand size particles (0.0625 mm to 0.25 mm) are not found in large quantities in the bed (d_{10} of bed material = 0.36 mm (Figure 3-16)) at flows close to 5,000 cfs, which suggest that they behave as washload (Appendix G, Table 5-1). In addition, the amount of sand particles in suspension finer than 0.36 mm (d_{10} of the bed material) is about 50% or more at flows close to 5,000 cfs (Table 5-1, Appendix G). As a result, the bed material load comprises only the sediment particles coarser than 0.36 mm at flows close to 5,000 cfs.

Table 5-1 Percents of total load that behave as washload and bed material load at flows close to 5,000 cfs

Date	Inst. Discharge (cfs)	d_{10} bed material mm	% washload	% bed material load
4/23/79	4980	0.14	47	53
5/29/79	6610	0.17	50	50
6/7/82	4570	0.17	55	45
5/8/84	4440	0.14	43	57
6/13/94	5030	0.074	67	33
6/27/94	4860	0.2	54	46
6/6/95	4960	0.29	45	55
7/3/95	5620	0.26	31	69
6/3/97	5040	0.26	30	70
5/24/99	4080	0.21	60	40

Total sediment input to the reach was estimated using the Modified Einstein Procedure (MEP) (Colby and Hembree 1955, USBR 1955). Cross-section geometry measurements, suspended sediment and bed material samples at the Albuquerque gage from 1978 to 1999 were used for the purpose of estimating the incoming total sediment load and sand-load to the reach using the MEP. The Albuquerque gage is located downstream from the study reach. As a result, the total load might be slightly over estimated since sediment is probably mined from the bed and banks between the study reach and the gage. The data were subdivided by separating snowmelt and summer flows. The snowmelt period was defined as April to July based on interpretation of the mean-daily discharge record for the Albuquerque gaging station from 1978 to 1999. Non-linear regression functions were fit to the MEP results to develop sand-load rating curves.

Channel transport capacities were estimated for each reach using different sediment transport equations. The following equations were used to estimate the transport capacity for 1992: Laursen, Engelund and Hansen, Ackers and White (d_{50} and d_{35}), Yang – sand (d_{50} and size fraction), Einstein, and Toffaleti (Stevens et al. 1989, Julien 1995). Between 1992 and 2001, the bed material gradation analysis indicate that subreaches 1 and 2 have become coarser with median grain sizes of medium to coarse gravel and very coarse sand to coarse gravel, respectively (Figure3-15 and 3-16). Therefore, usage of the majority of bed-material transport relationships would not be appropriate (Table 5-2). As a result, the 2001 transport capacities were computed with two bed-material load relationships (Yang-gravel, Yang-mixture) and three bedload relationships (Einstein, Meyer-Peter & Müller, Schoklitsch) for subreaches 1 and 2.

Subreach 3 had an opposite trend, whereby becoming finer since 1992 (Figure 3-17). This gradation curve yields a classification of the median grain size of medium to coarse sand. As a result, the same relationships analyzed for the 1992 data were used with the 2001 data. Transport capacities were estimated for 1992 and 2001 for comparative purposes. Unfortunately, the comparison between the 1992 and 2001 results for subreaches 1 and 2 are not possible, due to the different transport equations used for each year.

The input data to the sediment transport equations are the reach-averaged channel geometry values resulting from HEC-RAS runs at 5,000 cfs. Table 5-3 summarizes the 1992 and 2001 input data for all subreaches.

Table 5-2 Appropriateness of bedload and bed-material load transport equations (Stevens et al. 1989).

Author of Formula	*Date*	*Bedload (BL) or Bed-material Load (BML)*	*Type of Formula (D/P)*	*Sediment Type (S/M/O)*	*Sediment Size (S/G)*
Ackers & White	1973	BML	D	S	S,G
Einstein (BL)	1950	BL	P	M	S,G
Einstein (BML)	1950	BML	P	M	S
Engelund & Hansen	1967	BML	D	S	S
Laursen	1958	BML	D	M	S
Meyer-Peter and Muller	1948	BL	D	S	S,G
Schoklitsch	1934	BL	D	M	S,G
Toffaleti	1968	BML	D	M	S
Yang (sand)	1973	BML	D	O	S
Yang (gravel)	1984	BML	D	O	G

D/P - Deterministic/Probabilistic
S/M/O - Single Size Fraction/Mixture/Optional
S/G - Sand/Gravel

Table 5-3 Hydraulic input data at all subreaches for sediment transport capacity computations from 1992 and 2001 HEC-RAS runs at 5,000 cfs.

1992 Data				
Subreach #	**Width (ft)**	**Depth (ft)**	**Velocity (ft/s)**	**WS slope (ft/ft)**
1	565	2.34	3.86	0.0009
2	501	2.56	4.17	0.0010
3	418	2.75	4.58	0.0011
Total	501	2.52	4.20	0.0010

2001 Data				
Subreach #	**Width (ft)**	**Depth (ft)**	**Velocity (ft/s)**	**WS slope (ft/ft)**
1	560	3.12	2.95	0.00086
2	421	3.79	3.37	0.00091
3	546	3.17	3.01	0.00091
Total	504	3.38	3.12	0.00090

Hydraulic Geometry

Hydraulic geometry equations have been developed to estimate geometric characteristics of stable channels based on a channel-forming discharge. Some methods use bed material size, channel slope, and/or sediment concentration. Most hydraulic geometry methods have been developed from man-made canals or single-thread natural channels.

The equilibrium width of the Bernalillo Bridge reach for 1962, 1972, 1992 and 2001 were

estimated by the following hydraulic geometry equations:

- Leopold & Maddock (1953) developed a set of empirical equations that relate the hydraulic geometry variables (width, depth and velocity) to discharge in the form of power functions:

$$W = aQ^{b}$$
$$D = cQ^{e}$$
$$V = kQ^{m}$$

  Where, ack = 1 and b+e+m = 1 by continuity of water (Q = V.D.W) and the exponent of the equations b,f and m are on average equal to 0.5, 0.4 and 0.1 regardless the flow regime, sediment characteristics and physiographic location of the rivers (ASCE Task Committee on Hydraulics 1998).

- Julien and Wargadalam's (1995) regime geometry equations are "semi-theoretical" equations based on four fundamental hydraulic relationships – continuity, resistance, sediment transport and secondary flow. Depth, width, velocity and Shield's parameter are expressed as functions of discharge, bed material size and slope as follows:

$$D = 0.200 Q^{\frac{2}{6m+5}} d_s^{\frac{6m}{6m+5}} S^{-\frac{1}{6m+5}}$$
$$W = 1.330 Q^{\frac{4m+2}{6m+5}} d_s^{-\frac{4m}{6m+5}} S^{-\frac{2m+1}{6m+5}}$$
$$V = 3.758 Q^{\frac{2m+1}{6m+5}} d_s^{-\frac{2m}{6m+5}} S^{\frac{2m+1}{6m+5}}$$
$$\tau_* = 0.121 Q^{\frac{2}{6m+5}} d_s^{-\frac{5}{6m+5}} S^{\frac{6m+4}{6m+5}}$$
$$m = \frac{1}{(\ln \frac{12.2D}{d_{50}})}$$

- Simons & Albertson (1963), developed equations from analysis of Indian and American canals. Five data sets were used in the development of the equations. Simons and Bender's data were collected from irrigation canals in Wyoming, Colorado and Nebraska during the summers of 1953 and 1954 and consisted of cohesive and non-cohesive bank material. The USBR data were collected from canals in the San Luis Valley of Colorado. This data consisted of coarse non-

cohesive material. Indian canal data were collected from the Punjab and Sind canals. The average diameter of the bed material is approximately 0.43 mm for the Punjab canals and between 0.0346 mm to 0.1642 mm for the Sind canals. The Imperial Valley canal data were collected in the Imperial Valley canal systems. Bed and bank conditions of these canals are similar to the Punjab, Sind and Simons and Bender canals (Simons et. al 1963).

The relationship between wetted perimeter (P) and water discharge is represented in Figure 5-1. Once the wetted perimeter is obtained from Figure 5-1, the averaged channel width is estimated using Figure 5-2.

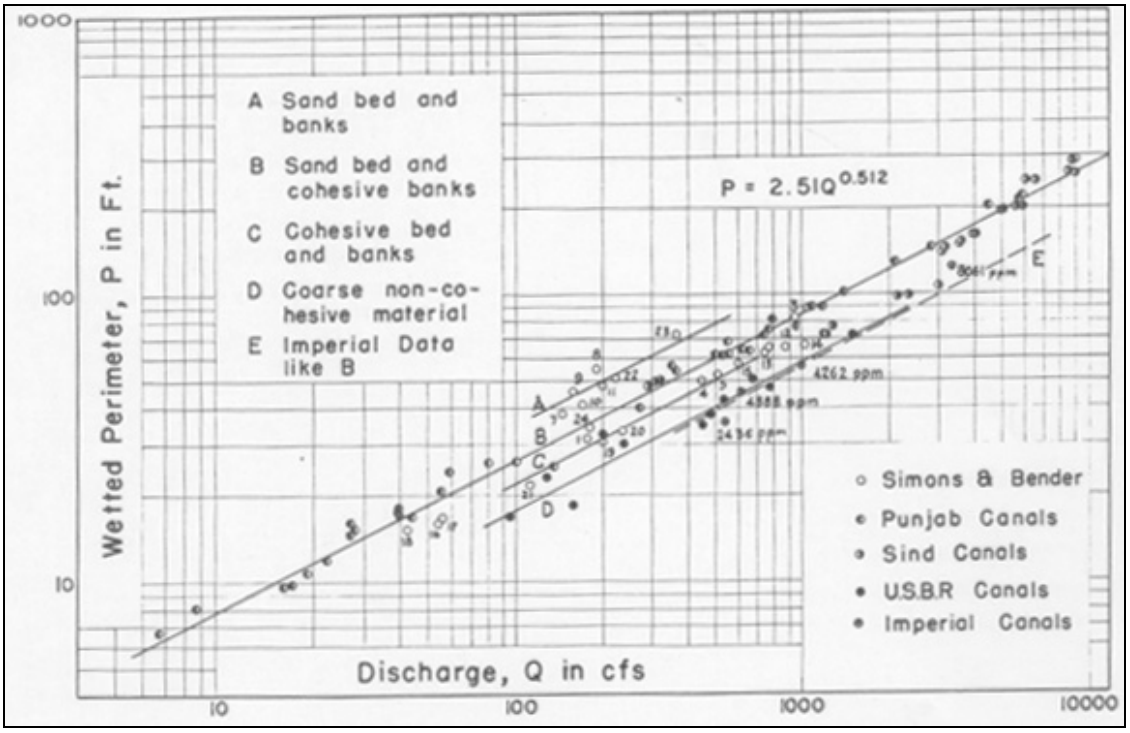

Figure 5-1 Variation of wetted perimeter P with discharge Q and type of channel (after Simons and Albertson 1963)

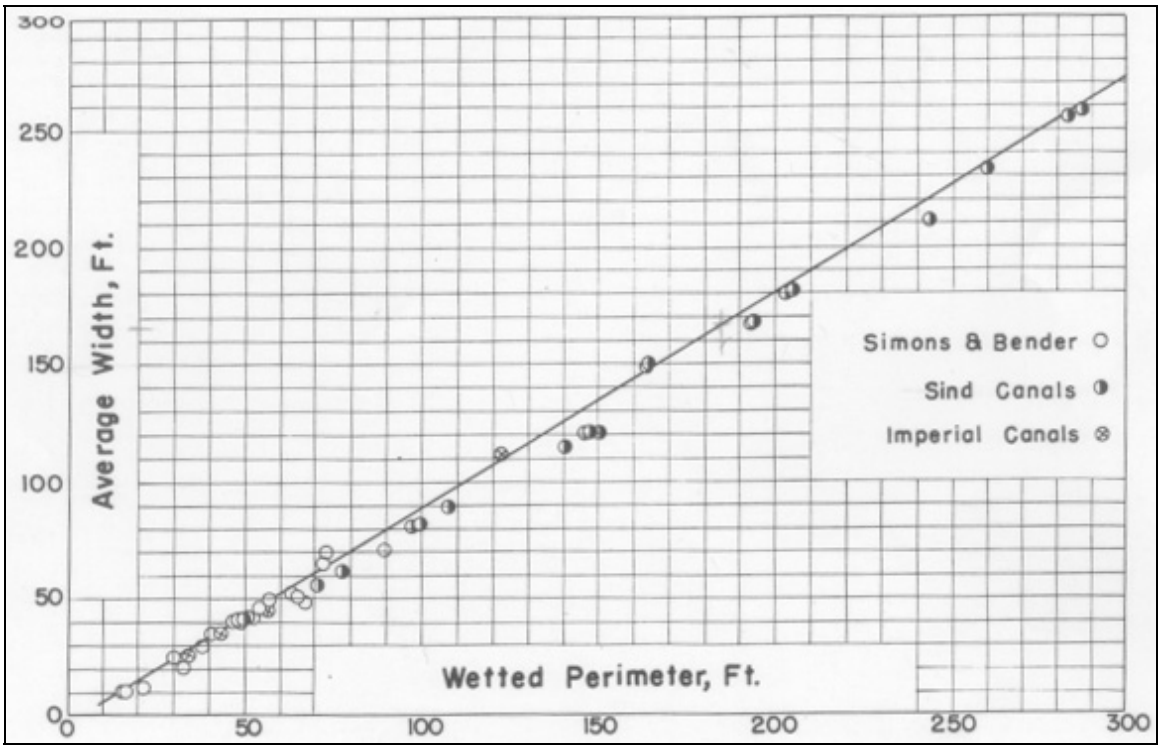

Figure 5-2 Variation of average width W with wetted perimeter P (after Simons and Albertson 1963)

- Blench (1957) developed regime equations from flume data. The equations account for the differences in bed and bank material by means of a bed and a side factor (F_s) (Thorne et al. 1997). The range of application of Blench's equation is (Thorne et al. 1997):

  Discharge (Q): 0.03-2800 m^3/s

  Sediment concentration (c): 30-100 ppm

  Bed material size (d): 0.1-0.6 mm

  Bank material type: cohesive

  Bedforms: ripples – dunes

  Planform: straight

  Profile: uniform

  The size factor is defined by $F_s = V^3/b$, where b is defined as the breadth, that multiplied by the mean depth d, gives the area of a mean trapezoidal

section, and V is the mean flow velocity (Blench 1957).

The regime equation for channel width (W) is [from Wargadalam (1993)]:

$$W = \left(\frac{9.6(1 + 0.012c)}{F_s} \right)^{\frac{1}{2}} d^{\frac{1}{4}} Q^{\frac{1}{2}} \text{ , (ft)}$$

Where,

c = sediment load concentration (ppm),

d = d_{50} (mm), and

F_s = 0.1 for slight cohesiveness of banks

- Lacey [(1930-1958), from Wargadalam (1993)]

$$P = 2.667Q^{0.5} \text{ (ft)}$$

Where,

P = wetted perimeter (feet)

Q = water discharge (ft^3/s)

- Klaassen-Vermeer (1988) developed a width relationship for braided rivers based on work on the Jamuna River in Bangladesh:

$$W = 16.1Q^{0.53} \text{ (m)}$$

Where,

Q = water discharge (m^3/s)

- Nouh (1988) developed regime equations from ephemeral channels located in the South and Southwest regions of Saudi Arabia. The equations provide information of channel dimensions under varying flash flood and sediment flow conditions in an extremely arid zone. The following regression equation was obtained for the channel width:

$$W = 28.3\left(\frac{Q_{50}}{Q} \right)^{0.83} + 0.018(1 + d)^{0.93} c^{1.25} \text{ , (m)}$$

Where,

Q_{50} = peak discharge for 50 yr. return period (m^3/s)

Q = annual mean discharge (m^3/s)

d = d_{50} (mm)

c = mean suspended sediment concentration (Kg/m^3).

Additionally, an empirical width-discharge relationship specific to the Bernalillo Bridge Reach and subreaches was developed from the digitized active channel widths from GIS coverage's and the peak flows from the 5-years prior to the survey date. Peak flows were obtained from the Rio Grande at Otowi Gage for 1918 and Rio Grande at San Felipe Gage for the remaining years. The resulting equation takes the following form:

$$W = a\,Qb$$

Where,

W = Active channel width (feet)

Q = Peak discharge (cfs)

Table 5-4 contains the input data for the empirical width-discharge equations. Peak flow data are included in Appendix E.

Table 5-4 Input data for the empirical width-discharge relationship

	1918	1935	1949	1962	1972	1985	1992	2001
Averaged 5-yr peak flows (cfs)	11630	6608	8010	5768	3490	6256	4142	4522
Subreach 1 Width (ft)	1165	669	561	521	583	592	524	418
Subreach 2 Width (ft)	1055	656	569	539	541	500	488	347
Subreach 3 Width (ft)	579	455	408	410	413	415	406	371
Total Width (ft)	954	607	527	501	524	512	479	378

Table 5-5 contains the input data for the hydraulic geometry calculations. The peak discharges for 50 year-return period are from Bullard and Lane (1993) report. The averaged suspended sediment concentration values are estimated from the double mass curve (Figure 4-3), which was developed from the Rio Grande near Bernalillo and Rio Grande at Albuquerque USGS gaging stations.

Table 5-5 Input data for the hydraulic geometry calculations

1962	Q (cfs)	Q_{50} (cfs)	d_{50} (mm)	Channel Slope (ft/ft)	Avg C (ppm)
Reach 1	5,000	23500	0.21	0.0007	3,732
Reach 2	5,000	23500	0.21	0.0008	3,732
Reach 3	5,000	23500	0.21	0.0010	3,732
Total Reach	5,000	23500	0.21	0.0008	3,732
1972					
Reach 1	5,000	10000	0.21	0.0009	3,732
Reach 2	5,000	10000	0.21	0.0009	3,732
Reach 3	5,000	10000	0.24	0.0010	3,732
Total Reach	5,000	10000	0.22	0.0009	3,732
1992					
Reach 1	5,000	10000	1.38	0.0008	255
Reach 2	5,000	10000	1.09	0.0011	255
Reach 3	5,000	10000	4.43	0.0008	255
Total Reach	5,000	10000	2.3	0.0009	255
2001					
Reach 1	5,000	10000	15.43	0.0011	663
Reach 2	5,000	10000	11.29	0.0008	663
Reach 3	5,000	10000	1.24	0.0008	663
Total Reach	5,000	10000	9.32	0.0008	663

Equilibrium Channel Width Analyses

- Williams and Wolman (1984) Hyperbolic Model

Williams and Wolman (1984) studied the downstream effects of dams on alluvial rivers. The changes in channel width with time were described by hyperbolic equations of the form $(1/Y) = C_1 + C_2\ (1/t)$, where Y is the relative change in channel width, C_1 and C_2 are empirical coefficients and t is time in years after the onset of the particular channel change. The relative change in channel width is equal to the ratio of the width at time t (W_t) to the initial width (W_i). Coefficients C_1 and C_2 might be a function, at least, of flow discharges and boundary materials.

Hyperbolic equations were fitted to the entire Bernalillo Bridge and to each subreach data set from 1918 to 1992. Width data for 2001 was not used, because the channel narrowed from 1992 to 2001 and seems to follow a trend different from the 1918-1992 trend (see Figure 3-14). The time t = 0 was taken as 1918, when narrowing of the channel began. To adjust the data to an origin of 0, 1.0 was subtracted from each W_t/W_1 before performing the regression. The data to which the hyperbolic regressions were applied are in Table 5-6.

Table 5-6 Hyperbolic regression input data

Subreach 1					
Year	t (year)	1/t	Wi (ft)	Wt (ft)	1/(Wt/Wi)-1
1918	0		1165	1165	
1935	17	0.05882		669	-2.3493
1949	31	0.03226		561	-1.9274
1962	44	0.02273		521	-1.8081
1972	54	0.01852		583	-2.0023
1985	67	0.01493		592	-2.0339
1992	74	0.01351		524	-1.8178
Subreach 2					
Year	t (year)	1/t	Wi (ft)	Wt (ft)	1/(Wt/Wi)-1
1918	0		1055	1055	
1935	17	0.0588		656	-2.6438
1949	31	0.0323		569	-2.1704
1962	44	0.0227		539	-2.0436
1972	54	0.0185		541	-2.0537
1985	67	0.0149		500	-1.9018
1992	74	0.0135		488	-1.8609
Subreach 3					
Year	t (year)	1/t	Wi (ft)	Wt (ft)	1/(Wt/Wi -1)
1918	0		579	579	
1935	17	0.0588		455	-4.6643
1949	31	0.0323		408	-3.3985
1962	44	0.0227		410	-3.4274
1972	54	0.0185		413	-3.4865
1985	67	0.0149		415	-3.5304
1992	74	0.0135		406	-3.3557
Bernalillo Bridge Reach					
Year	t (year)	1/t	Wi (ft)	Wt (ft)	1/(Wt/Wi -1)
1918	0		954	954	
1935	17	0.0588		607	-2.7502
1949	31	0.0323		527	-2.2354
1962	44	0.0227		501	-2.1037
1972	54	0.0185		524	-2.2187
1985	67	0.0149		512	-2.1564
1992	74	0.0135		479	-2.0095

- Richard (2001) Exponential Model

Richard (2001) selected an exponential function to describe the changes in width with time of the Cochiti reach of the Rio Grande. The hypothesis of the model is that the magnitude of the slope of the width vs. time curve increases with deviation from the equilibrium width, W_e. The exponential function is:

$$W = W_e + (W_0 - W_e).e^{-k_1 t}$$

Where,

k_1 = rate constant;

W_e = Equilibrium width toward which channel is moving (ft);

W_0 = Channel width (ft) at time t_0 (yrs); and

W = Channel width (ft) at time t (yrs)

Richard (2001) used three methods to estimate k_1 and W_e. The first method consists of empirically estimating the value of k_1 and W_e by plotting the width change rate vs. the width and generating a regression line. The rate constant, k_1, is the slope of the regression line and the intercept is k_1W_e. The second method consists of using the empirically determined k-values from the first method and varying the equilibrium width values to produce a "best-fit" equation that minimized the sum-square error (SSE) between the predicted and observed widths. This method was developed in an effort to better estimate the equilibrium width. The third method consists of estimating the equilibrium width, W_e, using a hydraulic geometry equation. The k_1-value was determined by varying it until the SSE between the predicted and observed width was minimized. The input data used in this analysis is included in Appendix F.

5.2 RESULTS

Sediment Transport Analysis

The total load computed from MEP comprises mostly sand material. Gravel load occurs with flows close to 5,000 cfs and represents less than 8% of the total MEP load. Figure 5-3 presents the Spring and Summer sand-load (0.0625 mm – 2 mm) data. Non-linear regression functions were fit to the data to obtain the rating curves at the Albuquerque gage. Using a channel forming discharge of 5,000 cfs, the estimated MEP sand-load at the Albuquerque gage station is 21,672 tons/day. It is evident that the variability of the data points around the regression line is about one order of magnitude (Figure 5-3). As a result, the real sand-load could considerably vary from the estimated value.

Table 5-7 lists the bed-material transport capacity calculations for the 1992 hydraulic geometry data for subreaches 1 and 2. The slopes indicated in Table 5-7 correspond to the water surface slopes. The different equations yield varying results. Engelund and Hansen's, Ackers and White's (d_{50} and d_{35}) and Yang's (sand d_{50} and mixture) equations yield comparable results for subreach 1. Engelund and Hansen's, Ackers and White's (d_{35}), and Yang's sand (d_{50}) equations produce similar results for subreach 2, while Einstein's and Toffaleti's results are also comparable. No sediment transport capacity exceeds 14,000 tons/day.

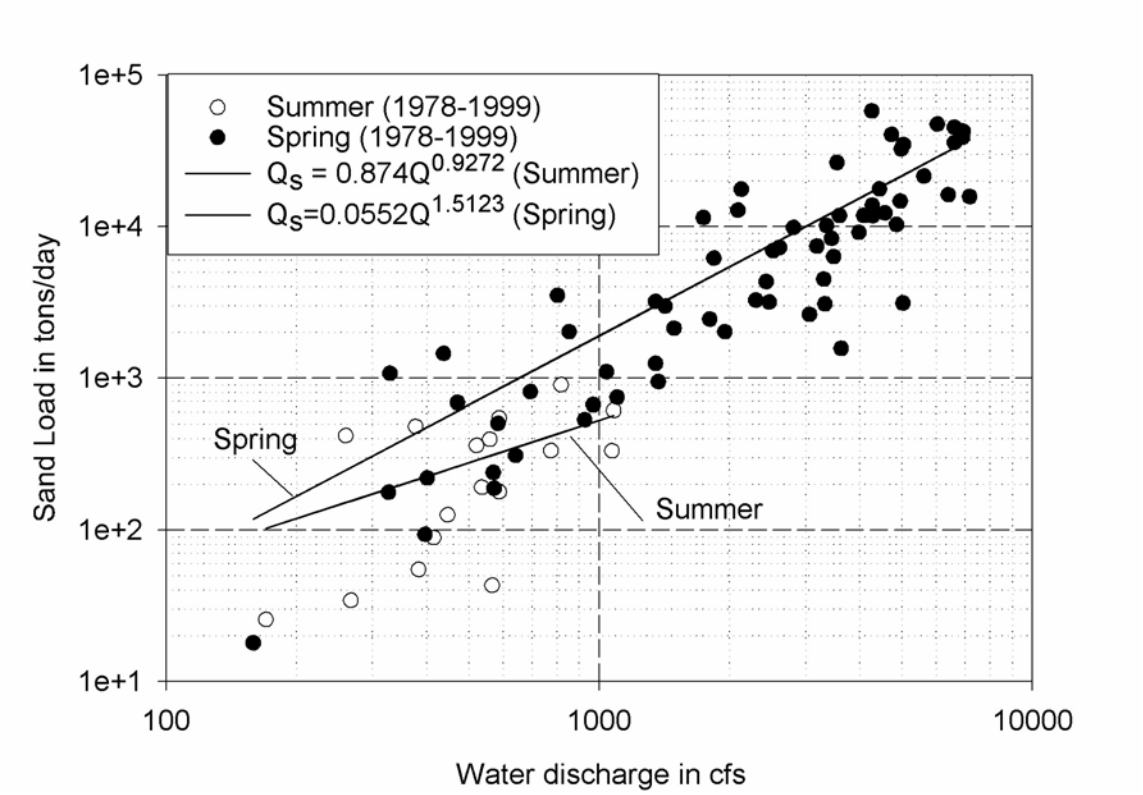

Figure 5-3 Albuquerque gage sand-load rating curve for the Spring and Summer seasons from 1978 to 1999

Table 5-7 Bed-material transport capacity for the 1992 channel geometry data for subreaches 1 and 2

	Existing Slopes in ft/ft	
	s = 0.0009	***s=0.0011***
Bed-material Transport Equations	***Subreach 1 BML in tons/day***	***Subreach 2 BML in tons/day***
Laursen	3518	5094
Engelund & Hansen	6052	11646
Ackers and White (d50)	6323	8863
Ackers and White (d35)	8239	11392
Yang Sand (d50)	7025	10555
Yang Sand (size fraction)	10050	13533
Einstein	2080	6019
Toffaleti	4257	6173
Average =	5943	9159

BML = Bed Material Load, S = water surface slopes

Table 5-8 lists the bedload and bed-material load transport capacity calculations for the 2001 hydraulic geometry data for subreaches 1 and 2. The different equations yield varying results. For both subreaches, Yang's (gravel), Einstein, and Meyer-Peter & Müller produce similar results, while Yang's (mixture) and Schoklitsch's results are also comparable. The average transport capacity for subreaches 1 and 2 is 401 tons/day and 997 tons/day respectively (Table 5-8), which are both less than the incoming sand load (21,672 tons/day). No sediment transport capacity exceeds 4,000 tons/day for these two subreaches. These low transport capacities are a direct result of the coarse material present in the bed.

Table 5-8 Bed-material and bedload transport capacity for the 2001 channel geometry data for subreaches 1 and 2

	Existing Slopes in ft/ft	
BML/BL Transport Equations	***s=0.00086***	***s=0.00091***
	Subreach 1 BML/BL in tons/day	***Subreach 2 BML/BL in tons/day***
Yang Gravel (size fraction) - BML	60	104
Yang Mixture (size fraction) - BML	1336	3618
Einstein (BL)	0	1.5
Meyer-Peter & Muller (BL)	0	0
Schoklitsch (BL)	609	1261
Average =	401	997

BML - Bed Material Load
BL - Bedload
s - Water surface slopes

Table 5-9 lists the bed-material transport capacity calculations for the 1992 and 2001 hydraulic geometry data for subreach 3. The slopes indicated in Table 5-9 correspond to the water surface slopes. The different equations yield varying results. Ackers and White's and Yang's sand (d_{50}) equations yield similar results for subreach 3 in 1992. For 2001, Laursen's, Ackers and White's (d_{50} and d_{35}), and Toffaleti's equations yield comparable results, while Engelund and Hansen's and Yang's (sand d_{50} and sand size fraction) results are also comparable. The average transport capacities for subreach 3 are 6,313 and 3,693 tons/day for 1992 and 2001 respectively (Table 5-9), which are less than the incoming sand load (21,672 tons/day). No sediment transport capacity exceeds 15,000 tons/day in 1992, while the maximum transport capacity does not exceed 7,500 tons/day in 2001.

Table 5-9 Bed material transport capacity for the 1992 and 2001 channel geometry data for subreach 3

	1992 Slope s=0.0008	*2001 Slope s=0.00091*
Bed-material Transport Equations	***Subreach 3 BML in tons/day***	***Subreach 3 BML in tons/day***
Laursen	5896	2302
Engelund & Hansen	3592	5159
Ackers and White (d50)	4604	2223
Ackers and White (d35)	8733	3497
Yang Sand (d50)	8189	5361
Yang Sand (size fraction)	14315	7050
Einstein	591	647
Toffaleti	4586	3306
Average =	6313	3693

BML = Bed Material Load, S = water surface slopes

The average transport capacity for the entire reach (subreaches 1 to 3) is 7,139 tons/day in 1992, which is less than the incoming sand load (21,672 tons/day). The transport capacities for the three reaches in 2001 are lower than the transport capacities for 1992.

In general, the washload comprises the fine particles not found in large quantities in the bed ($d_s < d_{10}$) (Julien 1995). The d_{10} of the bed material is on average 0.36 mm (Figure 3-18). The percent of material in suspension finer than 0.36 mm is about 50% at flows close to 5,000 cfs (Appendix G), which suggests that very fine and fine sand particles behave as washload. As a result, the incoming bed-material load is about 10,836 tons/day, which represents 50% of the sand-load (Appendix G). This methodology assumes that the silt load is very small, and thus negligible as compared to the sand load.

The incoming bed-material load is closer to the transport capacities for 1992 than for 2001. According to the results for 1992, the equation that yields closer results to the bed-material load is Yang sand for the three reaches. The 1992 average capacity load computed from the results of all the equations for all the subreaches (7,139 tons/day) is slight lower than the incoming bed-material load (10,836 tons/day). However, given the uncertainty involve in the estimation of the bed-material load (Figure 5-3), the average capacity load is comparable to the bed-material load. As a result, the channel slope in 1992 seems appropriate to transport the incoming bed-material load of 10,836 tons/day at a discharge of 5,000 cfs. However, this result is not in agreement with observed degradation in the channel bed that occurred between 1992

and 2001 (Figures 3-8 and 3-9).

The bed material gradation curves for subreaches 1 and 2 (Figures 3-15 and 3-16) represent a much coarser material than the bed material gradation curves collected at the Albuquerque gage and used for the estimation of the bed-material load (see Appendix G). The median grain size (d_{50}) of the bed material at Albuquerque gage is finer than medium sand for most of the samples (see Appendix G). As a result, the transport capacities computed for subreaches 1 and 2 do not compare with the bed-material load estimated with the MEP. It is likely that a layer of sand coming from tributaries and mined from the bed and banks of the channel upstream from the study reach overlay and move above a layer of coarser material (armor layer) that the river cannot transport. The averaged transport capacity of subreach 3 for 2001 is less than 50 % of the bed-material load (10,836 tons/day) and is about half of the capacity of that subreach in 1992. According to the HEC-RAS results for 2001, the reach-averaged velocity and the water surface slope decreased with respect to the 1992 results in subreach 3. As a result, the transport capacity is also reduced.

Hydraulic Geometry

The equilibrium widths predicted by the downstream hydraulic geometry equations for a discharge of 5,000 cfs are summarized in Table 5-10. Klaassen and Vermeer's, Simons and Albertson's, Lacey's and Julien-Wargadalam's equations under estimate the width for all subreaches for all the years. In Julien-Wargadalam (1995) equations the width-depth ratio cannot vary from a value of 20-40. Width-depth ratios of the Bernalillo Bridge reach are above 150 (Figure 3-13 d). Therefore, Julien-Wargadalam equation predicts narrower channels than the widths obtained from the HEC-RAS analysis.

Blench's equation overestimate the width for all the subreaches and years and Nouh's equations produce varying results. Nouh's and Blench's equations produce large width values for 1962, 1972 and 2001 (Table 5-10). These two equations are not applicable for the conditions of the Rio Grande (See Section 5. Equilibrium State Predictors).

Figure 5-4 is a plot of the measured reach-averaged active channel width versus the predicted width from the downstream hydraulic geometry equations. None of the equations produces channel width values close to the non-vegetated active channel widths obtained from the HEC-RAS analysis. The predicted widths are nearly constant for all the subreaches from 1962 to 2001. This trend is in agreement with the historical trends of channel width during the

1962 – 1992 time period (Figures 3-13 and 3-14). In summary, none of the equations predicts the historical widths. However, they do predict the nearly constant channel width observed between 1962 and 1992 (Figure 3-13 and 3-14).

Table 5-10 Predicted Equilibrium Widths in ft from downstream hydraulic geometry equations for Q = 5,000 cfs

Q = 5,000 cfs		Reach-Averaged HEC-RAS Main Channel Width (feet)	Klaassen & Vermeer (feet)	Nouh (feet)	Blench (feet)	Simons and Albertson (feet)	Julien-Wargadalam (feet)	Lacey (feet)
1962	**1**	595	729	2064	1417	167	283	189
	2	586	729	2064	1417	167	273	189
	3	432	729	2064	1417	167	265	189
	Total	546	729	2064	1417	167	274	189
1972	**1**	641	729	2060	1417	167	267	189
	2	595	729	2060	1417	167	269	189
	3	446	729	2107	1465	167	263	189
	Total	574	729	2076	1433	167	267	189
1992	**1**	565	729	138	675	167	273	189
	2	501	729	123	637	167	258	189
	3	418	729	294	904	167	273	189
	Total	501	729	186	767	167	266	189
2001	**1**	560	729	2686	1834	167	252	189
	2	421	729	2052	1696	167	265	189
	3	546	729	424	976	167	272	189
	Total	504	729	1744	1617	167	267	189

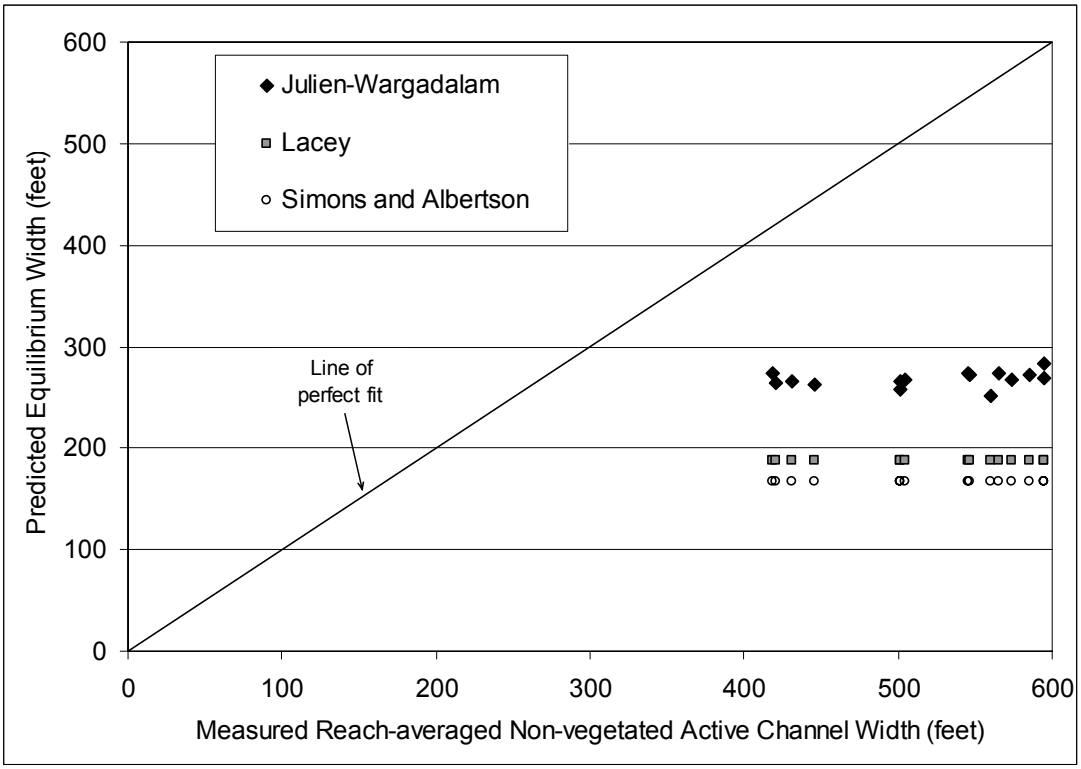

Figure 5-4 – Downstream hydraulic geometry equation results – Predicted equilibrium width in feet vs. measured reach-averaged non-vegetated active channel width in feet

Empirical width-discharge relationships ($w=aQ^b$) were developed for the subreaches and the entire study reach based on the non-vegetated active channel width measured from the GIS coverages of the non-vegetated active channel (Figure 3-13, Table 5-3). The results of this analysis are shown in Figure 5-5. The exponent b of the relationship for subreach 3 is almost half of the exponents of the relationships for subreaches 1 and 2. Therefore, for the same change in discharge, subreaches 1 and 2 seems to change their widths more than subreach 3.

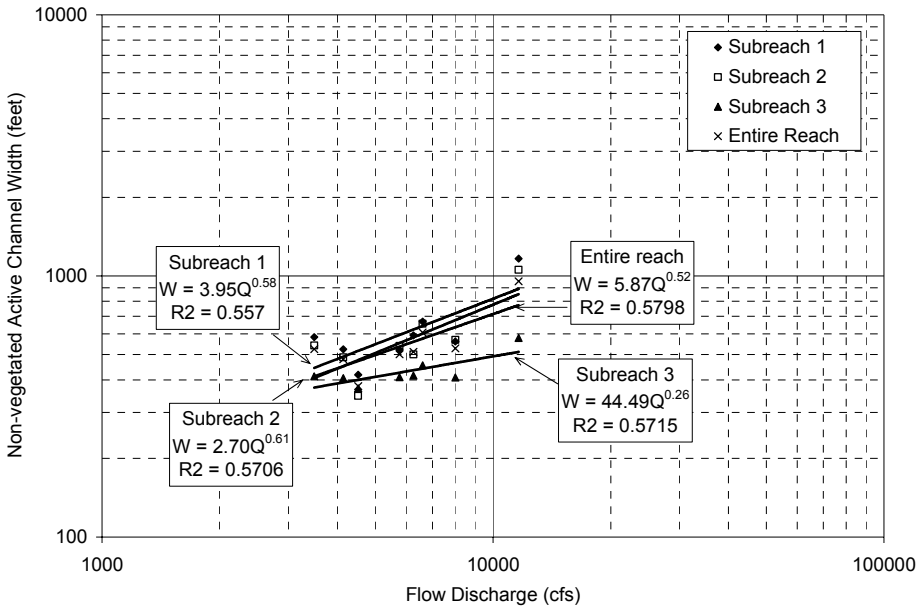

Figure 5-5 Empirical width-discharge relationships for the Bernalillo Bridge reach and subreaches

Equilibrium Channel Width Analyses

- Williams and Wolman (1984) Hyperbolic Model

Four hyperbolic equations were fitted to the subreaches and entire study reach data to describe the changes in channel width with time. Table 5-11 lists the fitted equations and the regression coefficients. Figures 5-6 (a, b, c and d) illustrate the results. The hyperbolic functions fit the data very well and could be used to describe past trends of channel width. This model indicates that the channel width did not change significantly between 1962 and 1992.

Table 5-11 Change in width with time hyperbolic equations and regression coefficients

Reach	Fitted Equation	r^2
1	$\frac{W_t}{W_i} = \frac{t}{-1.74069t - 9.30086} + 1$	0.6377
2	$\frac{W_t}{W_i} = \frac{t}{-1.67265t - 16.41757} + 1$	0.979
3	$\frac{W_t}{W_i} = \frac{t}{-2.93345t - 26.52193} + 1$	0.8084
Total	$\frac{W_t}{W_i} = \frac{t}{-1.85820t - 14.46590} + 1$	0.8995

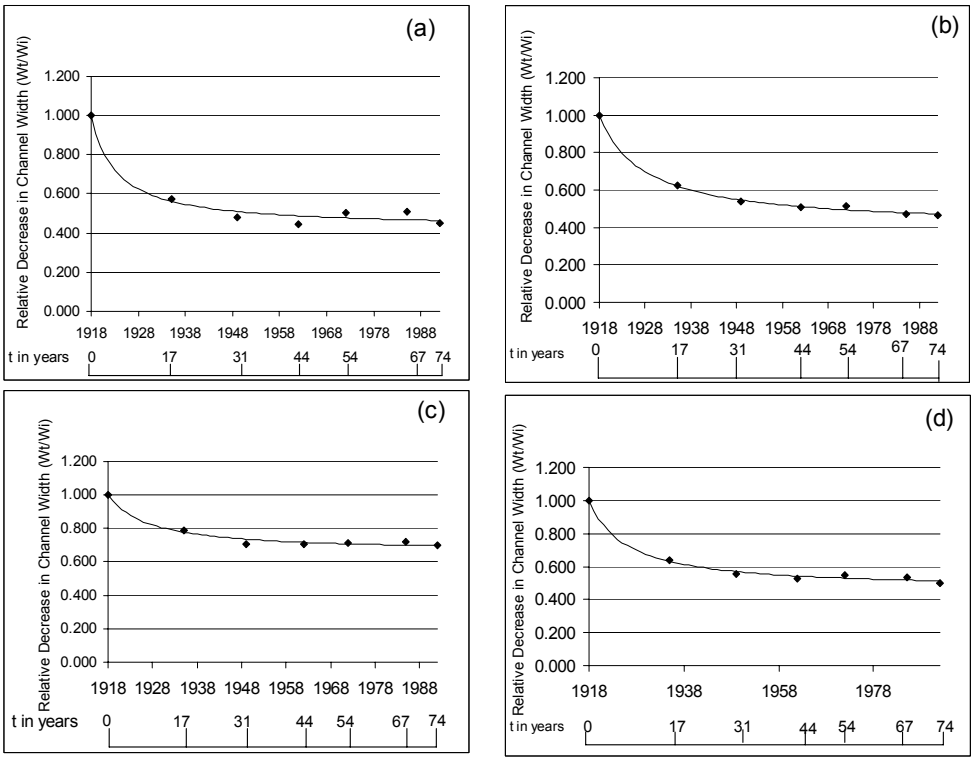

Figure 5-6 Relative decrease in channel width in (a) Subreach 1, (b) Subreach 2, (c) Subreach 3 and (d) Bernalillo Bridge Reach

- Richard (2001) Exponential Model

The exponential model was fitted to the Bernalillo Bridge reach data. The k_1 and W_e values were estimated using methods 1 and 2. Method 3 was not used because none of the hydraulic geometry equations yielded good results. Figures 5-7 (a,b,c,d) represent the regression lines between the width change rate vs. the non-vegetated active channel width for the subreaches and the entire reach from 1918 to 1992. The resulting empirically determined k_1 and W_e values and the r^2 of the regressions are listed in Table 5-12 (method 1).

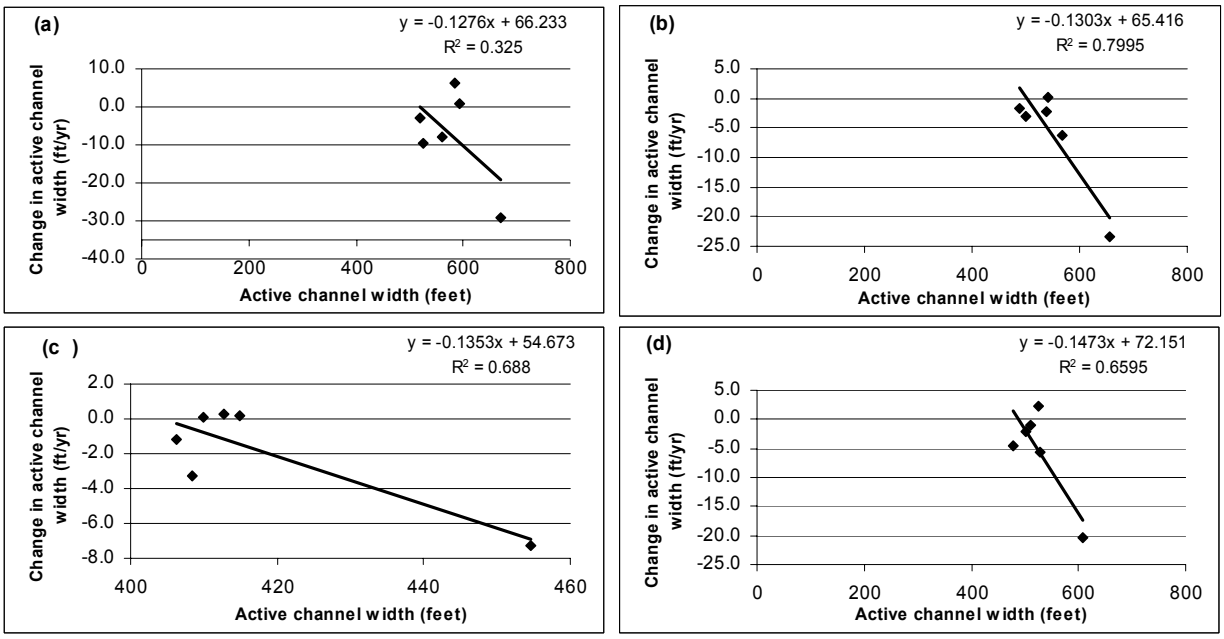

Figure 5-7 Linear regression results of subreach and entire reach data – observed width change (ft/year) with observed channel width (feet). (a) Subreach 1, (b) Subreach 2, (c) Subreach 3, (d) Entire Reach

Table 5-12 Empirical estimation of k_1 and W_e from linear regressions of width vs. width change data (Method 1)

	K_1	K_1W_e	W_e	r-sq
Subreach 1	0.1276	66.233	519	0.33
Subreach 2	0.1303	65.416	502	0.80
Subreach 3	0.1353	54.673	404	0.69
Entire reach	0.1473	72.151	490	0.66

The empirically determined k-values were used and the equilibrium width values were varied to produce a "best-fit" equation that minimized the SSE between the predicted and observed widths from 1918 to 1992 (method 2). Figures 5-8 (a,b,c,d) show the resulting exponential models from both methods. Table 5-13 summarizes the results and Table 5-14 summarizes the exponential equations.

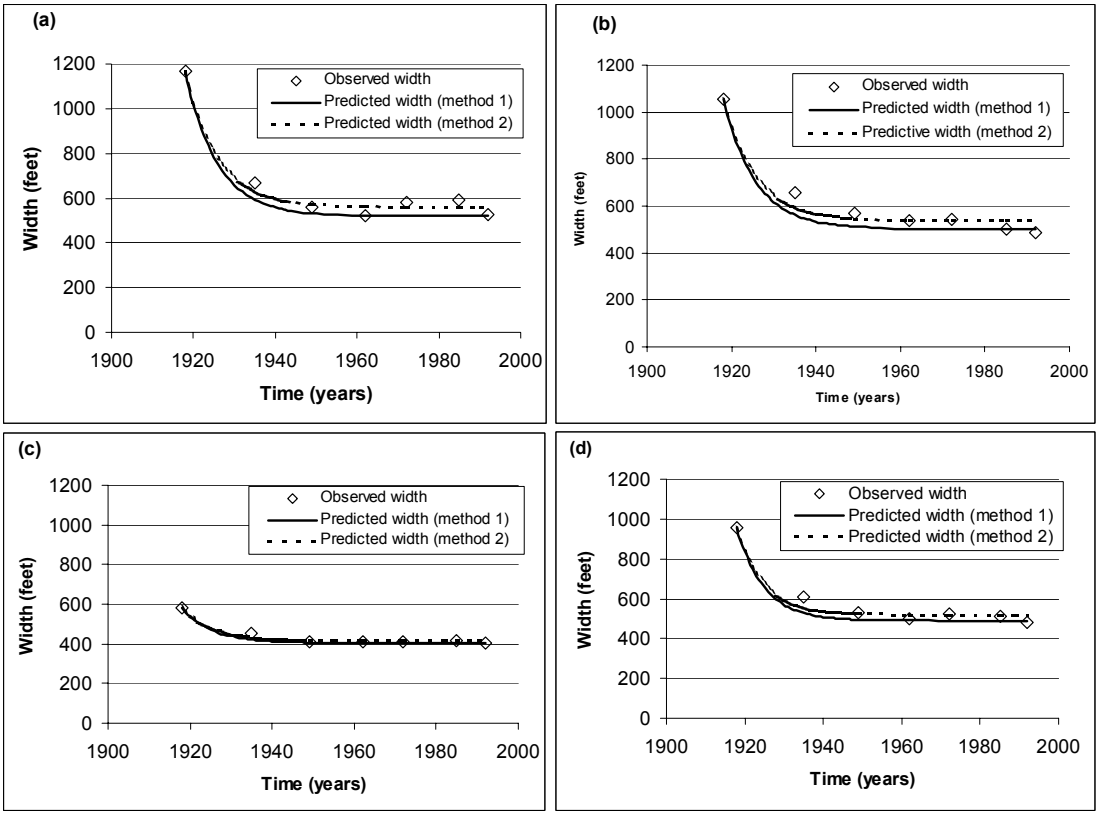

Figure 5-8 Application of exponential model of width change using methods 1 and 2 to estimate k_1 and W_e values. (a) Subreach 1, (b) Subreach 2, (c) Subreach 3 and (d) Entire Reach

Both models fit the data very well and could be used to describe past trends of channel width. These models indicate that the channel width did not change significantly between 1962 and 1992.

Table 5-13 Exponential model results using methods 1 and 2

Subreach 1		Method 1	Method 2		
Year	Wt (ft)	Predicted width (ft) with empirical k_1 and W_e	Predicted width (ft) with empirical k_1 and varying W_e	Guessed W_e	SSE
1918	1165	1165	1165	560	0
1935	669	593	629		1574.63
1949	561	531	572		128.888
1962	521	521	563		1751.962
1972	583	520	561		494.062
1985	592	519	560		1008.736
1992	524	519	560		1315.517
				SSE =	6273.796
Subreach 2					
1918	1055	1055	1055	536	0
1935	656	562	593		3972
1949	569	512	546		550
1962	539	504	538		1
1972	541	503	537		20
1985	500	502	536		1308
1992	488	502	536		2334
				SSE =	8185
Subreach 3					
1918	579	579	579	414	0
1935	455	422	431		575.7871
1949	408	407	417		67.30634
1962	410	405	415		22.2117
1972	413	404	414		2.350109
1985	415	404	414		0.3875
1992	406	404	414		62.40738
				SSE =	730.4502
Entire reach					
1918	954	954	954	518	0
1935	607	528	553		2924.805
1949	527	495	522		28.41353
1962	501	491	518		307.4722
1972	524	490	518		42.30177
1985	512	490	518		33.61447
1992	479	490	518		1454.069
				SSE =	4790.676

Table 5-14 Exponential equations of change in width with time using methods 1 and 2

Subreach	Method 1	Method 2
1	$W_1 = 519 + 646 * e^{-0.1276*t}$	$W_1 = 560 + 605 * e^{-0.1276*t}$
2	$W_2 = 502 + 553 * e^{-0.1303*t}$	$W_2 = 536 + 519 * e^{-0.1303*t}$
3	$W_3 = 404 + 175 * e^{-0.1353*t}$	$W_3 = 414 + 165 * e^{-0.1353*t}$
Entire reach	$W_t = 490 + 464 * e^{-0.1473*t}$	$W_t = 518 + 436 * e^{-0.1473*t}$

6 DISCUSSION

6.1 HISTORIC TREND ANALYSIS AND CURRENT CONDITIONS

Entire Bernalillo Bridge Reach

Discharge - Total annual water discharge at the Albuquerque gage increased from 1978 to 1987 by a factor of two (Figure 4-1). After 1987, the total annual water discharge declined to a value slightly higher than the total annual water discharge prior to 1978. Factors such as management of Cochiti Dam, climatic changes, irrigation and other water diversions could be responsible for these changes.

Suspended Sediment - The total annual suspended sediment discharge at the Albuquerque gage reveal a decreasing trend of suspended sediment load though time. This decreasing trend exacerbates after 1973, when Cochiti Dam started to impound water (Figure 4-2).

Bed Material – The median bed material size in the Bernalillo Bridge reach comprises fine sand in 1962, fine to medium sand in 1972, medium sand to very fine and medium gravel in 1992, and from medium sand to very coarse gravel in 2001.

The channel bed was composed of sand at all water discharges during the 1952 - 1969 period at the Bernalillo gage (Nordin and Beverage 1964, León C. 1998). Bed material surveyed during early summer in 2001, exhibit a bimodal size distribution (0.46mm < d_{50} < 18.13 mm) (Table 3-7). This conclusion is corroborated with recent field observations (Massong pers. comm. 2000). In summary, the bed material in the study reach has changed from sand to a bimodal sand and gravel bed material distribution from 1972 to 2001.

Channel Pattern – Qualitative observation of the GIS coverages of the non-vegetated active channel show that the greatest change in channel width occurred from 1918 to 1935. Channel width of the study reach has been controlled since the 1930's after the construction of the floodway during the 1930 to 1935 period (Woodson and Martin 1962). The floodway was built to contain the river in its channel and prevent avulsions from forming in the adjacent areas (Sanchez et. al 1997). According to the non-vegetated active channel widths computed from the GIS coverages, no significant change in width is observed between 1949 and 1992. Channel width decreased from 1992 to 2001 for subreaches 1 and 2, and increased for subreach 3 during this same time period.

The 1962, 1972 and 1992 aerial photos reveal a straight river with multiple channels at discharges below bankfull. Aerial photos of the river for 2001 reveal vegetated islands lateral to the low flow channel in the upper end of the study reach and several sediment bars within the low flow channel in other short reaches.

Channel Classification - Based on the results of the channel classification methods, the observed 2001 channel planform is represented best by Henderson's method, which predicts a braided channel. Other methods, such as Leopold and Wolman's and Schumm and Khan's methods, which all predicted straight channel planform at 5,000 cfs, illustrate the low sinuosity (<1.5) of the channel throughout the time period analyzed.

Vertical Movement - Analysis of the mean bed elevation indicates that the channel aggraded approximately 1.3 feet from 1962 to 1972 and degraded approximately 2.6 feet from 1972 to 1992 (Figure 3-8). The net change in channel elevation between 1962 and 1992 is approximately 1.3 feet. CO-line surveys show small degradation (about 1 foot) in the 1990's in the upper and middle part of the reach and almost constant thalweg elevation in the lower part of the reach (Figure 3-6). The apparent degradation trend observed in the upper and middle sections of the reach might be due to the fact that the bed material sediment is finer in those sections and therefore, more easily entrained by the spring runoffs. The 1972 to 1992 bed degradation trend continued until 2001, the bed degraded up to 2 feet in subreaches 1 and 2 and aggraded up to 1 foot in subreach 3 between 1992 and 2001.

Channel Geometry - General trends in channel geometry based on HEC-RAS results at 5,000 cfs from 1962 to 2001 include a decrease in width, width-depth ratio, wetted perimeter, and velocity and an increase in cross sectional area and depth. Water surface and energy slopes did not change. The changes in non-vegetated active channel width measured from the GIS coverages also show decreasing width since 1918 (Figure 3-13). Channel width remained almost constant between 1949 and 1992 and declined during the 1992-2001 period (Figure 3-13).

Overbank flow/channel capacity - Based on the results from HEC-RAS runs at 5,000 the overbank flow area is greater for the 1972 data than for 1962, 1992 and 2001. The 1972 channel had the largest cross sections in which the channel-forming discharges flowed out of the main channel into the overbank area. This illustrates the aggradational trend evident in the mean bed elevation profiles.

Subreach Trends

Channel Pattern - In general, the channel has maintained virtually the same width from 1949 to 1992. Channel width decreased from 1992 to 2001. The greatest change in width occurred between 1918 and 1935. Subreaches 1 and 2 have experienced almost the same changes in width. Subreach 3, which is the narrowest of the three subreaches, depicts the smallest change in width since 1918. The three subreaches are fairly straight and reflect a multi-channel configuration at flows below bankfull (< 5,000 cfs). Subreach 1 reflects a multi-channel configuration at high flows as well.

Vertical Movement – The three subreaches aggraded about 1.3 feet from 1962 to 1972 and degraded almost 2.5 feet from 1972 to 1992 (Figure 3-8, Table 3-5). Maximum changes in mean bed elevation occurred in subreaches 1 and 3 during 1972 and 1992 period. Minimum changes in mean bed elevation (< 2 ft) occurred in the transition from subreaches 1 to 2 and at the upper end of subreach 3 during the same time period. Subreaches 1 degraded while subreaches 2 and 3 aggraded during the 1992-2001 period (Figure 3-7).

Channel Geometry – Width, width/depth ratio, wetted perimeter, and velocity decreased while cross sectional area and flow depth increased in subreaches 1 and 2 between 1962 and 2001. Area, wetted perimeter and velocity decreased in subreach 3 while width, depth, and width-depth ratio increased. Energy and water surface slope did not change in subreach 1 and decreased in subreach 2. Energy slope decreased and water surface slope increased in subreach 3. Table 6-1 summarizes the net channel changes between 1962 and 2001 for all the subreaches and the entire reach. A plus (+) indicates an increase in the magnitude of the parameter, a minus (-) a decrease and the equal sign (=) indicates no change.

Table 6-1 Summary of channel changes between 1962 and 2001 based on reach-averaged main channel parameters from HEC-RAS modeling runs at Q = 5,000 cfs.

1962-2001 Period								
Reach	**W**	**EG-Slope**	**Velocity**	**Area**	**D**	**F =W/D**	**WP**	**WS slope**
1	-	=	-	+	+	-	-	=
2	-	-	-	+	+	-	-	-
3	+	-	-	-	+	+	-	+
Total	-	=	-	+	+	-	-	=

W = width, EG-Slope = energy grade line slope, D = depth, F = width/depth ratio, WP = wetted perimeter, WS slope = water surface slope

Table 6-2 summarizes the channel changes during 1962-1972, 1972-1992, and 1992-2001 periods. The active channel width slightly increased in all subreaches in the 1962-1972 period as a result of the aggradation of the river bed. Channel area increased and mean velocity decreased in subreaches 1 and 2. The opposite trends are observed in subreach 3. Active channel width, width/depth ratio and wetted perimeter decreased while mean velocity increased in all subreaches during the 1972-1992 time period. These changes are the result of the degradation trend after 1972. The increase in cross section area, flow depth, and wetted perimeter between 1992 and 2001 also reflect the effect of the degradation of the bed during that time period. The decrease in velocity is likely the primary result of the increase in roughness of the channel in 2001.

GIS coverage's reflect the same trends in channel width obtained from the HEC-RAS analysis. In summary, the overall reach-averaged changes are a decrease in width, width/depth ratio, wetted perimeter and flow velocity and an increase in area and depth in the 1962-2001 time period.

Table 6-2 Summary of channel changes during 1962-1972 and 1972-1992 periods based on reach-averaged main channel parameters from HEC-RAS modeling run at Q = 5,000 cfs.

1962-1972 Period								
Reach	**W**	**EG-Slope**	**Velocity**	**Area**	**D**	**F =W/D**	**WP**	**WS slope**
1	+	-	-	+	+	-	+	+
2	+	=	-	+	-	+	+	-
3	+	+	+	-	-	+	+	+
Total	+	-	-	+	+	+	+	=

1972-1992 Period								
Reach	**W**	**EG-Slope**	**Velocity**	**Area**	**D**	**F =W/D**	**WP**	**WS slope**
1	-	+	+	-	-	-	-	-
2	-	=	+	-	+	-	-	+
3	-	=	+	+	+	-	-	=
Total	-	+	+	-	-	-	-	=

1992-2001 Period								
Reach	**W**	**EG-Slope**	**Velocity**	**Area**	**D**	**F =W/D**	**WP**	**WS slope**
1	-	=	-	+	+	-	-	=
2	-	-	-	+	-	+	+	-
3	+	-	-	+	+	+	+	-
Total	+	-	-	+	+	-	+	-

W = width, EG-Slope = energy grade line slope, D = depth, F = width/depth ratio, WP = wetted perimeter, WS slope = water surface slope.

6.2 SCHUMM'S (1969) RIVER METAMORPHOSIS MODEL

Schumm's (1969) qualitative model of channel metamorphosis is based on the concept that the dimensions, shape, gradient and pattern of stable alluvial rivers are controlled by the quantity of water and sediment as well as the type of sediment moved through their channels. The application of this model is appropriate for rivers in semi-arid regions because they are usually more adjustable than rivers in humid regions due to their less cohesive and less developed bank vegetation. The following equations summarize Schumm's results. A plus exponent indicates an increase in the magnitude of a parameter and a minus indicates a decrease:

- Decrease in bed material load:

$$Q_s^- \sim \frac{W^- L^- S^-}{D^+ P^+}$$

- Increase in bed material load:

$$Q_s^+ \sim \frac{W^+ L^+ S^+}{D^- P^-}$$

- Increase in water discharge:

$$Q^+ \sim \frac{W^+ D^+ L^+}{S^-}$$

- Decrease in water discharge:

$$Q^- \sim \frac{W^- D^- L^-}{S^+}$$

- Increase in water discharge and bed material load:

$$Q^+ Q_t^+ \sim \frac{W^+ F^+ L^+ S^{\pm} D^{\pm}}{P^-}$$

- Decrease in water discharge and decrease in bed material load:

$$Q^- Q_t^- \sim \frac{W^- F^- L^- S^{\pm} D^{\pm}}{P^+}$$

Where,

Q = water discharge,

Q_s = bed material load,

Q_t = percentage of total sediment load that is bed-load or ratio of bedload (sand size or larger) to total sediment load x 100 at mean annual discharge,

W = channel width,

D = flow depth,

F = width/depth,

L = meander wavelength,

P = sinuosity, and

S = channel slope.

These equations are summarized in Table 6-3. Table 6-4 summarizes the trends in channel changes in the Bernalillo Bridge reach for the 1962 to 1972, 1972 to 1992, and 1992 to 2001 time periods in a similar manner as Table 6-3 for purposes of comparison.

Table 6-3 Summary of Schumm's (1969) channel metamorphosis model.

	W	D	S	W/D =F	P	L
Qs^-	-	+	-		+	-
Q^+	+	+	-			+
Qs^+	+	-	+		-	+
Q^-	-	-	+			-
Q^-Qs^-	-	+ -	+ -	-	+	-
Q^+Qs^+	+	+ -	+ -	+	-	+

Table 6-4 Summary of channel changes during 1962-1972, 1972-1992, and 1992-2001 periods.

1962-1972 Period					
Reach	W	D	F =W/D	EG-Slope	P
1	+	+	-	-	-
2	+	-	+	=	-
3	+	-	+	+	+
Total	+	+	+	-	-

1972-1992 Period					
Reach	W	D	F =W/D	EG-Slope	P
1	-	-	-	+	+
2	-	+	-	=	+
3	-	+	-	=	=
Total	-	-	-	+	+

1992-2001 Period					
Reach	W	D	F =W/D	EG-Slope	P
1	-	+	-	=	+
2	-	-	+	-	-
3	+	+	+	-	+
Total	+	+	-	-	=

According to Schumm's (1969) metamorphosis model, changes in channel geometry, slope and planform in the Bernalillo Bridge Reach from 1962 to 1972 were the response to increasing mean annual flood (Q^+) and increasing bed-material load (Q_s^+). The large suspended sediment concentration (Figures 4-2 and 4-3) observed at the Bernalillo and Albuquerque gages are in agreement with the modeled results, assuming that the bed-material load was also large during the 1962-1972 period. Conversely, annual peak flows appear to be lower between 1962 and 1972 than during previous years (Figure 2-8, Appendix C).

The 1972-1992 changes in channel geometry, slope and planform in the study reach are best explained by decrease in discharge (Q^-) and bed-material load (Q_s^-). The model results are supported by the decrease in suspended sediment concentration since 1973 (Figure 4-2 and 4-3). However, the decrease in annual peak flows at San Felipe and Albuquerque are not in agreement with the model prediction (Figure 2-8, Appendix C).

The channel width changed only from 501 ft to 504 ft from 1992 to 2001, which is not a

significant change. The channel depth increased during the same time period. Therefore, the width-depth ratio decreased. The changes in channel geometry between 1992 and 2001 are also best explained by the decrease in discharge (Q^-) and bed-material load (Q_s^-).

Schumm's (1969) model uses mean-annual flows instead of annual peak flows. The annual peak flows are more uniformly distributed after 1963 (Figure 2-8). There are fewer low and high flows and therefore, more frequent flows between 3,000 cfs and 7,000 cfs. It is possible that peak discharges are not indicative of the channel forming discharge regime. Additionally, changes in water regime could have been less significant than changes in sediment load and therefore, the channel could have been responding primarily to the changes in the sediment regime.

6.3 POTENTIAL FUTURE EQUILIBRIUM CONDITIONS

Sediment Transport Analysis

Sediment transport equations predict bed-material loads lower than the incoming sand-load (0.0625 mm to 2 mm) to the reach (21,672 tons/day) for 1992 and 2001. The incoming bed-material load (0.36 mm < d_s < 2 mm) to the reach (10,836 tons/day) is comparable to the sediment transport capacities estimated by most sediment transport equations for 1992 (Tables 5-7 and 5-9). The equation that yields closer results to the incoming bed-material load is Yang sand (d_{50} and size fraction) for all subreaches. The channel slope in 1992 seems appropriate to transport the incoming bed-material load of 10,836 tons/day. However, the degradation of the river bed between 1992 and 2001 indicates that the transport capacity of the stream is larger than the sediment supply and therefore, is not in agreement with the results of the sediment transport analysis for 1992.

The transport capacities computed for subreaches 1 and 2, based on the 2001 bed material gradation analyses, are much lower than the estimated bed-material load. It is likely that a layer of sand coming from tributaries and mined from the bed and banks of the channel upstream from the study reach overlay and move above a layer of coarser material (armor layer) that the river cannot transport. The averaged transport capacity of subreach 3 for 2001 is less than 50 % of the bed-material load (10,836 tons/day) and is about half of the capacity of that subreach in 1992, likely due to the reduction of flow velocity and friction slope from 1992 to 2001. In summary, the transport capacity of this reach has decreased from 1992 to 2001.

Equilibrium Channel Width Analysis

- Williams and Wolman (1984) Hyperbolic Model

Hyperbolic equations fit the historical data very well and therefore could be used to describe the past trends in channel width. Table 6-5 contains the 1991-1992 rate of decrease in channel width in feet per year, the 2001 active channel widths in feet from GIS and the 2001 channel widths in feet predicted with the hyperbolic functions. 1991-1992 rates of decrease in channel width were computed as the slope of the hyperbolic function between 1991 and 1992. These rates are very low and suggest that the channel widths are still decreasing at a slow rate. The active channel widths for 2001 from the digitized aerial photos are less than the 2001 widths calculated from the regression equations. The coarsening of the bed material between 1992 and 2001 might have caused the reduction of width during that period. This model indicates that the channel width did not change significantly between 1962 and 1992.

Table 6-5 1991-1992 rate of decrease in channel width according to the hyperbolic model and 2001 predicted and measured widths

Reach	1991-1992 rate of decrease in channel width (ft/yr)	Predicted 2001 width from hyperbolic equations (ft)	2001 non-vegetated width from GIS in ft
1	-0.6	536	418
2	-0.9	491	347
3	-0.3	401	371
Total	-0.6	485	378

- Richard (2001) Exponential Model

Exponential equations fit the historical data very well and therefore could be used to describe the past trends in channel width. Table 6-6 summarizes the 1985-1992 rate of change of width in feet per year, the predicted 2001 widths in feet from the exponential equations and the 2001 non-vegetated channel widths in feet from the digitized aerial photos. The exponential model produces lower rates of decreasing channel width with time than the hyperbolic model. The predicted 2001 widths are greater than the measurements. This model indicates that the channel width did not change significantly between 1962 and 1992.

Table 6-6 1985-1992 rate of decrease in channel width according to the exponential model and 2001 predicted and measured widths

Reach	1985-1992 rate of decrease in channel width (ft/yr)		Predicted 2001 width from hyperbolic equations (ft)		2001 non-vegetated width from GIS in ft
	Method 1	Method 2	Method 1	Method 2	
1	-0.011	-0.010	519	560	418
2	-0.008	-0.007	502	536	347
3	-0.002	-0.002	404	414	371
Total	-0.002	-0.002	490	518	378

Hydraulic Geometry

The hydraulic geometry equations do not predict the historical width values well. However, the predicted widths illustrate the nearly constant width of the channel between 1962 and 1992. The conditions of the Bernalillo Bridge reach are out of the range of applicability of Nouh's and Blench's equations. Lacey's, Simons and Albertson's, Julien-Wargadalam's and Klassen and Vermeer's equations under estimate the channel width for all the reaches and years.

7 SUMMARY

This work pertains to the hydraulic modeling analysis of the Bernalillo Bridge reach of the Middle Rio Grande, which spans 5.10 miles from New Mexico Highway 44 (agg/deg 298) to cross section CO-33 (agg/deg line 351). This report characterizes the historic conditions of the study reach and evaluates potential future equilibrium conditions. The general trend of the study reach includes decrease in width, width-depth ratio, wetted perimeter, and velocity and increase in cross sectional area and depth during the 1962 to 2001 time period. Water surface and friction slopes did not change during this same time period. The main conclusions are:

1. The entire reach aggraded approximately 1.3 feet between 1962 and 1972 and degraded approximately 2.6 feet between 1972 and 1992. The bed degraded as much as 2 feet in subreaches 1 and 2 and aggraded as much as 1 foot in subreach 3 from 1992 to 2001.
2. The active channel width of the study reach decreased from 954 feet in 1918 to 378 feet in 2001. The largest change in channel width occurred between 1918 and 1935. After 1949, the channel width remained fairly constant until 1992 (Figure 3-13). A slight increase in channel width occurred as a result of the river bed aggradation between 1962 and 1972. Bed degradation after 1972 induced some narrowing of the channel. The channel width has narrowed from 1992 to 2001, likely due to the coarsening of the bed. Subreach 3 has been narrower than subreaches 1 and 2 throughout the entire period analyzed.
3. Hyperbolic and exponential equations fit the historical width data from 1918 to 1992 well. Both models indicate that the channel width did not change significantly between 1962 and 1992.
4. The four downstream hydraulic geometry equations (Julien-Wargadalam, Lacey, Klaassen and Vermeer, Simons and Albertson) shown in Figure 5-4 under predict the historical channel widths.
5. Planform geometry of the entire reach is a straight single-thread channel with few vegetated islands at bankfull discharge of 5,000 cfs. The channel sinuosity for the entire reach remained nearly constant at 1.10 throughout the entire period analyzed, indicative of a nearly straight channel.

6. According to the modeling results from HEC-RAS, the 1962, 1992, and 2001 channels have greater capacity to convey the modeled discharge (5,000 cfs) without overbank flow than the channel in 1972. The simulated decrease in flow velocity from 1992 to 2001 reduced the capacity of the reach to transport the bed-material load (0.36 mm < d_s < 2 mm) in 2001. This decrease in flow velocity is likely due to the increased roughness in the channel.
7. At the Albuquerque gage, at a flow discharge of 5,000 cfs, very fine and fine sand particles (0.0625 mm < d_s < 0.36 mm) behave as washload. The bed-material load is about 50% of the sand-load (21,672 tons/day). Therefore, the incoming bed-material load is 10,836 tons/day and the washload is 10,836 tons/day.
8. The sediment transport capacity for the sand fractions (0.0625 mm to 2 mm) was calculated using six different equations (Laursen, Engelund and Hansen, Ackers and White, Yang, Einstein and Toffaleti) and the 1992 channel geometry data. The results shown in Tables 5-7 and 5-9 give an average capacity of 7,139 tons/day and vary from 591 tons/day to 14,315 tons/day. None of the calculations exceed 15,000 tons/day.
9. The sediment transport capacities calculated with these equations are comparable to the incoming bed-material load at the Albuquerque gage (10,836 tons/day). The equation that yields closer results to the bed-material load is Yang's equation for sand (d_{50} and size fraction) for all reaches. These results suggest that the measured channel slope in 1992 is appropriate to transport this bed-material load.
10. The transport capacities for the coarse sand and gravel fractions were calculated using five different equations (Yang for gravel, Yang for sand and gravel, Einstein, Meyer-Peter and Muller, and Schoklitsch) and the hydraulic geometry data of 2001 for subreaches 1 and 2. The results shown in Table 5-8 give an average capacity of 401 tons/day and 997 tons/day for subreaches 1 and 2 respectively. None of the calculations exceed 4,000 tons/day.

    The sediment transport capacities calculated with these equations are lower than the bed-material load (10,836 tons/day) at the Albuquerque gage. This is likely due to the coarsening of the bed material.

11. The sediment transport capacity for the sand fractions (0.0625 mm to 2 mm) was calculated using six different equations (Laursen, Engelund and Hansen, Ackers and White, Yang, Einstein and Toffaleti) and the 2001 channel geometry data for subreach 3. The results shown in Table 5-9 give an average capacity of 3,693 tons/day for subreach 3. None of the calculations exceed 8,000 tons/day. The transport capacity of subreach 3 is less than 50 % of the bed-material load (10,836 tons/day) and is about half of the capacity of that subreach in 1992. This reduction of capacity is likely due to the decrease in velocity and water surface slope from 1992 to 2001.

8 REFERENCES

Ackers, P. 1982. Meandering Channels and the Influence of Bed Material. *Gravel Bed Rivers. Fluvial Processes, Engineering and Management*. Edited by R. D. Hey, J.C. Bathurst and C.R. Thorne. John Wiley & Sons Ltd. pp 389-414.

Arritt, S. 1996. Rio Grande Silvery Minnow: Symbol of an Embattled River. New Mexico Wildlife. 41. pp 8-10

ASCE Task Committee on Hydraulics, Bank Mechanics and Modeling of River Width Adjustment. 1998. River Width Adjustment. I: Processes and Mechanisms. Journal of Hydraulic Engineering, ASCE. 124 (9): 881-902.

Baird, D. C. 1996. River Mechanics Experience on the Middle Rio Grande. 6th Federal Interagency Sediment Conference. March 11-14. 8 pp.

Bestgen, K.R. and Platania, S.P.1991. Status and Conservation of the Rio Grande Silvery Minnow, Hybognathus Amarus. The Southwestern Naturalist. 36(2): 225-232.

Blench, T. 1957. *Regime Behaviour of Canals and Rivers*. Butterworths Scientific Publications, London.138 pp.

Brownlie, W.R. 1981. Prediction of Flow Depth and Sediment discharge in Open Channels. W. M. Keck Laboratory of Hydraulics and Water Resources. Division of Engineering and Applied Science. California Institute of Technology. Pasadena, California. Report No. KH-R-43A. 228 pp.

Bullard, K. L. and Lane, W. L. 1993. Middle Rio Grande Peak Flow Frequency Study. U.S. Department of Interior, Bureau of Reclamation, Albuquerque, NM. 36+p.

Burton, G.L. 1997. America's National Wildlife Refuges. Where Wildlife Comes Naturally! Rio Grande Silvery Minnow [Web Page]. Available at: http:// refuges.fws.gov/NWRSFiles/Wildli...nts/Fish/Rio_Grande_Silvery_Minnow.html.

Chang, H.H. 1979. Minimum stream power and river channel patterns. *Journal of Hydrology*, 41, 303-327.

Colby, B.R. and Hembree, C.H. 1955. Computations of Total Sediment Discharge Niobrara River near Cody, Nebraska. Geological Survey Water-Supply Paper 1357. pp.187

Henderson, F.M. 1966. *Open channel flow.* Macmilllan Publishing Co., Inc. New York, NY, 522 pp.

Julien, P. Y. 1995. *Erosion and Sedimentation*, Cambridge University Press, Ny, Ny, 280 pp.

Julien, P. Y. and Wargadalam, J. 1995. Alluvial Channel Geometry: Theory and Applications. *Journal of Hydraulic Engineering*, 121(4), 312-25.

Klaassen, G. J. and Vermeer, K. 1988. Channel Characteristics of the Braiding Jamuna River, Bangladesh. In *International Conference on River Regime, 18-20 May, 1988*, W.R. White (ed.), Hydraulics Research Limited, Wallingford, UK, 173-89.

Knighton, A.D. and Nanson, G.C. 1993. Anastomosis and the continuum of channel pattern. *Earth Surface Processes and Landforms*, 18, 613-625.

Lagasse, P.F. 1981. Geomorphic Response of the Rio Grande to Dam Construction. New Mexico Geological Society, Special Publication. No. 10. pp. 27-46.

León C. 1998. Morphology of the Middle Rio Grande from Cochiti Dam to Bernalillo Bridge, New Mexico. Master Thesis, Colorado State University, 210 pp.

Leopold, L. B. and Maddock, T. Jr. 1953. The Hydraulic Geometry of Stream Channels and Some Physiographic Implications: USGS Professional Paper 252, 57 pp.

Leopold, L.B. and Wolman, M.G. 1957. River Channel Patterns: Braided, Meandering and Straight, USGS Professional Paper 282-B, 85 pp.

Massong, T. 2000. Personal Communication. U.S. Bureau of Reclamation, Albuquerque, NM.
Molnár, P. 2001. Precipitation and Erosion Dynamics in the Rio Puerco Basin. Ph.D. Dissertation. Department of Civil Engineering. Colorado State University, Fort Collins, Colorado. pp. 258.
Mosley, H. and S. Boelman. 1998. Santa Ana Geomorphic Report. Draft. U.S. Bureau of Reclamation, Albuquerque, NM. pp.29.
Nordin, C. and Beverage J. 1965. *Sediment Transport in the Rio Grande, New Mexico*. Geological Survey Professional Paper 462-F, 35 pp.
Nordin, C. and J.K. Culbertson. 1961. Particle-size distribution of stream bed material in the Middle Rio Grande Basin. New Mexico. *Short Papers in the Geologic and Hydrologic Sciences*, Article 147-292, C-323-C-326.
Nouh, M. 1988. Regime channels of an extremely arid zone. *International Conference on River Regime, 18-20 May, 1988*, W.R. White (ed.), Hydraulics Research Limited, Wallingford, UK, 55-66.
Parker, G. 1976. On the cause and characteristic scales of meandering and braiding in rivers. *Journal of Fluid Mechanics*, vl.76, part 3, pp. 457-480.
Pemberton, E.L. 1964. Sediment Investigations-Middle Rio Grande. Journal of the Hydraulic Division. Proceedings of the American Society of Civil Engineers. Vol.90, No. HY2. pp. 163-185.
Platania, S.P. 1991. Fishes of the Rio Chama and Upper Rio Grande, New Mexico, with Preliminary Comments on their Longitudinal Distribution. The Southwestern Naturalist. Vol 36, No. 2. pp.186-193.
Richard G. 2001. Quantification and Prediction of Lateral Channel Adjustments Downstream from Cochiti Dam, Rio Grande, NM. Ph.D. Dissertation. Department of Civil engineering. Colorado State University, Fort Collins, Colorado. pp. 276.
Richardson, E.V, D.B. Simons and P.Y. Julien 1990. Highways in the River Environment. U.S. Department of Transportation. Federal Highway Administrartion, 610 pp.
Robinson, S. 1995. The Life & Times of Rio Grande Minnows. New Mexico Wildlife. 40(6):2-5.
Rosgen, D., 1996. *Applied River Morphology*, Pagosa Springs, CO, Wildland Hydrology. 360+p.
Sanchez, V. and D. Baird, 1997. River Channel Changes Downstream of Cochiti Dam. Middle Rio Grande, New Mexico. Sam S.Y. Wang, E.J. Langendoen and F.D. Shields Jr. Proceedings of the Conference on Management of Landscapes Disturbed by Channel Incision. The University of Mississippi, Oxford, Mississippi: The Center for Computational Hydroscience and Engineering. 6 pp.
Scurlock, D. 1998. From the Rio to the Sierra. An Environmental History of the Middle Rio Grande Basin. USDA, Forest Service, Rocky Mountain Research Station, Fort Collins. General Thechnical Report RMRS-GTR5. 440 p.
Schumm, S. A. 1969. *River Metamorphosis*. Journal of the Hydraulics Division. Vol 95, No. 1. pp. 255-273.
Schumm, S.A. and Khan, H.R. 1972. Experimental study of channel patterns. *Geological Society of America Bulletin,* 83, 1755-1770.
Simons, D.B and Albertson, M.L.1963. Uniform Water Conveyance Channels in Alluvial Material. Transactions of the American Society of Civil engineers. Paper No. 3399. Vol.128, PartI. pp. 65-107.
Stevens, H.H. and Yang, C.T. 1989. Summary and use of selected fluvial sediment-discharge formulas, USGS Water Resources Investigations Report 80-4026, 62 pp.

Taylor, J.P. and Mcdaniel, K.C. Accessed 2001. Restoration of Saltcedar Infested Flood Plains on the Bosque del Apache National Wildlife Refuge [Web page]. Available at : http://bhg.fws.gov/Literatur/newpage12.htm.

Thorne, C. R., R.D. Hey and M. D. Newson. 1997. *Applied Fluvial Geomorphology for River Engineering and Management*. John Wiley & Sons Ltd. 375 pp.

Tofaletti, F.B. 1969. Definitive computations of Sand Discharge in Rivers. *Journal of the Hydraulics Division*, 95, HY1, 225-246

US Army Corps of Engineers. 1998. Hydrologic Engineering Center-River Analysis System User's Manual. Version 2.2. Hydrologic Engineering Center, Davis, California, 227+p.

US Bureau of Reclamation. 1955. Step Method for Computing Total Sediment Load by the Modified Einstein Procedure. Prepared by the Sedimentation Section, Hydrology Branch. pp.18.

US Fish and Wildlife Service. 2000. http://pacific.fws.gov/vfwo/SpeciesAccount/birds/SWWF.htm

Van den Berg, J.H. 1995. Prediction of alluvial channel pattern of perennial rivers. *Geomorphology*. 12, 259-279.

Wargadalam, J. 1993. Hydraulic Geometry Equations of Alluvial Channels, Ph.D. Dissertation. Fort Collins, CO, Colorado State University, 203 pp.

Williams G. and G. Wolman. 1984. *Downstream Effects of Dams on Alluvial Rivers*. Geological Survey Professional Paper 1286, 83pp.

Woodson, R.C. 1961. Stabilization of the Middle Rio Grande in New Mexico. Journal of the Waterways and Harbors Division. Proceedings of the American Society of Civil Engineers. Vol.87, No. WW4. pp.1-15.

Woodson, R. C. and Martin, J. T. 1962. The Rio Grande comprehensive plan in New Mexico and its effects on the river regime through the middle valley, Control of Alluvial Rivers by Steel Jetties, *American Society of Civil Engineers Proceedings, Waterways and Harbors Division Journal 88,* E.J. Carlson and E.A. Dodge (eds.), NY, NY, American Society of Civil Engineers, 53-81.

APPENDIX A – DATA LISTS

TABLE A-1 AERIAL PHOTO
(SOURCE: RICHARD ET AL. 2000)

Aerial Photos digitized in the Rio Grande Geomorphology Study, v. 1 by the USBR, Remote Sensing and Geographic Information Group, Denver, CO:

1) 1918 – Scale: 1:12,000, Hand drafted linens (39 sheets), USBR Albuquerque Area Office. Surveyed in 1918, published in 1922.

2) 1935 – Scale: 1:8,000. Black and white photography, USBR Albuquerque Area Office. Flown in 1935, published 1936.

3) 1949 – Scale 1:5,000. Photo-mosaic. J. Ammann Photogrammetric Engineers, San Antonio, TX. USBR Albuquerque Area Office.

4) March 15, 1962 – Scale: 1:4,800. Photo-mosaic. Abram Aerial Survey Corp. Lansing, MI. USBR Albuquerque Area Office.

5) April 1972 – Scale: 1:4,800. Photo-mosaic. Limbaugh Engineers, Inc., Albuquerque, NM. USBR Albuquerque Area Office.

6) March 31, 1985 – Scale: 1:4,800. Orthophoto. M&I Consulting Engineers, Fort Collins, CO. Aero-Metric Engineering, Sheboygan, MN. USBR Albuquerque Area Office.

7) February 24, 1992 – Scale: 1:4,800. Ratio-rectified photo-mosaic. Koogle and Poules Engineering, Albuquerque, NM. USBR Albuquerque Area Office.

8) Winter 2001 – Scale: 1:4,800. Photo-mosaic. USBR Albuquerque Area Office.

Table A-2 Aerial photo dates and main daily discharge on those days.

Aerial Photo Dates	Mean Daily Discharge at Bernalillo (cfs)	Mean Daily Discharge at Albuquerque (cfs)
February 24, 1992	No data	159
March 31, 1985	No data	109
April 1972	No data	Mean = 705 Max = 2540 Min = 116
March 15, 1962	493	No data
1949 (unknown date)	Extreme low flow (from meta-data file)	No data
1935 (unknown date)	Annual data from Otowi: Mean = 1,520 Max = 7,490 Min = 350	No data
1918 (unknown date)	No data	No data

APPENDIX B – CROSS-SECTION PLOTS

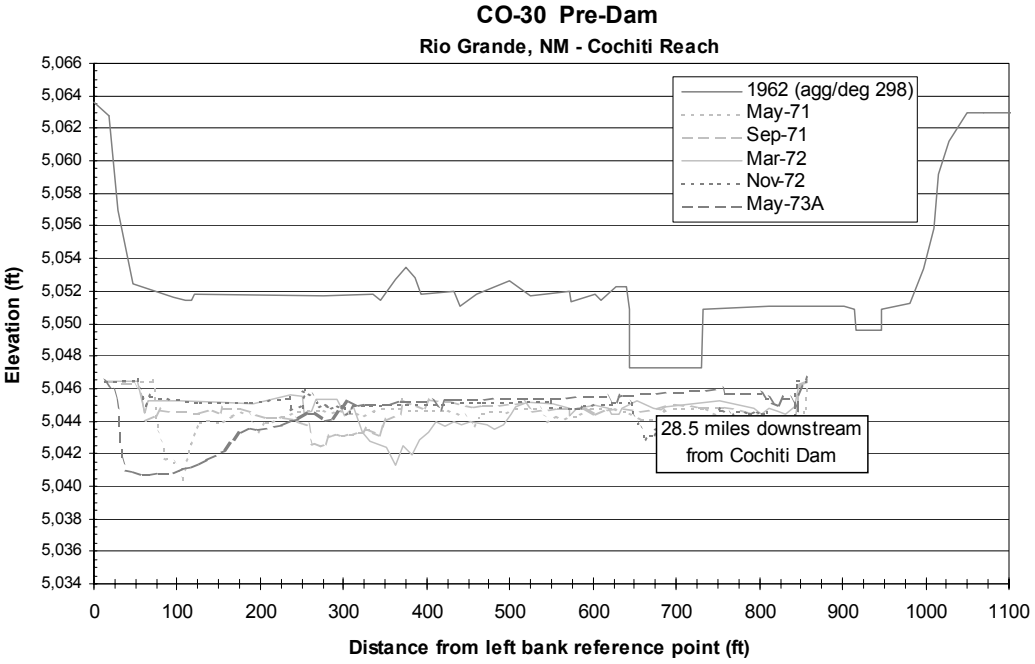

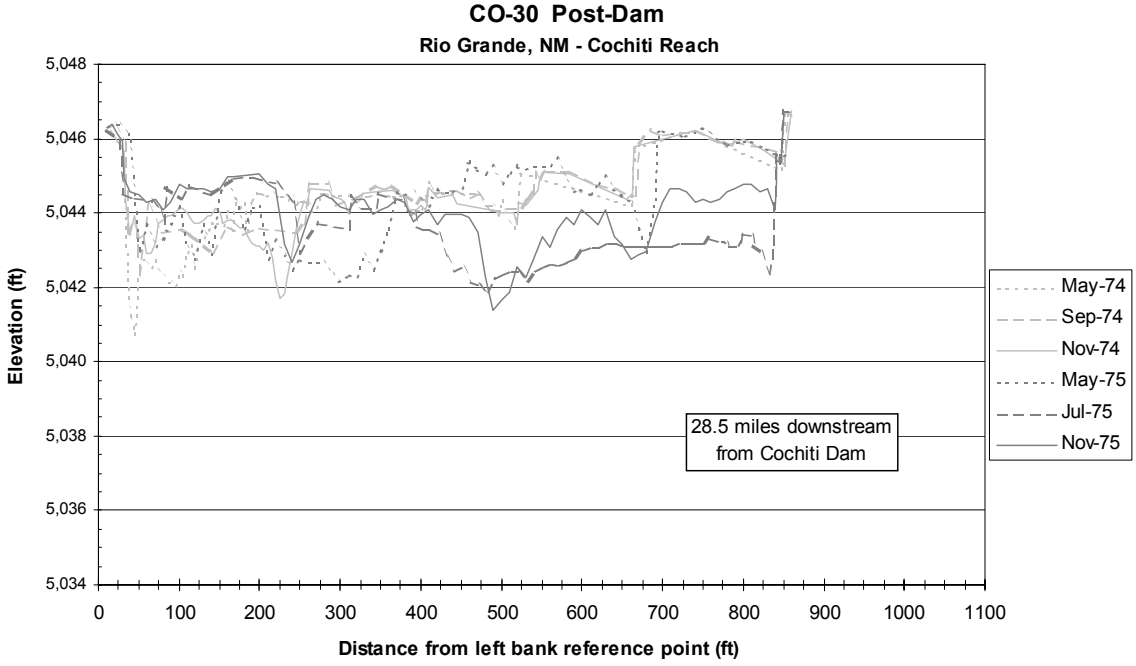

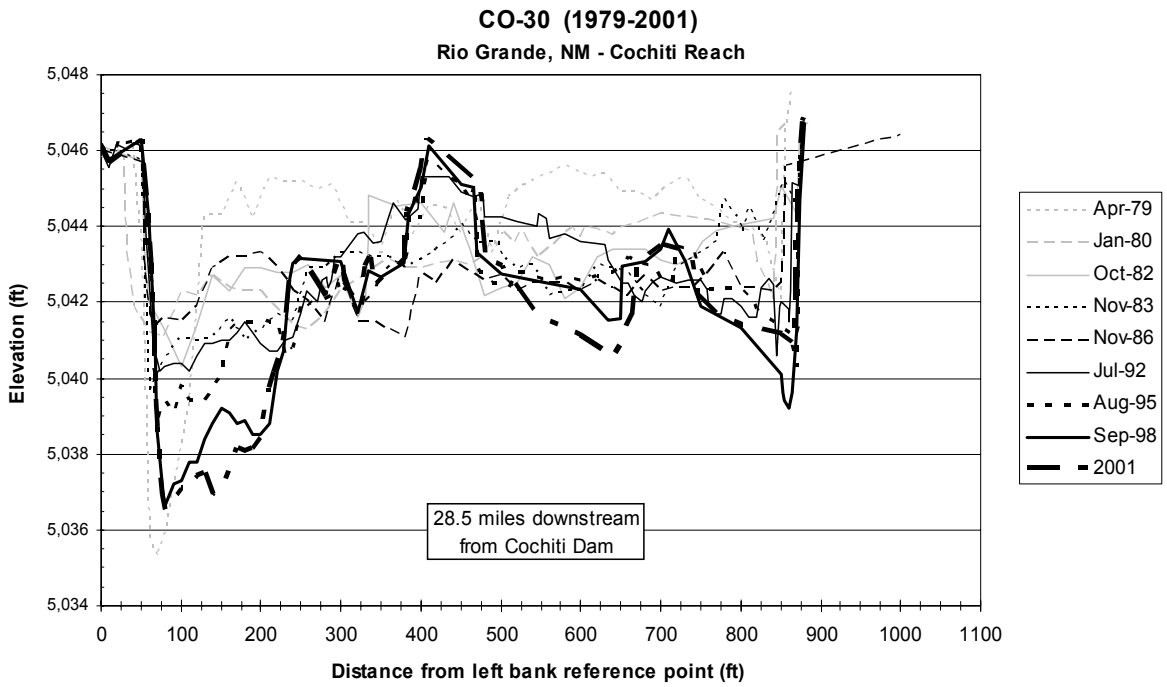
CO-30 (1979-2001)
Rio Grande, NM - Cochiti Reach
Elevation (ft)
5,048
5,046
5,044
5,042
5,040
5,038
5,036
5,034
0
100
200
300
400
500
600
700
800
900
1000
1100
Distance from left bank reference point (ft)
28.5 miles downstream from Cochiti Dam
Apr-79
Jan-80
Oct-82
Nov-83
Nov-86
Jul-92
Aug-95
Sep-98
2001

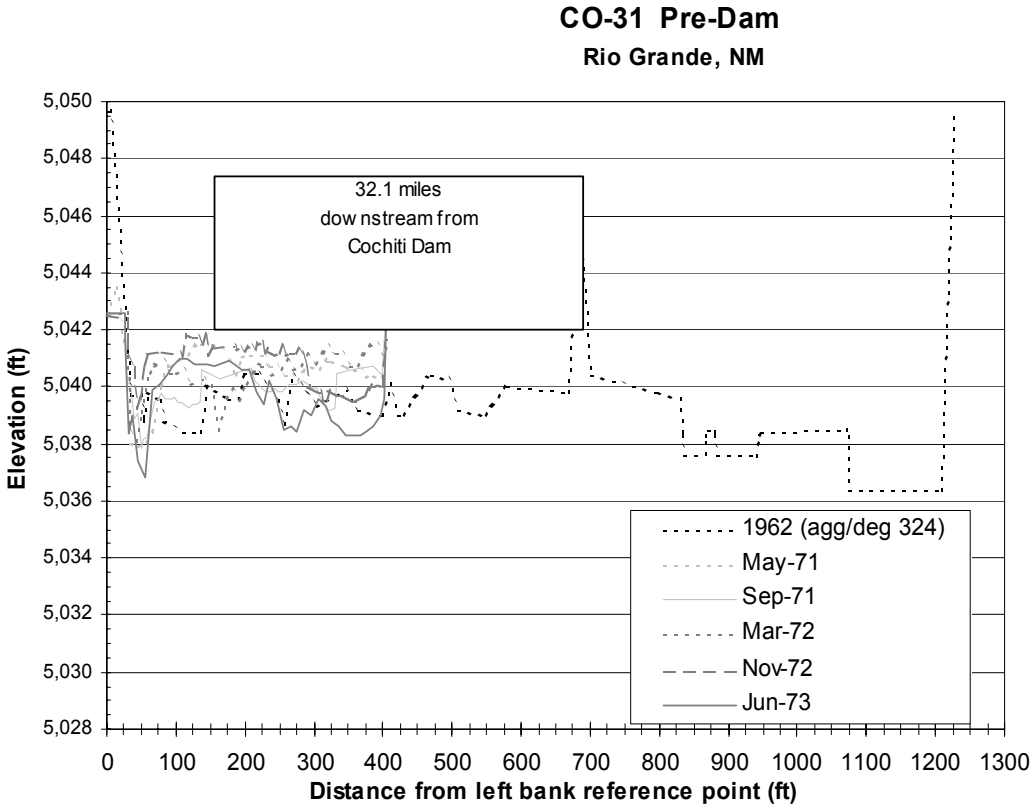
CO-31 Pre-Dam
Rio Grande, NM
Elevation (ft)
5,050
5,048
5,046
5,044
5,042
5,040
5,038
5,036
5,034
5,032
5,030
5,028
0
100
200
300
400
500
600
700
800
900
1000
1100
1200
1300
Distance from left bank reference point (ft)
32.1 miles downstream from Cochiti Dam
1962 (agg/deg 324)
May-71
Sep-71
Mar-72
Nov-72
Jun-73

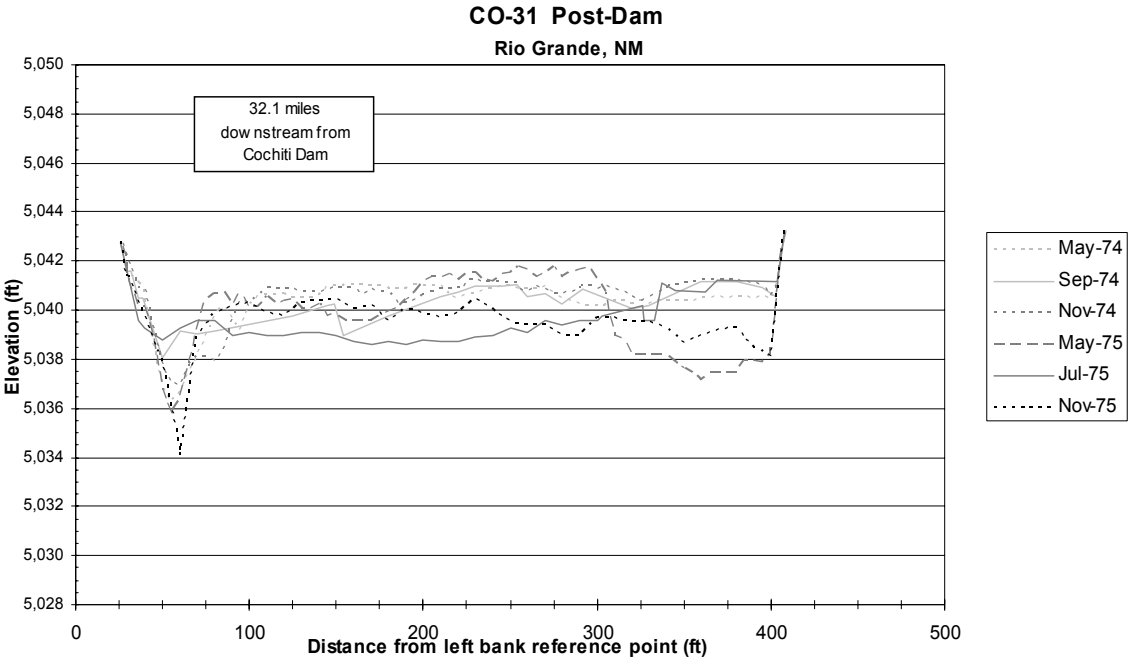
CO-31 Post-Dam
Rio Grande, NM
32.1 miles
dow nstream from
Cochiti Dam
Elevation (ft)
5,050
5,048
5,046
5,044
5,042
5,040
5,038
5,036
5,034
5,032
5,030
5,028
0
100
200
300
400
500
Distance from left bank reference point (ft)
May-74
Sep-74
Nov-74
May-75
Jul-75
Nov-75

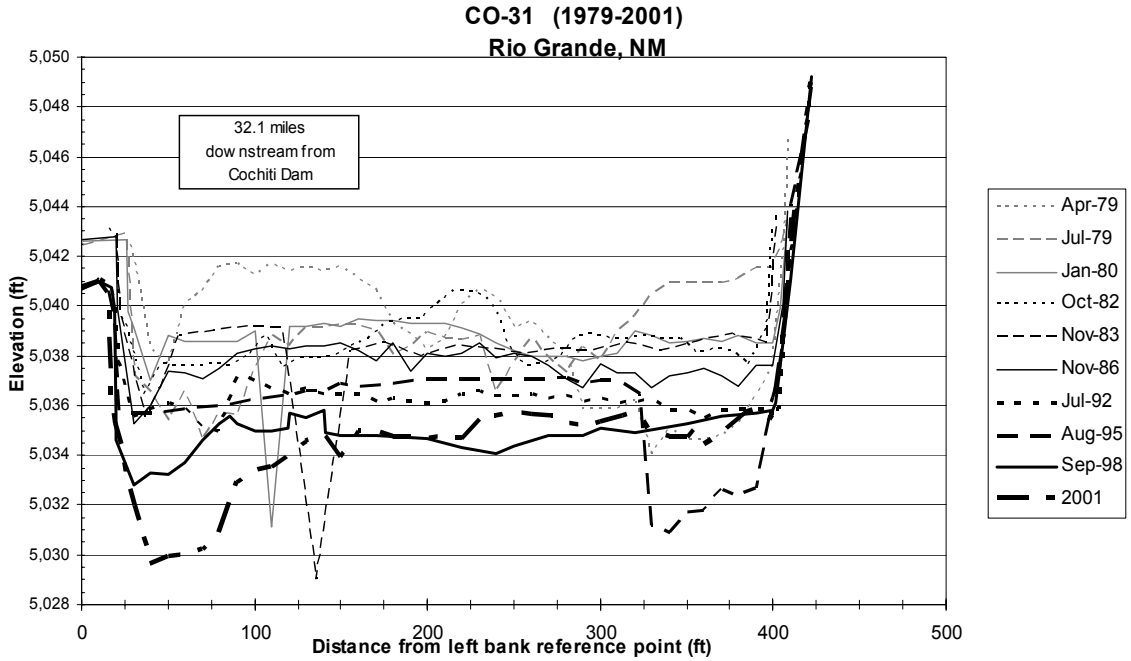
CO-31 (1979-2001)
Rio Grande, NM
32.1 miles
dow nstream from
Cochiti Dam
Elevation (ft)
5,050
5,048
5,046
5,044
5,042
5,040
5,038
5,036
5,034
5,032
5,030
5,028
0
100
200
300
400
500
Distance from left bank reference point (ft)
Apr-79
Jul-79
Jan-80
Oct-82
Nov-83
Nov-86
Jul-92
Aug-95
Sep-98
2001

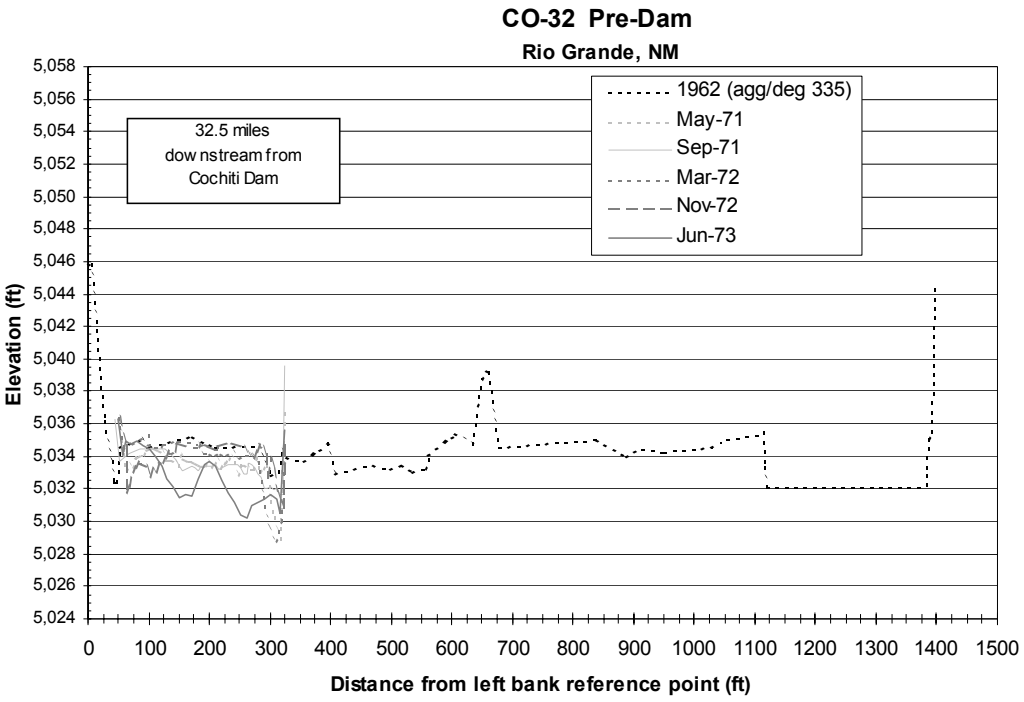
CO-32 Pre-Dam
Rio Grande, NM
32.5 miles
dow nstream from
Cochiti Dam
1962 (agg/deg 335)
May-71
Sep-71
Mar-72
Nov-72
Jun-73
Elevation (ft)
5,058
5,056
5,054
5,052
5,050
5,048
5,046
5,044
5,042
5,040
5,038
5,036
5,034
5,032
5,030
5,028
5,026
5,024
0
100
200
300
400
500
600
700
800
900
1000
1100
1200
1300
1400
1500
Distance from left bank reference point (ft)

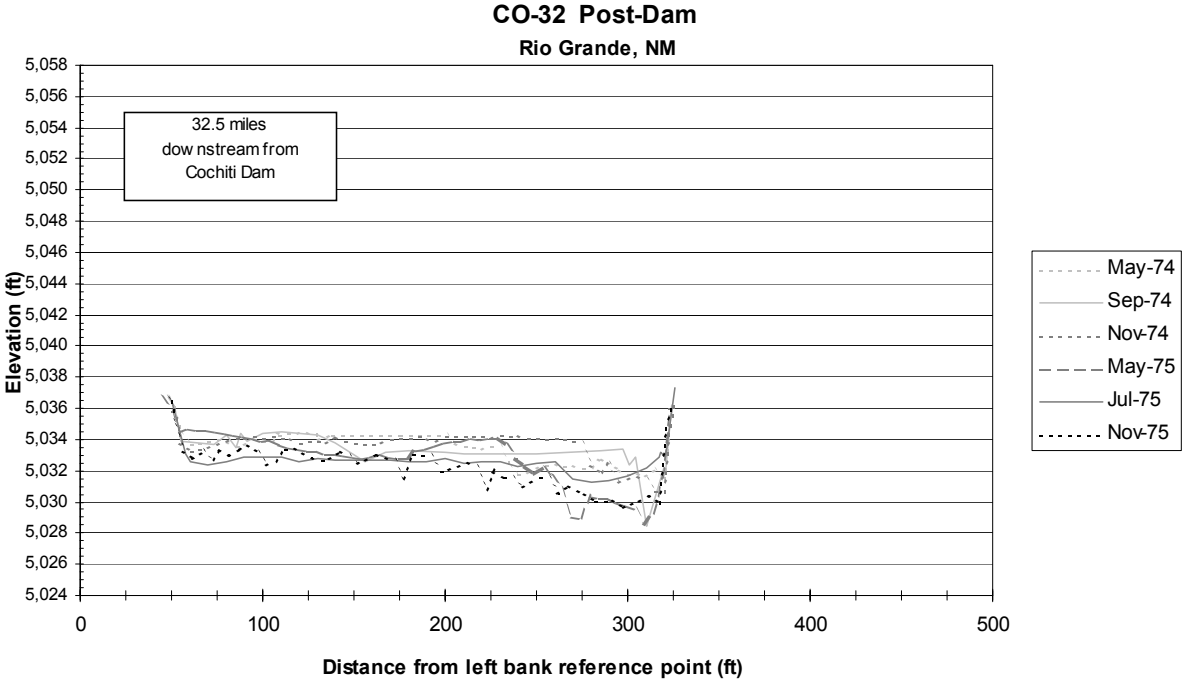
CO-32 Post-Dam
Rio Grande, NM
32.5 miles
dow nstream from
Cochiti Dam
May-74
Sep-74
Nov-74
May-75
Jul-75
Nov-75
Elevation (ft)
5,058
5,056
5,054
5,052
5,050
5,048
5,046
5,044
5,042
5,040
5,038
5,036
5,034
5,032
5,030
5,028
5,026
5,024
0
100
200
300
400
500
Distance from left bank reference point (ft)

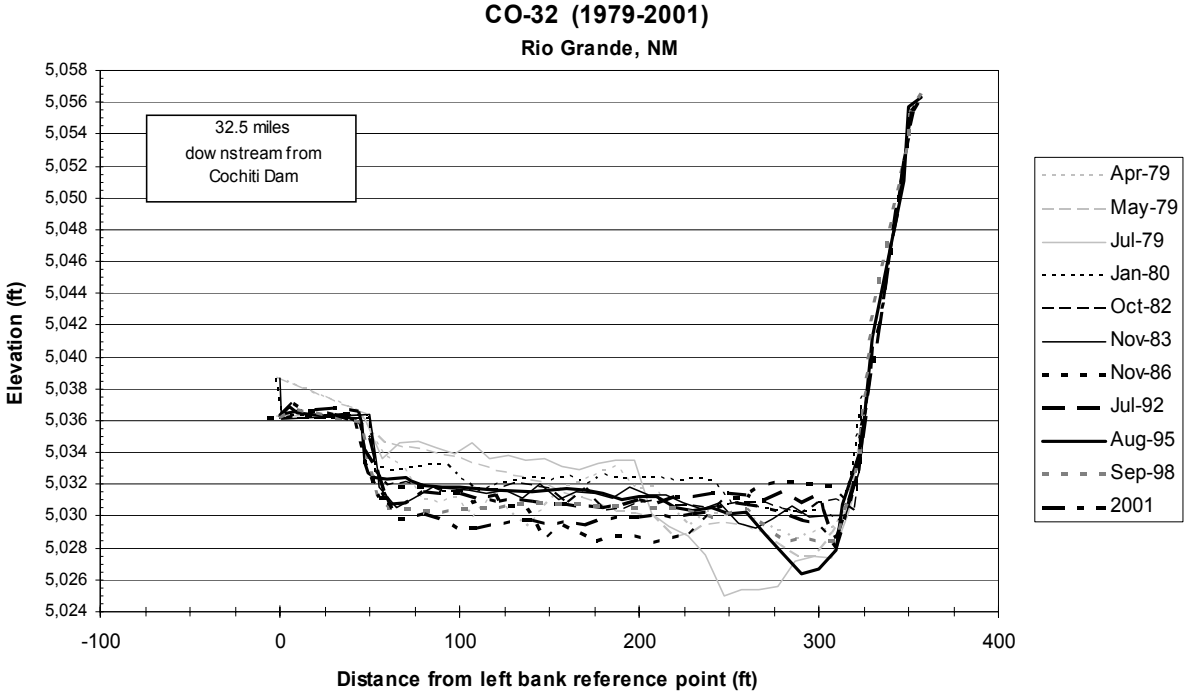
CO-32 (1979-2001)
Rio Grande, NM
32.5 miles
dow nstream from
Cochiti Dam
Elevation (ft)
5,058
5,056
5,054
5,052
5,050
5,048
5,046
5,044
5,042
5,040
5,038
5,036
5,034
5,032
5,030
5,028
5,026
5,024
-100
0
100
200
300
400
Distance from left bank reference point (ft)
Apr-79
May-79
Jul-79
Jan-80
Oct-82
Nov-83
Nov-86
Jul-92
Aug-95
Sep-98
2001

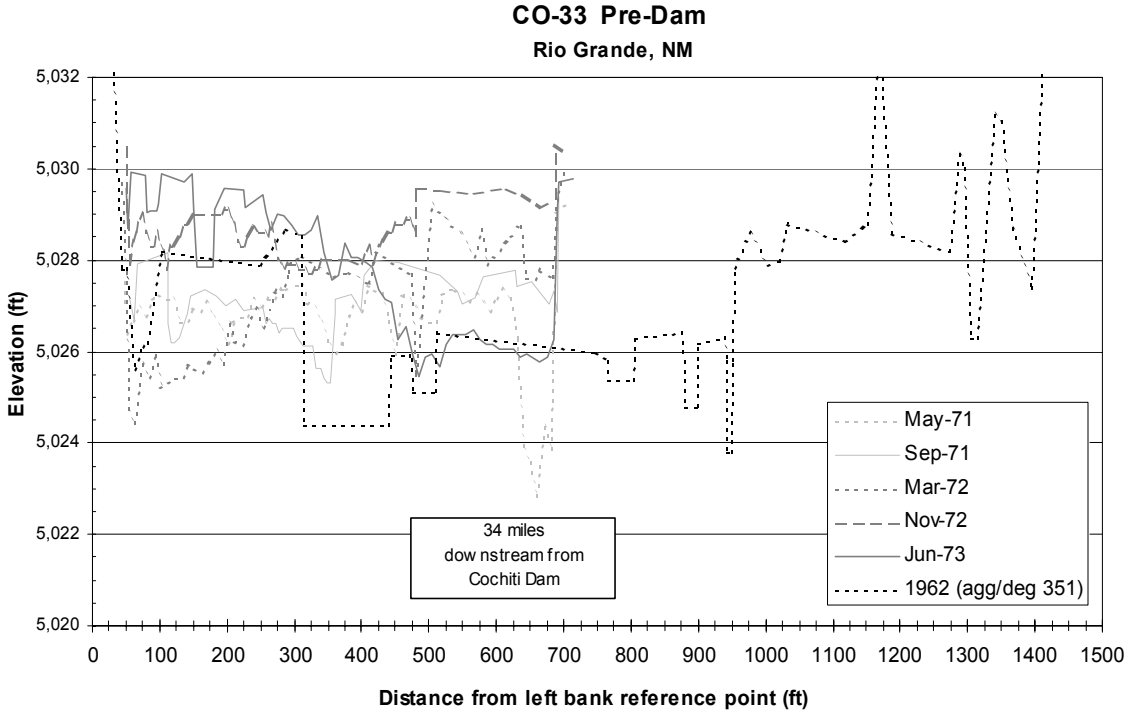
CO-33 Pre-Dam
Rio Grande, NM
Elevation (ft)
5,032
5,030
5,028
5,026
5,024
5,022
5,020
0
100
200
300
400
500
600
700
800
900
1000
1100
1200
1300
1400
1500
Distance from left bank reference point (ft)
34 miles
dow nstream from
Cochiti Dam
May-71
Sep-71
Mar-72
Nov-72
Jun-73
1962 (agg/deg 351)

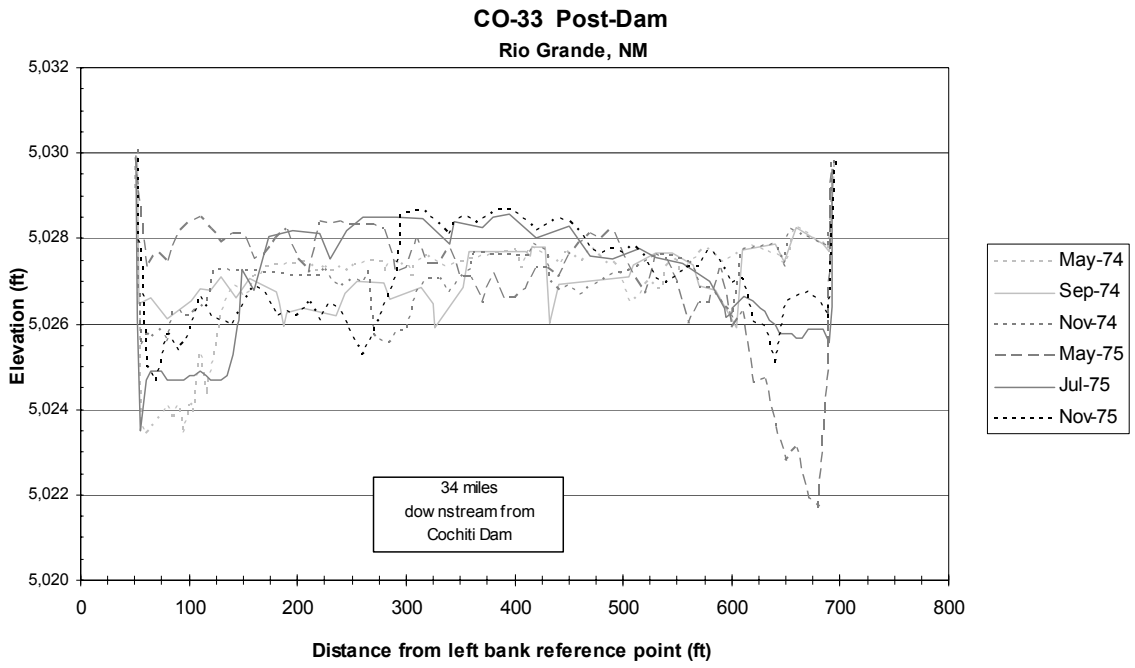
CO-33 Post-Dam
Rio Grande, NM
Elevation (ft)
5,032
5,030
5,028
5,026
5,024
5,022
5,020
0
100
200
300
400
500
600
700
800
Distance from left bank reference point (ft)
34 miles
downstream from
Cochiti Dam
May-74
Sep-74
Nov-74
May-75
Jul-75
Nov-75

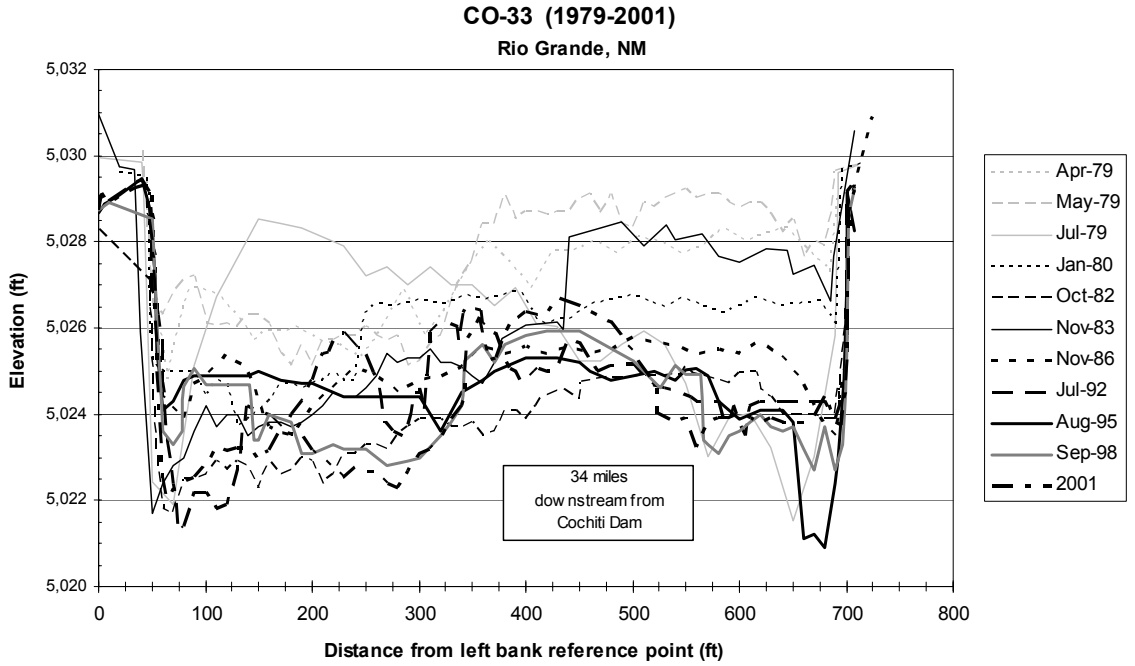
CO-33 (1979-2001)
Rio Grande, NM
Elevation (ft)
5,032
5,030
5,028
5,026
5,024
5,022
5,020
0
100
200
300
400
500
600
700
800
Distance from left bank reference point (ft)
34 miles
downstream from
Cochiti Dam
Apr-79
May-79
Jul-79
Jan-80
Oct-82
Nov-83
Nov-86
Jul-92
Aug-95
Sep-98
2001

APPENDIX C – ANNUAL PEAK MEAN DISCHARGE PLOTS

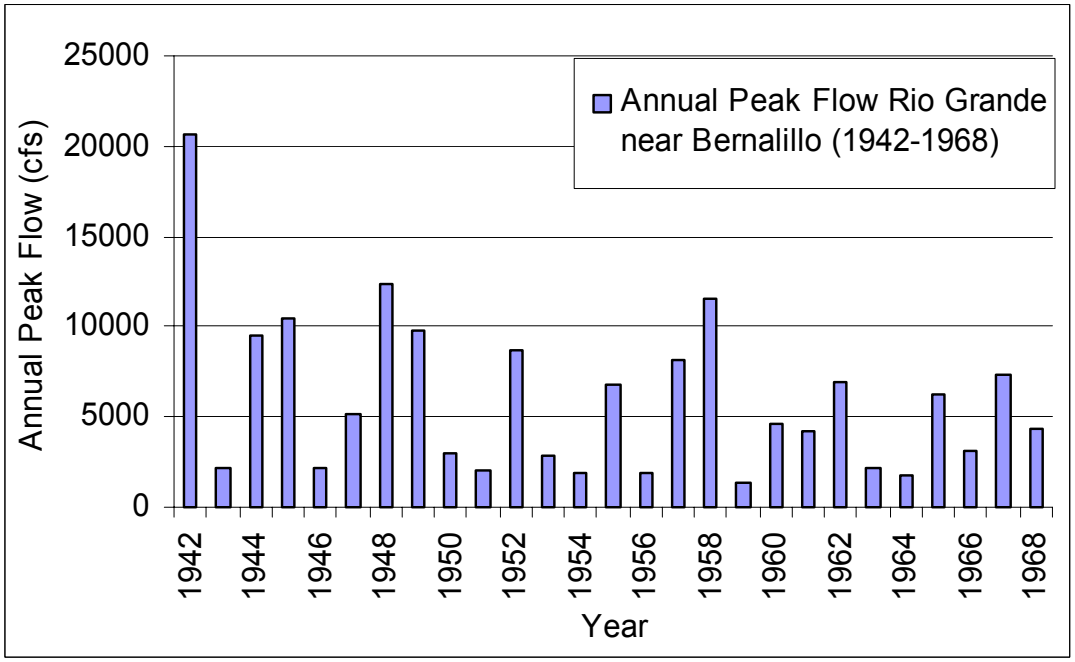

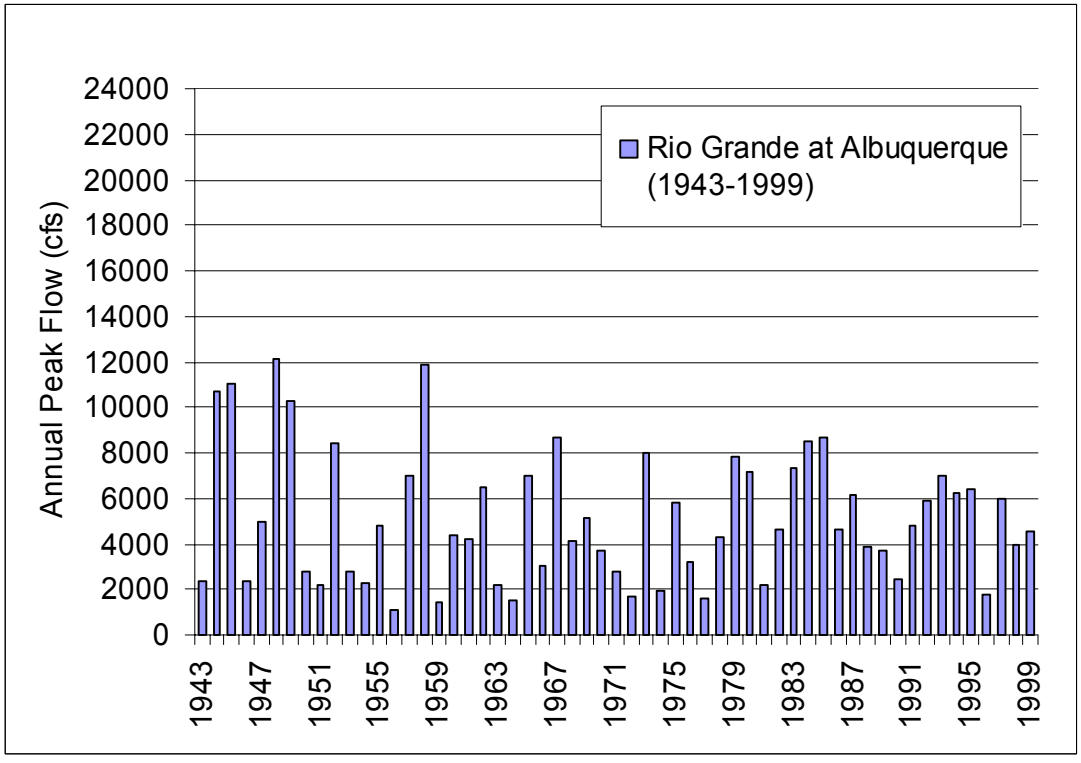

APPENDIX D – REACH-AVERAGED RESULTS FROM HEC-RAS

	Subreach 1								
Year	**Width**	**EG Slope**	**Velocity**	**Area**	**Depth**	**W/D**	**WP**	**WS slope**	**MBE**
1962	595	0.0009	3.89	1327	2.36	286	608	0.0009	5045
1972	641	0.0006	2.60	2119	3.38	270	632	0.0010	5047
1992	565	0.0009	3.86	1319	2.34	245	570	0.0009	5044
2001	560	0.0009	2.95	1715	3.12	180	565	0.0009	5044
	Subreach 2								
Year	**Width**	**EG Slope**	**Velocity**	**Area**	**Depth**	**W/D**	**WP**	**WS slope**	**MBE**
1962	586	0.0010	3.99	1282	2.38	272	581	0.0010	5036
1972	595	0.0010	3.80	1315	2.29	277	597	0.0009	5038
1992	501	0.0010	4.17	1240	2.56	208	505	0.0010	5035
2001	421	0.0009	3.37	1522	3.79	111	424	0.0009	5034
	Subreach 3								
Year	**Width**	**EG Slope**	**Velocity**	**Area**	**Depth**	**W/D**	**WP**	**WS slope**	**MBE**
1962	432	0.0010	4.35	1168	2.74	162	436	0.0009	5028
1972	446	0.0012	4.43	1092	2.50	185	448	0.0011	5030
1992	418	0.0012	4.58	1119	2.75	166	422	0.0011	5027
2001	546	0.0009	3.01	1676	3.17	173	551	0.0009	5026
	Total								
Year	**Width**	**EG Slope**	**Velocity**	**Area**	**Depth**	**W/D**	**WP**	**WS slope**	**MBE**
1962	546	0.0009	4.05	1269	2.48	245	550	0.0009	
1972	574	0.0008	3.50	1551	2.74	250	572	0.0010	
1992	501	0.0010	4.20	1225	2.52	211	505	0.0010	
2001	504	0.0009	3.12	1632	3.38	149	508	0.0009	5035

APPENDIX E – FLOW DISCHARGE DATA USED IN THE DEVELOPMENT OF THE EMPIRICAL WIDTH-DISCHARGE RELATIONSHIPS

Rio Grande at Otowi				*Rio Grande near Bernalillo*			
Years	**Annual Peak Flows (cfs)**	**Years**	**Annual Peak Flows (cfs)**	**Years**	**Annual Peak Flows (cfs)**	**Years**	**Annual Peak Flows (cfs)**
1914	12500	1931	4600	1945	10500	1958	11600
1915	15600	1932	13500	1946	2200	1959	1400
1916	17200	1933	5570	1947	5190	1960	4670
1917	4440	1934	1880	1948	12400	1961	4270
1918	8410	1935	7490	1949	9760	1962	6900
1918 Average	**11630**	**1935 Average**	**6608**	**1949 Average**	**8010**	**1962 Average**	**5768**

Rio Grande at Albuquerque							
Years	**Annual Peak Flows (cfs)**	**Years**	**Annual Peak Flows (cfs)**	**Years**	**Annual Peak Flows (cfs)**	**Years**	**Annual Peak Flows (cfs)**
1968	4160	1981	2170	1988	3880	1995	6370
1969	5120	1982	4630	1989	3710	1996	1770
1970	3710	1983	7330	1990	2420	1997	5980
1971	2780	1984	8500	1991	4800	1998	3940
1972	1680	1985	8650	1992	5900	1999	4550
1972 Average	**3490**	**1985 Average**	**6256**	**1992 Average**	**4142**	**1999 Average**	**4522**

APPENDIX F – EQUILIBRIUM CHANNEL WIDTH ANALYSIS. EXPONENTIAL MODEL DATA

Subreach 1			Width change rate
Year	t (year)	Wt (ft)	dW (ft/year)
1918	0	1165	
1935	17	669	-29.2
1949	31	561	-7.8
1962	44	521	-3.1
1972	54	583	6.2
1985	67	592	0.7
1992	74	524	-9.7
Subreach 2			
Year	t (year)	Wt (ft)	dW (ft/year)
1918	0	1055	
1935	17	656	-23.48
1949	31	569	-6.22
1962	44	539	-2.32
1972	54	541	0.25
1985	67	500	-3.16
1992	74	488	-1.74

Subreach 3			
Year	t (year)	Wt (ft)	dW (ft/year)
1918	0	579	
1935	17	455	-7.30
1949	31	408	-3.30
1962	44	410	0.11
1972	54	413	0.29
1985	67	415	0.16
1992	74	406	-1.22

Entire reach			
Year	t (year)	Wt (ft)	dW (ft/year)
1918	0	954	
1935	17	607	-20.41
1949	31	527	-5.71
1962	44	501	-2.06
1972	54	524	2.35
1985	67	512	-0.96
1992	74	479	-4.62

APPENDIX G – MODIFIED EINSTEIN PROCEDURE INPUT DATA AND RESULTS

Table 1 – MEP input data for Albuquerque Gage G-2

Table 2 – MEP results for Albuquerque Gage and bed-material load estimations.....G-11

Table 2 - MEP results for Albuquerque gage and bed-material load estimations

		MEP results						
Date	Inst. Discharge (cfs)	Total load	Sand load	Gravel load	d10 bed material	% washload	% bed material load	Bed material load (t/day)
4/10/1978	326	498	177.8	0	0.16	92	8	40
4/24/1978	329	1319.9	1075.3	71.7	0.15	31	69	911
5/8/1978	1420	5186.7	2984.6	0	0.14	71	29	1504
5/22/1978	4260	69638.5	58057.7	0	0.15	36	64	44569
5/30/1978	2520	9891.2	6931.3	0	0.14	60	40	3956
6/5/1978	2810	12581.3	9882.1	0	0.17	51	49	6165
6/26/1978	1350	3967.6	3206.7	6.9	0.14	50	50	1984
7/24/1978	1040	7854.2	1099.4	0	0.14	96	4	314
4/2/1979	1840	7402.1	6199.2	0	0.14	54	46	3405
4/23/1979	4980	46703.6	32668.3	63.2	0.14	47	53	24753
5/29/1979	6610	56805.4	45329.2	589.6	0.17	50	50	28403
6/18/1979	6920	47923.7	42714.1	718	0.17	42	58	27796
7/9/1979	6040	50108.4	47521.4	465.8	0.15	31	69	34575
4/7/1980	926	632.5	535	0	0.18	60	40	253
4/28/1980	4730	44563.5	40624.3	586	0.2	41	59	26292
5/12/1980	6900	101837.1	39079.1	130.8	0.13	32	68	69249
6/9/1980	6610	94407.8	36004.9	170.2	0.14	22	78	73638
4/20/1981	641	382.7	311.3	0	0.15	62	38	145
6/22/1981	694	1223	813.7	0	0.15	58	42	514
7/27/1981	584	1527.7	506.4	0	0.15	94	6	92
4/26/1982	1740	12907.8	11471.2	0	0.16	21	79	10197
5/3/1982	3350	15377.6	10182.8	0	0.13	62	38	5843
5/24/1982	4280	15493.5	11800.8	15	0.12	47	53	8212
6/7/1982	4570	14722.7	12313.3	52	0.17	55	45	6625
6/21/1982	3480	7363.3	6331.5	6.8	0.25	81	19	1399
7/7/1982	1100	944.3	746.8	0.2	0.18	60	40	378
7/26/1982	159	42.4	18	0	0.19	90	10	4
4/3/1984	1350	1600.6	1250.6	12	0.048		100	1601
4/24/1984	4270	16901.2	13834.9	0	0.12	52	48	8113
5/8/1984	4440	20624.1	17745.6	0	0.14	43	57	11756
7/10/1984	396	232.4	93.8	0	0.19	84	16	37
5/15/1985	7170	21145.9	15792.6	0	0.039		100	21146
6/17/1985	3620	2060	1568.9	0	0.26	99	1	21
5/6/1986	2430	4713.4	4334.6	10.2	0.16	41	59	2781
5/20/1986	2300	3625.9	3274	37.7	0.2	60	40	1450
6/3/1986	3440	9018.5	8383	11.4	0.15	40	60	5411
6/30/1986	3320	5074.7	3089.8	0	0.24	95	5	254
5/11/1988	1800	6156.2	2448.1	0	0.046	94	6	369
5/8/1990	1950	2721.4	2022.2	1.7	0.065	74	26	708
7/2/1990	570	380	240.4	0	0.19	95	5	19
4/4/1991	1490	2590.6	2128.5	0	0.18	69	31	803
4/10/1991	2130	18967.7	17698	20.9	0.3	35	65	12329
4/22/1991	3060	4027	2628.7	9	0.1	86	14	564
6/3/1991	3590	15609.6	11825	2152	0.16	45	55	8585
7/2/1991	2470	4588.4	3182.9	0	0.18	85	15	688
7/10/1991	401	335.8	220.7	0	0.24	53	47	158
6/18/1992	2610	9164.3	7276.8	985.4	0.042		100	9164
6/29/1992	853	2162.6	2024.2	0	0.24	19	81	1752
7/31/1992	801	3884.5	3509.8	1.5	0.18	15	85	3302
4/1/1994	1370	1191.1	947.9	7.6	0.29	84	16	191
5/2/1994	3300	5670.8	4495.7	48.1	0.25	70	30	1701
6/13/1994	5030	4493.5	3129.8	0	0.074	67	33	1483
6/27/1994	4860	11452.3	10331.9	18	0.2	54	46	5268
5/5/1995	3980	11194	9148.1	6.1	0.26	65	35	3918
5/24/1995	6400	19248.6	16235	63.7	0.26	65	35	6737
6/6/1995	4960	16225.7	14723.8	200.5	0.29	45	55	8924
7/3/1995	5620	25603.1	21572.6	2069.4	0.26	31	69	17666

Table 2 - MEP results for Albuquerque gage and bed-material load estimations

		MEP results						
Date	Inst. Discharge (cfs)	Total load	Sand load	Gravel load	d10 bed material	% washload	% bed material load	Bed material load (t/day)
4/5/1996	437	1494.9	1454.8	0	0.21	6	94	1405
5/3/1996	471	734.3	691.2	0	0.19	12	88	646
6/20/1996	572	282.8	189.4	0	0.22	80	20	57
4/4/1997	2090	14852.7	12854.9	0	0.16	28	72	10694
6/3/1997	5040	54393.6	34813.5	247.4	0.26	30	70	38076
5/5/1998	3180	8875.1	7447.3	6.5	0.20	62	38	3373
6/3/1998	3540	27598	26510.6	47	0.25	48	52	14351
4/27/1999	969	1031.9	669.6	0.1	0.25	93	7	72
5/24/1999	4080	14002.3	11851	152.6	0.21	60	40	5601
8/7/1978	817	2504.4	902.9	0	0.13	90	10	250
8/22/1978	559	1075.7	397.8	0	0.14	94	6	65
8/13/1979	588	1160.1	549.9	0	0.16	69	31	360
9/10/1979	521	539.3	362.4	0	0.16	87	13	70
8/18/1980	377	633.5	483.1	0	0.16	30	70	443
9/15/1980	447	393.6	126.2	0				
8/24/1981	260	1484.8	421.6	0	0.14	95	5	74
8/6/1990	415	220.6	89.1	0	0.25	97	3	7
9/4/1990	267	84.8	34.4	0	0.18			
8/31/1992	1070	1153.8	333.8	0	0.21	94	6	69
8/13/1993	536	413.4	191.6	0	0.25	94	6	25
8/4/1994	588	2807.3	179.4	0	0.18	99	1	28
9/30/1994	383	155.1	55	0	0.12	87	13	20
9/2/1997	774	1355.1	335.1	0	0.27	98	2	27
9/17/1999	1080	980.3	615.3	0.7	0.27	91	9	88
			Average (spring)		0.175	57		
			Average (summer)		0.187	87		